PHYSICAL REVIEW D **96,** 075005 (2017)

Implications of residual *CP* symmetry for leptogenesis in a model with two right-handed neutrinos

Cai-Chang Li[*] and Gui-Jun Ding[†]

Interdisciplinary Center for Theoretical Study and Department of Modern Physics, University of Science and Technology of China, Hefei, Anhui 230026, China

(Received 27 February 2017; published 5 October 2017)

We analyze the interplay between leptogenesis and residual symmetry in the framework of a model with two right-handed neutrinos. Working in the flavor basis, we show that all the leptogenesis *CP* asymmetries are vanishing for the case of two residual *CP* transformations or a cyclic residual flavor symmetry in the neutrino sector. If a single remnant *CP* transformation is preserved in the neutrino sector, the lepton mixing matrix is determined up to a real orthogonal matrix multiplied from the right side. The *R*-matrix is found to depend on only one real parameter. It can take three viable forms, and each entry is either real or purely imaginary. The baryon asymmetry is generated entirely by the *CP* violating phases in the mixing matrix in this scenario. We perform a comprehensive study for the $\Delta(6n^2)$ flavor group and *CP* symmetry which are broken into a single remnant *CP* transformation in the neutrino sector and an Abelian subgroup in the charged lepton sector. The results for lepton flavor mixing and leptogenesis are presented.

DOI: 10.1103/PhysRevD.96.075005

I. INTRODUCTION

A large amount of experiments with solar, atmospheric, reactor, and accelerator neutrinos have provided compelling evidence for oscillations of neutrinos caused by nonzero neutrino masses and neutrino mixing [1–3]. Both three-flavor neutrino and antineutrino oscillations can be described by three lepton mixing angles θ_{12}, θ_{13}, and θ_{23}; one leptonic Dirac *CP* violating phase δ; and two independent mass-squared splittings $\delta m^2 \equiv m_2^2 - m_1^2 > 0$ and $\Delta m^2 \equiv m_3^2 - (m_1^2 + m_2^2)/2$, where $m_{1,2,3}$ are the three neutrino masses and $\Delta m^2 > 0$ and $\Delta m^2 < 0$ correspond to the normal ordering (NO) and inverted ordering (IO) mass spectrum, respectively. All of these mixing parameters except for δ have been measured with good accuracy [4–8]. The experimentally allowed regions at 3σ confidence level (taken from Ref. [4]) are

$$\begin{gathered}0.259 \leq \sin^2\theta_{12} \leq 0.359,\\ 1.76(1.78)\times 10^{-2} \leq \sin^3\theta_{13} \leq 2.95(2.98)\times 10^{-2},\\ 0.374(0.380) \leq \sin^2\theta_{23} \leq 0.626(0.641),\\ 6.99\times 10^{-5}\ \text{eV}^2 \leq \delta m^2 \leq 8.18\times 10^{-5}\ \text{eV}^2,\\ 2.23(-2.56)\times 10^{-3}\ \text{eV}^2 \leq \Delta m^2 \leq 2.61(-2.19)\times 10^{-3}\ \text{eV}^2\end{gathered} \tag{1.1}$$

for the NO (IO) neutrino mass spectrum. At present, both T2K [9–11] and NOνA [12,13] report a weak evidence for a nearly maximal *CP* violating phase $\delta \sim -\pi/2$, and hits of $\delta \sim -\pi/2$ also show up in the global fit of neutrino oscillation data [4–8]. Moreover, several experiments are being planned to look for *CP* violation in neutrino oscillation, including long-baseline facilities, superbeams, and neutrino factories. The above structure of lepton mixing, so different from the small mixing in the quark sector, provides a great theoretical challenge. The idea of flavor symmetry has been extensively exploited to provide a realistic description of the lepton masses and mixing angles. The finite discrete non-Abelian flavor symmetries have been found to be particularly interesting as they can naturally lead to certain mixing patterns [14]; please see Refs. [15–17] for review.

Although the available data are not yet able to determine the individual neutrino mass m_i, the neutrino masses are known to be of order eV from tritium end point, neutrinoless double beta decay, and cosmological data. The smallness of neutrino masses can be well explained within the seesaw mechanism [18], in which the standard model (SM) is extended by adding new heavy states. The light neutrino masses are generically suppressed by the large masses of the new states. In a type I seesaw model [18], the extra states are right-handed (RH) neutrinos which have Majorana masses much larger than the electroweak scale, unlike the standard model fermions which acquire mass proportional to electroweak symmetry breaking. Apart from elegantly explaining the tiny neutrino masses, the seesaw mechanism provides a simple and attractive explanation for the observed baryon asymmetry of the Universe, one of the most longstanding cosmological puzzles. The *CP* violating decays of heavy RH neutrinos can produce a lepton asymmetry in the early Universe, which is then converted into a baryon

[*]lcc0915@mail.ustc.edu.cn
[†]dinggj@ustc.edu.cn

asymmetry through $B+L$ violating anomalous sphaleron processes at the electroweak scale. This is the so-called leptogenesis mechanism [19].

It is well known that in the paradigm of the unflavored thermal leptogenesis, the CP phases in the neutrino Yukawa couplings in general are not related to the low energy leptonic CP violating parameters (i.e., Dirac and Majorana phases) in the mixing matrix. However, the low energy CP phases could play a crucial role in the flavored thermal leptogenesis [20] in which the flavors of the charged leptons produced in the heavy RH neutrino decays are relevant. In models with flavor symmetry, the total number of free parameters is greatly reduced; therefore the observed baryon asymmetry could possibly be related to other observable quantities [21]. In general, the leptogenesis CP asymmetries would vanish if a Klein subgroup of the flavor symmetry group is preserved in the neutrino sector [22].

Recent studies show that the extension of discrete flavor symmetry to include CP symmetry is a very predictive framework [23–35]. If the given flavor and CP symmetries are broken to an Abelian subgroup and $Z_2 \times CP$ in the charged lepton and neutrino sectors, respectively, the resulting lepton mixing matrix would be determined in terms of a free parameter θ whose value can be fixed by the reactor angle θ_{13}. Hence all the lepton mixing angles, the Dirac CP violating phase, and the Majorana CP phases can be predicted [35]. Moreover, other phenomena involving CP phases such as neutrinoless double beta decay and leptogenesis are also strongly constrained in this approach [22,33,36]. In fact, we find that the leptogenesis CP asymmetries are exclusively due to the Dirac and Majorana CP phases in the lepton mixing matrix, and the R-matrix depends on only a single real parameter in this scenario [22].

In this paper we shall extend upon the work of [22] in which the SM is extended to introduce three RH neutrinos. Here we shall study the interplay between residual symmetry and leptogenesis in the seesaw model with two RH neutrinos. We find that all the leptogenesis CP asymmetries would be exactly vanishing if two residual CP transformations or a cyclic residual flavor symmetry were preserved by the seesaw Lagrangian. On the other hand, if only one remnant CP transformation is preserved in the neutrino sector, all mixing angles and CP phases are then fixed in terms of three real parameters $\theta_{1,2,3}$ which can take values between 0 and π, and the R-matrix would be constrained to depend on only one free parameter. The total CP asymmetry $\epsilon_1 \equiv \epsilon_e + \epsilon_\mu + \epsilon_\tau$ in leptogenesis is predicted to be zero. Hence our discussion will be entirely devoted to the flavored thermal leptogenesis scenario in which the lightest RH neutrino mass is typically in the interval of 10^9 GeV $\leq M_1 \leq 10^{12}$ GeV. Our approach is quite general and it is independent of the explicit form of the residual symmetries and how the vacuum alignment achieving the residual symmetries is dynamically realized. In order to show concrete examples, we apply this general formalism to the flavor group $\Delta(6n^2)$ combined with CP symmetry, which is broken down to an Abelian subgroup in the charged lepton sector and a remnant CP transformation in the neutrino sector. The expressions for the lepton mixing matrix as well as mixing parameters in each possible case are presented. We find that for small values of the flavor group index n, the experimental data on lepton mixing angles can be accommodated for certain values of the parameters $\theta_{1,2,3}$. The corresponding predictions for the cosmological matter-antimatter asymmetry are discussed.

The rest of the paper is organized as follows. In Sec. II we briefly review some generic aspects of leptogenesis in the two RH model and present some analytic approximations which will be used later. In Sec. III we study the scenario that one residual CP transformation is preserved in the neutrino sector. The lepton mixing matrix is determined up to an arbitrary real orthogonal matrix multiplied from the right-hand side. The R-matrix contains only one free parameter, and each element is either real or purely imaginary. The total CP asymmetry ϵ_1 is vanishing; consequently the unflavored leptogenesis is not feasible unless subleading corrections are taken into account. The scenario of two remnant CP transformations or a cyclic residual flavor symmetry is discussed in Sec. IV. All leptogenesis CP asymmetries $\epsilon_{e,\mu,\tau}$ are found to vanish in both cases. Leptogenesis could become potentially viable only when higher order contributions lift the postulated residual symmetry. In Sec. V we apply our general formalism to the case that the single residual CP transformation of the neutrino sector arises from the breaking of the most general CP symmetry compatible with the $\Delta(6n^2)$ flavor group, which is broken down to an Abelian subgroup in the charged lepton sector. The predictions for lepton flavor mixing and baryon asymmetry are studied analytically and numerically. Finally, in Sec. VI we summarize our main results and draw the conclusions.

II. GENERAL SETUP OF LEPTOGENESIS IN A MODEL WITH TWO RIGHT-HANDED NEUTRINOS

The seesaw mechanism is a popular extension of the SM to explain the smallness of neutrino masses. In the famous type I seesaw mechanism [18], one generally introduces three additional right-handed neutrinos which are singlets under the SM gauge group. Although the seesaw mechanism describes qualitatively well the observations in neutrino oscillation experiments, it is quite difficult to make quantitative predictions for neutrino mass and mixing without further hypothesis for underlying dynamics. The reason is that the seesaw mechanism involves a large number of undetermined parameters at high energies, whereas many fewer parameters could be measured experimentally.

An intriguing way out of this problem is to simply reduce the number of right-handed neutrinos from three to two [37–39]. The two right-handed neutrino (2RHN) model can be regarded as a limiting case of three right-handed neutrinos in which one of the RH neutrinos decouples from the seesaw mechanism either because it is very heavy or because its Yukawa couplings are very weak. Since the number of free parameters is greatly reduced, the 2RHN model is more predictive than the standard scenario involving three RH neutrinos. Namely, the lightest left-handed neutrino mass automatically vanishes, while the masses of the other two neutrinos are fixed by δm^2 and Δm^2. Hence only two possible mass spectra can be obtained:

$$\begin{aligned}&\text{NO}:\ m_1=0, \quad m_2=\sqrt{\delta m^2}, \quad m_3=\sqrt{\Delta m^2+\delta m^2/2},\\ &\text{IO}:\ m_1=\sqrt{-\delta m^2/2-\Delta m^2}, \quad m_2=\sqrt{\delta m^2/2-\Delta m^2},\\ &\quad m_3=0.\end{aligned} \tag{2.1}$$

Moreover there is only one Majorana *CP* violating phase corresponding to the phase difference between these two nonzero mass eigenvalues. The Lagrangian responsible for lepton masses in the 2RHN model takes the following form,

$$\mathcal{L}=-y_\alpha\bar{L}_\alpha H l_{\alpha R}-\lambda_{i\alpha}\bar{N}_{iR}\tilde{H}^\dagger L_\alpha-\frac{1}{2}M_i\bar{N}_{iR}N^c_{iR}+\text{H.c.}, \tag{2.2}$$

where $L_\alpha\equiv(\nu_{\alpha L},l_{\alpha L})^T$ and $l_{\alpha R}$ indicate the lepton doublet and singlet fields with flavor $\alpha=e,\mu,\tau$, respectively; N_{iR} is the RH neutrino with mass M_i $(i=1,2)$; and $H\equiv(H^+,H^0)^T$ is the Higgs doublet with $\tilde{H}\equiv i\sigma_2H^*$. The Yukawa couplings $\lambda_{i\alpha}$ form an arbitrary complex 2×3 matrix. Here we have worked in the basis in which both the Yukawa couplings for the charged leptons and the Majorana mass matrix for the RH neutrinos are diagonal and real. After electroweak symmetry breaking, the light neutrino mass matrix is given by the famous seesaw formula

$$m_\nu=-v^2\lambda^TM^{-1}\lambda=U^*mU^\dagger, \tag{2.3}$$

where $v=175$ GeV refers to the vacuum expectation value of the Higgs field H^0; $M\equiv\text{diag}(M_1,M_2)$ and $m\equiv\text{diag}(m_1,m_2,m_3)$, with $m_1=0$ for NO and $m_3=0$ for IO; and U is the lepton mixing matrix. It is convenient to express the Yukawa coupling λ in terms of the neutrino mass eigenvalues, mixing angles, and *CP* violation phases as[1]

$$\lambda=iM^{1/2}Rm^{1/2}U^\dagger/v, \tag{2.4}$$

[1]For other parametrizations of the neutrino Yukawa coupling, see Ref. [40].

where R is a 2×3 complex orthogonal matrix having the following structure [41,42],

$$\text{NO}:\ R=\begin{pmatrix}0 & \cos\hat{\theta} & \xi\sin\hat{\theta}\\ 0 & -\sin\hat{\theta} & \xi\cos\hat{\theta}\end{pmatrix}, \tag{2.5a}$$

$$\text{IO}:\ R=\begin{pmatrix}\cos\hat{\theta} & \xi\sin\hat{\theta} & 0\\ -\sin\hat{\theta} & \xi\cos\hat{\theta} & 0\end{pmatrix}, \tag{2.5b}$$

where $\hat{\theta}$ is an arbitrary complex number and $\xi=\pm1$. From Eqs. (2.5a) and (2.5b) we can check that the R-matrix satisfies

$$\begin{aligned}&RR^T=\text{diag}(1,1), \quad \text{for NO and IO},\\ &R^TR=\text{diag}(0,1,1), \quad \text{for NO},\\ &R^TR=\text{diag}(1,1,0), \quad \text{for IO}.\end{aligned} \tag{2.6}$$

Leptogenesis is a natural consequence of the seesaw mechanism, and it provides an elegant explanation for the baryon asymmetry of the Universe [19]. For illustration, we shall work in the typical N_1-dominated scenario, and we assume that right-handed neutrinos are hierarchical $M_2\gg M_1$ such that the asymmetry is dominantly produced from the decays of the lightest RH neutrino N_1. The approach of this paper can also be applied to discuss the resonant leptogenesis [43]. The naturalness of the electroweak scale restricts the heavy RH neutrino mass to be $M_1\leq10^7$ GeV [44]. This bound arises from the naturalness requirement that the RH neutrino loops do not lead to unnaturally large radiative corrections to the Higgs mass. However, the unknown dynamics of quantum gravity at the Planck scale $M_{\rm P}$ would always introduce an unavoidable naturalness problem. In addition, the theoretical criterion of naturalness requires the presence of new physics at the TeV scale. But no any signal of new physics has been observed at the LHC or elsewhere. The argument for naturalness has failed so far as a guiding principle, and nature does not much care about our notion of naturalness. Therefore we do not require the Vissani bound $M_1\leq10^7$ GeV to be fulfilled in this paper. Actually we shall work in the two-flavored leptogenesis regime, that is, at 10^9 GeV $\leq M_1\leq10^{12}$ GeV.

The phenomenology of leptogenesis in the 2RHN model has been comprehensively studied [38,39,42,45]. The flavored *CP* asymmetries in the decays of N_1 into leptons of different flavors are of the form [46–49]

$$\begin{aligned}\epsilon_\alpha&\equiv\frac{\Gamma(N_1\to l_\alpha H)-\Gamma(N_1\to\bar{l}_\alpha\bar{H})}{\sum_\alpha\Gamma(N_1\to l_\alpha H)+\Gamma(N_1\to\bar{l}_\alpha\bar{H})}\\ &=\frac{1}{8\pi(\lambda\lambda^\dagger)_{11}}\sum_{j\neq1}\left\{\text{Im}[(\lambda\lambda^\dagger)_{1j}\lambda_{1\alpha}\lambda^*_{j\alpha}]g(x_j)\right.\\ &\quad\left.+\text{Im}[(\lambda\lambda^\dagger)_{j1}\lambda_{1\alpha}\lambda^*_{j\alpha}]\frac{1}{1-x_j}\right\},\end{aligned} \tag{2.7}$$

where $\Gamma(N_1 \to l_\alpha H)$ and $\Gamma(N_1 \to \bar{l}_\alpha \bar{H})$, with $\alpha = e, \mu, \tau$, denote the flavored decay rates of N_1 into lepton l_α and antilepton $\bar{l}_\alpha$, respectively; the parameter x_j is defined as $x_j \equiv M_j^2/M_1^2$, and the loop function $g(x)$ is

$$g(x) = \sqrt{x}\left[\frac{1}{1-x} + 1 - (1+x)\ln\left(\frac{1+x}{x}\right)\right] \simeq -\frac{3}{2\sqrt{x}} + \mathcal{O}(x^{-3/2}) \quad \text{for } x \gg 1. \tag{2.8}$$

In the hierarchical limit $M_2 \gg M_1$, i.e., $x_2 \gg 1$, the CP asymmetries can be written as[2]

$$\epsilon_\alpha \simeq -\frac{3}{16\pi}\sum_{j=1}^{2}\frac{M_1}{M_j}\frac{\Im[(\lambda\lambda^\dagger)_{1j}\lambda_{1\alpha}\lambda^*_{j\alpha}]}{(\lambda\lambda^\dagger)_{11}} = -\frac{3M_1}{16\pi v^2}\frac{\Im(\sum_{ij}\sqrt{m_i m_j}\, m_j R_{1i}R_{1j}U^*_{\alpha i}U_{\alpha j})}{\sum_j m_j |R_{1j}|^2}. \tag{2.9}$$

Actually, only the $j = 2$ term is relevant in the first line of Eq. (2.9), since $\Im[(\lambda\lambda^\dagger)_{1j}\lambda_{1\alpha}\lambda^*_{j\alpha}] = 0$ for the case of $j = 1$. Here the summation over j allows us to straightforwardly derive the compact expression of Eq. (2.9). We notice that ϵ_α is invariant under the transformation $\xi \to -\xi$ and $\hat{\theta} \to -\hat{\theta}$. Consequently we shall choose $\xi = 1$ as an illustration in the following numerical analysis. Inserting the expression for the Yukawa coupling in Eqs. (2.5) and (2.5b) into Eq. (2.9), we obtain the CP asymmetry

$$\begin{aligned}\epsilon_\alpha \simeq & -\frac{3}{16\pi v^2}\frac{M_1}{m_2|\cos\hat{\theta}|^2 + m_3|\sin\hat{\theta}|^2} \\ & \times \{(m_3^2|U_{\alpha 3}|^2 - m_2^2|U_{\alpha 2}|^2)\Im\sin^2\hat{\theta} \\ & + \xi\sqrt{m_2 m_3}[(m_2+m_3)\Re(U^*_{\alpha 2}U_{\alpha 3})\Im(\sin\hat{\theta}\cos\hat{\theta}) \\ & + (m_3 - m_2)\Im(U^*_{\alpha 2}U_{\alpha 3})\Re(\sin\hat{\theta}\cos\hat{\theta})]\}\end{aligned} \tag{2.10}$$

for the NO and

$$\begin{aligned}\epsilon_\alpha \simeq & -\frac{3}{16\pi v^2}\frac{M_1}{m_1|\cos\hat{\theta}|^2 + m_2|\sin\hat{\theta}|^2} \\ & \times \{(m_2^2|U_{\alpha 2}|^2 - m_1^2|U_{\alpha 1}|^2)\Im\sin^2\hat{\theta} \\ & + \xi\sqrt{m_1 m_2}[(m_1+m_2)\Re(U^*_{\alpha 1}U_{\alpha 2})\Im(\sin\hat{\theta}\cos\hat{\theta}) \\ & + (m_2 - m_1)\Im(U^*_{\alpha 1}U_{\alpha 2})\Re(\sin\hat{\theta}\cos\hat{\theta})]\}\end{aligned} \tag{2.11}$$

for the IO neutrino mass spectrum. If the RH neutrino mass M_1 is large enough (e.g., $M_1 > 10^{12}$ GeV), the interactions mediated by all three charged lepton Yukawa couplings are out of equilibrium. As a result, the one-flavor approximation rigorously holds, and the total CP asymmetry is

$$\epsilon_1 \equiv \sum_\alpha \epsilon_\alpha = -\frac{3M_1}{16\pi v^2}\frac{\Im(\sum_i m_i^2 R_{1i}^2)}{\sum_j m_j |R_{1j}|^2}, \tag{2.12}$$

which is completely independent of the lepton mixing matrix U. For the parametrization of the R-matrix in Eqs. (2.5) and (2.5b), we have

$$\text{NO:}\ \epsilon_1 = -\frac{3M_1}{16\pi v^2}\frac{(m_3^2 - m_2^2)\Im\sin^2\hat{\theta}}{m_2|\cos\hat{\theta}|^2 + m_3|\sin\hat{\theta}|^2}, \tag{2.13a}$$

$$\text{IO:}\ \epsilon_1 = -\frac{3M_1}{16\pi v^2}\frac{(m_2^2 - m_1^2)\Im\sin^2\hat{\theta}}{m_1|\cos\hat{\theta}|^2 + m_2|\sin\hat{\theta}|^2}. \tag{2.13b}$$

We see that the total CP asymmetry ϵ_1 would vanish when the parameter $\hat{\theta}$ is real or purely imaginary up to $\pi/2$. The total baryon asymmetry is the sum of each individual lepton asymmetry. In the present paper we will be concerned with the temperature window $(10^9 \le T \sim M_1 \le 10^{12})$ GeV. In this range only the τ charged lepton Yukawa interaction is in equilibrium, the e and μ flavors are indistinguishable, and the final baryon asymmetry is well approximated by [50–53]

$$Y_B \simeq -\frac{12}{37 g^*}\left[\epsilon_2\eta\left(\frac{417}{589}\tilde{m}_2\right) + \epsilon_\tau\eta\left(\frac{390}{589}\tilde{m}_\tau\right)\right], \tag{2.14}$$

where $\epsilon_2 \equiv \epsilon_e + \epsilon_\mu$, $\tilde{m}_2 \equiv \tilde{m}_e + \tilde{m}_\mu$, g_* is the number of relativistic degrees of freedom, and η is the efficiency factor which depends on the initial abundance of N_1. The washout mass $\tilde{m}_\alpha$ parametrizes the decay rate of N_1 into the leptons of flavor α with

$$\tilde{m}_\alpha \equiv \frac{|\lambda_{1\alpha}|^2 v^2}{M_1} = \left|\sum_i m_i^{1/2} R_{1i} U^*_{\alpha i}\right|^2, \quad \alpha = e, \mu, \tau. \tag{2.15}$$

Plugging Eqs. (2.5) and (2.5b) into the above equation, we find that the explicit expression of the washout mass is

$$\tilde{m}_\alpha = \begin{cases} |\sqrt{m_2}U^*_{\alpha 2}\cos\hat{\theta} + \xi\sqrt{m_3}U^*_{\alpha 3}\sin\hat{\theta}|^2, & \text{for NO,} \\ |\sqrt{m_1}U^*_{\alpha 1}\cos\hat{\theta} + \xi\sqrt{m_2}U^*_{\alpha 2}\sin\hat{\theta}|^2, & \text{for IO.} \end{cases} \tag{2.16}$$

Then the washout parameter K defined as $K = \sum_\alpha \tilde{m}_\alpha/\tilde{m}^*$ with $\tilde{m}^* \sim 10^{-3}$ eV takes the form

[2]The flavored CP asymmetry ϵ_α contains two terms: the lepton-number-violating (LNV) piece $\epsilon_\alpha^{\rm LNV} \propto \Im[(\lambda\lambda^\dagger)_{1j}\lambda_{1\alpha}\lambda^*_{j\alpha}]$ and the lepton-flavor-violating (LFV) piece $\epsilon_\alpha^{\rm LFV} \propto \Im[(\lambda\lambda^\dagger)_{j1}\lambda_{1\alpha}\lambda^*_{j\alpha}]$. Since $\epsilon_\alpha^{\rm LNV} \sim \mathcal{O}(x_j^{-1/2})$ and $\epsilon_\alpha^{\rm LFV} \sim \mathcal{O}(x_j^{-1})$ in the limit $x_j \gg 1$, the LFV term is suppressed with respect to the LNV one; hence we shall neglect the LFV contribution in this work.

$$K=\begin{cases}\frac{m_2|\cos\hat{\theta}|^2+m_3|\sin\hat{\theta}|^2}{\tilde{m}^*}\geq\frac{m_2}{\tilde{m}^*}\simeq 8.683, & \text{for NO},\\ \frac{m_1|\cos\hat{\theta}|^2+m_2|\sin\hat{\theta}|^2}{\tilde{m}^*}\geq\frac{m_1}{\tilde{m}^*}\simeq 48.397, & \text{for IO}.\end{cases} \tag{2.17}$$

Therefore the two right-handed models are always in the strong washout regime. As a consequence, the initial N_1 abundance is almost irrelevant [54], and the right-handed neutrinos are brought to thermal equilibrium by inverse decays and by $\Delta L=1$ scatterings. To a good accuracy, the efficiency factor $\eta(\tilde{m}_\alpha)$ is approximately given by [50]

$$\eta(\tilde{m}_\alpha)\simeq\left[\left(\frac{\tilde{m}_\alpha}{8.25\times10^{-3}\,\text{eV}}\right)^{-1}+\left(\frac{0.2\times10^{-3}\,\text{eV}}{\tilde{m}_\alpha}\right)^{-1.16}\right]^{-1}. \tag{2.18}$$

III. LEPTOGENESIS WITH ONE RESIDUAL *CP* TRANSFORMATION

In a series of papers [23–35], it has been shown that the residual *CP* symmetry of the light neutrino mass matrix can quite efficiently predict the lepton mixing angles as well as *CP* violation phases. If the residual *CP* symmetry is preserved by the seesaw Lagrangian, leptogenesis would also be strongly constrained [22,36,55]. We assume that the flavor and *CP* symmetries are broken at a scale above the leptogenesis scale. As a consequence, leptogenesis occurs in the standard framework of the SM plus two heavy RH neutrinos without involving any additional state in its dynamics. Otherwise if the flavor and *CP* symmetries are broken close to or below the leptogenesis scale, the additional interactions and new particles related to flavor and *CP* symmetries should be considered [56], and the resulting scenarios would be quite different from the standard one. In this section, we shall study the implications of residual *CP* for leptogenesis in the 2RHN model, and we assume that both the neutrino Yukawa coupling and the Majorana mass term in Eq. (A1) are invariant under one generic residual *CP* transformation, defined as

$$\nu_L\overset{\text{CP}}{\mapsto}iX_\nu\gamma_0C\bar{\nu}_L^T,\qquad N_R\overset{\text{CP}}{\mapsto}i\hat{X}_N\gamma_0C\bar{N}_R^T, \tag{3.1}$$

where $\nu_L\equiv(\nu_{eL},\nu_{\mu L},\nu_{\tau L})^T$; $N_R\equiv(N_{1R},N_{2R})^T$; C denotes the charge-conjugation matrix; X_ν is a 3×3 symmetric unitary matrix to avoid degenerate neutrino masses; and $\hat{X}_N$ is a 2×2 symmetric unitary matrix. For the symmetry to hold, λ and M have to fulfill

$$\hat{X}_N^\dagger\lambda X_\nu=\lambda^*,\qquad \hat{X}_N^\dagger M\hat{X}_N^*=M^*. \tag{3.2}$$

As we work in the basis in which the RH neutrino mass matrix M is real and diagonal, the residual *CP* transformation $\hat{X}_R$ should be diagonal with elements equal to ±1, i.e.,

$$\hat{X}_N=\text{diag}(\pm1,\pm1). \tag{3.3}$$

Notice that the conclusion would not be changed even if M is nondiagonal in a concrete flavor symmetry model [22], and the reason is explained in Appendix A. Thus we can find that the light neutrino mass matrix m_ν given by the seesaw formula satisfies

$$X_\nu^Tm_\nu X_\nu=m_\nu^*, \tag{3.4}$$

which means (as expected) that m_ν is invariant under the residual *CP* transformation X_ν. The light neutrino mass matrix can be diagonalized by a unitary transformation U_ν with $m_\nu=U_\nu^*\text{diag}(m_1,m_2,m_3)U_\nu^\dagger$. Then from Eq. (3.4) we can obtain

$$\begin{aligned}&(U_\nu^\dagger X_\nu U_\nu^*)^T\text{diag}(m_1,m_2,m_3)(U_\nu^\dagger X_\nu U_\nu^*)\\&\quad=\text{diag}(m_1,m_2,m_3).\end{aligned} \tag{3.5}$$

Note that $m_1=0$ for NO and $m_3=0$ for IO in the 2RHN model. Hence U_ν is subject to the following constraint from the residual *CP* transformation X_ν,

$$U_\nu^\dagger X_\nu U_\nu^*=\hat{X}_\nu, \tag{3.6}$$

with

$$\begin{aligned}\hat{X}_\nu&=\text{diag}(e^{i\alpha},\pm1,\pm1)\quad\text{for NO},\\ \hat{X}_\nu&=\text{diag}(\pm1,\pm1,e^{i\alpha})\quad\text{for IO},\end{aligned} \tag{3.7}$$

where α is a real parameter in the interval between 0 and 2π. Then it is easy to check that X_ν is a symmetric and unitary matrix for both the NO and IO cases. Moreover, with the definition of the R-matrix in Eq. (2.4), we can derive that the postulated residual symmetry leads to the following constraint on R as

$$\hat{X}_NR^*\hat{X}_\nu^{-1}=R, \tag{3.8}$$

Obviously $-\hat{X}_N$ and $-\hat{X}_\nu$ give rise to the same constraint on R as $\hat{X}_N$ and $\hat{X}_\nu$; therefore it is sufficient to only consider the cases of $\hat{X}_N=\text{diag}(1,\pm1)$, $\hat{X}_\nu=\text{diag}(e^{i\alpha},\pm1,\pm1)$ for NO and $\hat{X}_\nu=\text{diag}(\pm1,\pm1,e^{i\alpha})$ for IO. The explicit forms of the R-matrix for all possible values of $\hat{X}_N$ and $\hat{X}_\nu$ are collected in Table I. We see that there are three admissible forms of the R-matrix summarized as follows:

TABLE I. The explicit form of the R-matrix for all possible independent values of $\hat{X}_N$ and $\hat{X}_\nu$, where ϑ is a real free parameter. The symbol ✗ denotes that the solution for the R-matrix does not exist since it has to fulfill the equality of Eq. (2.6). The notation $\mathcal{D}(x,y)$ with $x,y=\pm 1$ refers to $\mathrm{diag}(e^{i\alpha},x,y)$ and $\mathrm{diag}(x,y,e^{i\alpha})$ for NO and IO, respectively.

$\hat{X}_N$	$\hat{X}_\nu$	R (NO)	R (IO)
$\mathrm{diag}(1,1)$	$\mathcal{D}(1,1)$	$\begin{pmatrix} 0 & \cos\vartheta & \xi\sin\vartheta \\ 0 & -\sin\vartheta & \xi\cos\vartheta \end{pmatrix}$	$\begin{pmatrix} \cos\vartheta & \xi\sin\vartheta & 0 \\ -\sin\vartheta & \xi\cos\vartheta & 0 \end{pmatrix}$
$\mathrm{diag}(1,1)$	$\mathcal{D}(1,-1)$	✗	✗
$\mathrm{diag}(1,1)$	$\mathcal{D}(-1,1)$	✗	✗
$\mathrm{diag}(1,1)$	$\mathcal{D}(-1,-1)$	✗	✗
$\mathrm{diag}(1,-1)$	$\mathcal{D}(1,1)$	✗	✗
$\mathrm{diag}(1,-1)$	$\mathcal{D}(1,-1)$	$\pm\begin{pmatrix} 0 & \cosh\vartheta & i\xi\sinh\vartheta \\ 0 & -i\sinh\vartheta & \xi\cosh\vartheta \end{pmatrix}$	$\pm\begin{pmatrix} \cosh\vartheta & i\xi\sinh\vartheta & 0 \\ -i\sinh\vartheta & \xi\cosh\vartheta & 0 \end{pmatrix}$
$\mathrm{diag}(1,-1)$	$\mathcal{D}(-1,1)$	$\pm\begin{pmatrix} 0 & i\sinh\vartheta & -\xi\cosh\vartheta \\ 0 & \cosh\vartheta & i\xi\sinh\vartheta \end{pmatrix}$	$\pm\begin{pmatrix} i\sinh\vartheta & -\xi\cosh\vartheta & 0 \\ \cosh\vartheta & i\xi\sinh\vartheta & 0 \end{pmatrix}$
$\mathrm{diag}(1,-1)$	$\mathcal{D}(-1,-1)$	✗	✗

$$\text{R-1st}: \begin{cases} R=\begin{pmatrix} 0 & \cos\vartheta & \xi\sin\vartheta \\ 0 & -\sin\vartheta & \xi\cos\vartheta \end{pmatrix} & \text{for NO,} \\ R=\begin{pmatrix} \cos\vartheta & \xi\sin\vartheta & 0 \\ -\sin\vartheta & \xi\cos\vartheta & 0 \end{pmatrix} & \text{for IO,} \end{cases}$$

$$\text{R-2nd}: \begin{cases} R=\pm\begin{pmatrix} 0 & \cosh\vartheta & i\xi\sinh\vartheta \\ 0 & -i\sinh\vartheta & \xi\cosh\vartheta \end{pmatrix} & \text{for NO,} \\ R=\pm\begin{pmatrix} \cosh\vartheta & i\xi\sinh\vartheta & 0 \\ -i\sinh\vartheta & \xi\cosh\vartheta & 0 \end{pmatrix} & \text{for IO,} \end{cases}$$

$$\text{R-3rd}: \begin{cases} R=\pm\begin{pmatrix} 0 & i\sinh\vartheta & -\xi\cosh\vartheta \\ 0 & \cosh\vartheta & i\xi\sinh\vartheta \end{pmatrix} & \text{for NO,} \\ R=\pm\begin{pmatrix} i\sinh\vartheta & -\xi\cosh\vartheta & 0 \\ \cosh\vartheta & i\xi\sinh\vartheta & 0 \end{pmatrix} & \text{for IO.} \end{cases} \tag{3.9}$$

We would like to point out that the R-matrix is constrained to depend on a single real parameter ϑ in this setup. Moreover, from Eq. (2.12) we can see that the total lepton asymmetry ϵ_1 is vanishing, i.e.,

$$\epsilon_1=\epsilon_e+\epsilon_\mu+\epsilon_\tau=0. \tag{3.10}$$

As a result, the net baryon asymmetry cannot be generated in the one-flavor approximation which is realized when the mass of the lightest right-handed neutrino M_1 is larger than about 10^{12} GeV, unless the residual CP symmetry is further broken by subleading order corrections. This result is quite general; it is independent of the explicit form of the residual CP transformation and how the residual symmetry is dynamically realized.

Next we proceed to determine the lepton mixing matrix from the postulated remnant CP transformation. Since X_ν must be a symmetric unitary matrix to avoid degenerate neutrino masses, by performing the Takagi factorization X_ν can be written as [23,35]

$$X_\nu=\Sigma_\nu\Sigma_\nu^T, \tag{3.11}$$

where Σ_ν is a unitary matrix and it can be expressed in terms of the eigenvalues and eigenvectors of X_ν [35]. Thus the constraint on the neutrino diagonalization matrix U_ν in Eq. (3.6) can be simplified into

$$\Sigma_\nu^T U_\nu^*\hat{X}_\nu^{-\frac{1}{2}}=\Sigma_\nu^\dagger U_\nu\hat{X}_\nu^{\frac{1}{2}}. \tag{3.12}$$

The matrices on the two sides of this equation are unitary and complex conjugates of each other. Therefore the combination $\Sigma_\nu^\dagger U_\nu\hat{X}_\nu^{\frac{1}{2}}$ is a generic real orthogonal matrix, and consequently the unitary transformation U_ν takes the form [35,55,57]

$$U_\nu=\Sigma_\nu O_{3\times 3}\hat{X}_\nu^{-\frac{1}{2}}, \tag{3.13}$$

where $O_{3\times 3}$ is a three-dimensional real orthogonal matrix, and it can be generally parametrized as

$$\begin{aligned} O_{3\times 3}(\theta_1,\theta_2,\theta_3)=&\begin{pmatrix} 1 & 0 & 0 \\ 0 & \cos\theta_1 & \sin\theta_1 \\ 0 & -\sin\theta_1 & \cos\theta_1 \end{pmatrix} \\ &\times\begin{pmatrix} \cos\theta_2 & 0 & \sin\theta_2 \\ 0 & 1 & 0 \\ -\sin\theta_2 & 0 & \cos\theta_2 \end{pmatrix} \\ &\times\begin{pmatrix} \cos\theta_3 & \sin\theta_3 & 0 \\ -\sin\theta_3 & \cos\theta_3 & 0 \\ 0 & 0 & 1 \end{pmatrix}, \end{aligned} \tag{3.14}$$

where θ_i $(i=1,2,3)$ are real free parameters in the range of $[0,\pi)$. In our working basis (usually called leptogenesis basis) where the charged lepton mass matrix is diagonal, lepton flavor mixing completely arises from the neutrino sector, and therefore the lepton mixing matrix U coincides with U_ν. Hence we conclude that the mixing matrix and all mixing angles and CP phases would depend on three free continuous parameters $\theta_{1,2,3}$ if only one residual CP transformation is preserved in the neutrino sector. In order to facilitate the discussion of leptogenesis, we separate out the CP parity matrices $\hat{X}_N$ and $\hat{X}_\nu$ and define the following three parameters,

$$\begin{aligned} &U'\equiv U\hat{X}_\nu^{\frac{1}{2}}, \qquad R'\equiv\hat{X}_N^{-\frac{1}{2}}R\hat{X}_\nu^{\frac{1}{2}}, \\ &K_i\equiv(\hat{X}_N)_{11}(\hat{X}_\nu^{-1})_{ii}, \qquad i=1,2,3. \end{aligned} \tag{3.15}$$

We see that R' is real and the parameter K_i is equal to $+1$, -1 or $\pm e^{-i\alpha}$. As a consequence, the flavored CP asymmetry ϵ_α can be expressed as

$$\epsilon_\alpha = -\frac{3M_1}{16\pi v^2}\frac{\Im(\sum_{ij}\sqrt{m_i m_j}\, m_j R'_{1i}R'_{1j}U'^{*}_{\alpha i}U'_{\alpha j}K_j)}{\sum_j m_j R'^2_{1j}}, \quad (3.16)$$

and the washout mass $\tilde{m}_\alpha$ is given by

$$\tilde{m}_\alpha = \left|\sum\nolimits_i \sqrt{m_i}\, R'_{1i}U'_{\alpha i}\right|^2. \quad (3.17)$$

Taking into account that the lightest neutrino is massless in the 2RHN model, we find that ϵ_α and $\tilde{m}_\alpha$ can be written into a rather simple form:

$$\text{NO:}\ \epsilon_\alpha = -\frac{3M_1}{16\pi v^2}W_{\rm NO}I^\alpha_{\rm NO},$$
$$\tilde{m}_\alpha = |\sqrt{m_3}R'_{13}U'_{\alpha 3} + \sqrt{m_2}R'_{12}U'_{\alpha 2}|^2, \quad (3.18a)$$

$$\text{IO:}\ \epsilon_\alpha = -\frac{3M_1}{16\pi v^2}W_{\rm IO}I^\alpha_{\rm IO},$$
$$\tilde{m}_\alpha = |\sqrt{m_2}R'_{12}U'_{\alpha 2} + \sqrt{m_1}R'_{11}U'_{\alpha 1}|^2, \quad (3.18b)$$

with

$$W_{\rm NO} = \frac{\sqrt{m_2 m_3}R'_{12}R'_{13}(m_3K_3 - m_2K_2)}{m_2R'^2_{12} + m_3R'^2_{13}},$$
$$I^\alpha_{\rm NO} = \Im(U'_{\alpha 3}U'^{*}_{\alpha 2}),$$
$$W_{\rm IO} = \frac{\sqrt{m_1 m_2}R'_{11}R'_{12}(m_2K_2 - m_1K_1)}{m_1R'^2_{11} + m_2R'^2_{12}},$$
$$I^\alpha_{\rm IO} = \Im(U'_{\alpha 2}U'^{*}_{\alpha 1}). \quad (3.19)$$

The explicit expressions of $W_{\rm NO}$ and $W_{\rm IO}$ for the three viable forms of the R-matrix are shown in Table II. Notice that $W_{\rm NO,IO}$ are fixed by the light neutrino masses $m_{2,3}$ and ϑ, which parametrize the R-matrix, and the bilinear invariants $I^\alpha_{\rm NO,IO}$ depend on the low energy CP phases contained in the mixing matrix U. As a result, if the signal of CP violation were observed in future neutrino oscillation experiments or neutrinoless double beta ($0\nu\beta\beta$) decay experiments, we would expect a nonzero baryon asymmetry to be generated through leptogenesis in this framework. In the following, we shall perform a general analysis of leptogenesis in the 2RHN model with a generic residual CP transformation, and the lepton mixing matrix can be parametrized as [58]

$$U = \begin{pmatrix} c_{12}c_{13} & s_{12}c_{13} & s_{13}e^{-i\delta} \\ -s_{12}c_{23} - c_{12}s_{13}s_{23}e^{i\delta} & c_{12}c_{23} - s_{12}s_{13}s_{23}e^{i\delta} & c_{13}s_{23} \\ s_{12}s_{23} - c_{12}s_{13}c_{23}e^{i\delta} & -c_{12}s_{23} - s_{12}s_{13}c_{23}e^{i\delta} & c_{13}c_{23} \end{pmatrix} \mathrm{diag}(1, e^{i\frac{\phi}{2}}, 1), \quad (3.20)$$

where $c_{ij} \equiv \cos\theta_{ij}$, $s_{ij} \equiv \sin\theta_{ij}$, and δ and ϕ are the Dirac type and Majorana type CP violating phases, respectively. Note that there is only one Majorana CP phase ϕ in the presence of one massless light neutrino.

Now we discuss the predictions for matter/antimatter asymmetry for each admissible R-matrix. The explicit expressions of the CP asymmetry parameter ϵ_α and the washout mass $\tilde{m}_\alpha$ are given in Appendix B. The contour regions of $Y_B/Y_B^{\rm obs}$ for the three types of R matrices R-1st, R-2nd, and R-3rd are displayed in the plane ϕ versus ϑ in Figs. 1, 2, and 3, respectively. Here both the three lepton mixing angles and the mass-squared splittings are set to

TABLE II. The parametrization of the first row of R' and the corresponding expressions of $W_{\rm NO}$ and $W_{\rm IO}$ for the three viable forms of the R-matrix.

	Mass ordering	K_i	$(R'_{11}, R'_{12}, R'_{13})$	$W_{\rm NO}$ $(W_{\rm IO})$
R-1st	NO	$K_2 = K_3 = 1$	$(0, \cos\vartheta, \xi\sin\vartheta)$	$\frac{\xi\sqrt{m_2m_3}(m_3-m_2)\sin 2\vartheta}{2(m_2\cos^2\vartheta + m_3\sin^2\vartheta)}$
	IO	$K_1 = K_2 = 1$	$(\cos\vartheta, \xi\sin\vartheta, 0)$	$\frac{\xi\sqrt{m_1m_2}(m_2-m_1)\sin 2\vartheta}{2(m_1\cos^2\vartheta + m_2\sin^2\vartheta)}$
R-2nd	NO	$K_2 = -K_3 = 1$	$\pm(0, \cosh\vartheta, -\xi\sinh\vartheta)$	$\frac{\xi\sqrt{m_2m_3}(m_2+m_3)\sinh 2\vartheta}{2(m_2\cosh^2\vartheta + m_3\sinh^2\vartheta)}$
	IO	$K_1 = -K_2 = 1$	$\pm(\cosh\vartheta, -\xi\sinh\vartheta, 0)$	$\frac{\xi\sqrt{m_1m_2}(m_1+m_2)\sinh 2\vartheta}{2(m_1\cosh^2\vartheta + m_2\sinh^2\vartheta)}$
R-3rd	NO	$-K_2 = K_3 = 1$	$\pm(0, -\sinh\vartheta, -\xi\cosh\vartheta)$	$\frac{\xi\sqrt{m_2m_3}(m_2+m_3)\sinh 2\vartheta}{2(m_2\sinh^2\vartheta + m_3\cosh^2\vartheta)}$
	IO	$-K_1 = K_2 = 1$	$\pm(-\sinh\vartheta, -\xi\cosh\vartheta, 0)$	$\frac{\xi\sqrt{m_1m_2}(m_1+m_2)\sinh 2\vartheta}{2(m_1\sinh^2\vartheta + m_2\cosh^2\vartheta)}$

their best fit values [4] and two representative values $\delta = 0, -\pi/2$ are considered. From Eqs. (2.9) and (2.14) we know that the final baryon asymmetry Y_B is proportional to M_1. We shall take $M_1 = 5 \times 10^{11}$ GeV for illustration in this work, and the conclusions would not change qualitatively for other values of M_1. The neutrino mass spectrum is NO and IO, respectively, in the first row and second row of these plots, and we choose $\delta = 0$ in the left column and $\delta = -\pi/2$ in the right column. Note that the period of ϑ for R-1st is π and there are no phenomenologically viable points in the region of $|\vartheta| > 0.6\pi$ for both R-2nd and R-3rd. For R-1st, we find that the experimentally measured value of the baryon asymmetry can be accommodated in the case of NO, while Y_B is too small to account for its observed value for IO. The second case R-2nd can result in successful leptogenesis regardless of whether the neutrino mass spectrum is NO or IO. From Fig. 3, we see that the realistic baryon asymmetry can be generated in the case of R-3rd plus IO, while Y_B is determined to be smaller than its measured value for R-3rd plus NO.

We have chosen the representative values $\delta = 0$ and $-\pi/2$ for illustration in Figs. 1–3. In view of the fact that

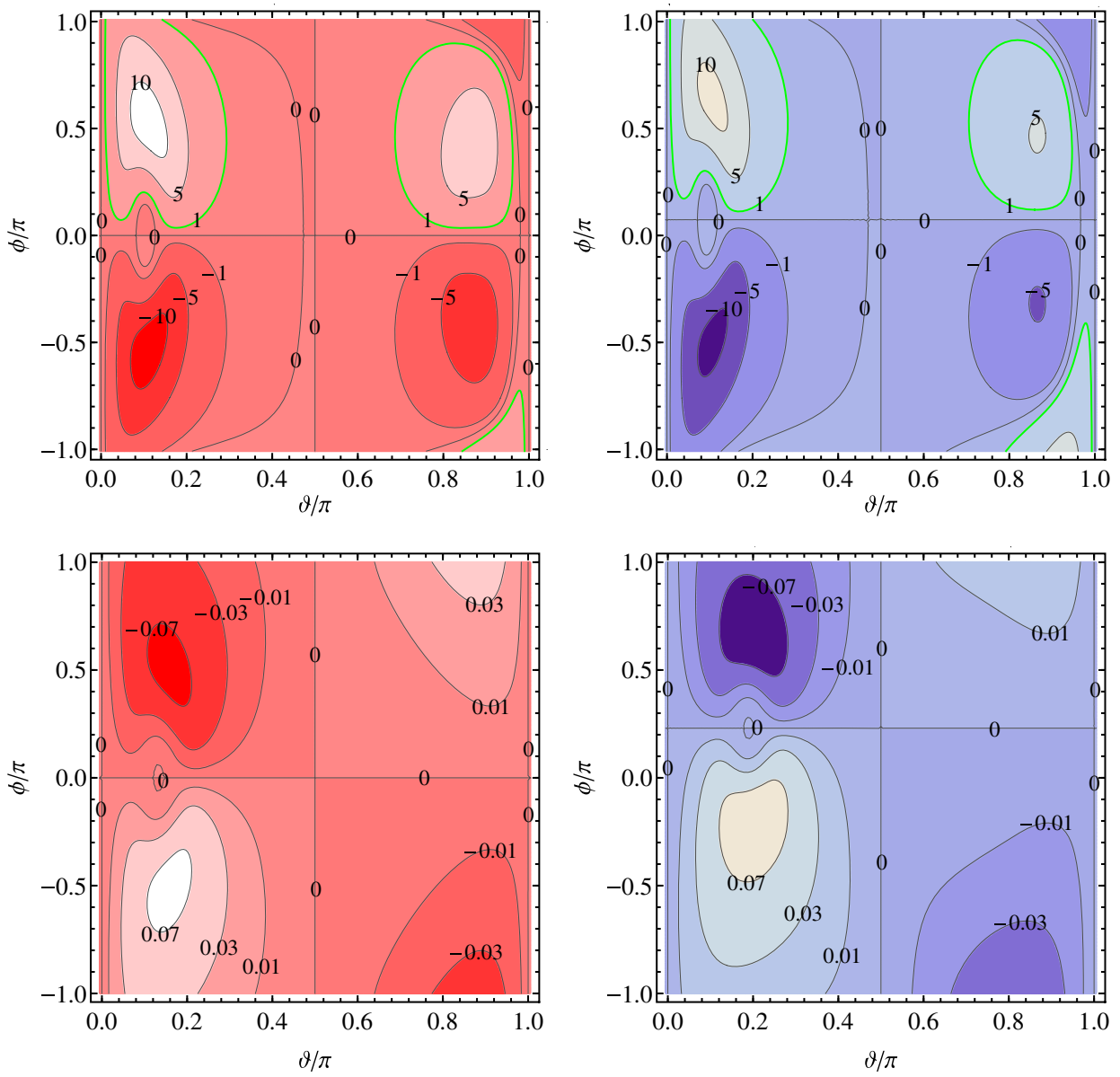

FIG. 1. The contour plots of $Y_B/Y_B^{\rm obs}$ in the $\vartheta - \phi$ plane for the case of R-1st. Here we choose $M_1 = 5 \times 10^{11}$ GeV, so that only the tau Yukawa couplings are in equilibrium. The first row and the second row are for the NO and IO spectra, respectively, and the Dirac CP phase δ is taken to be 0 in the left panels and $-\pi/2$ in the right panels. The neutrino oscillation parameters θ_{12}, θ_{13}, θ_{23}, δm^2, and Δm^2 are fixed at their best fit values [4]. The thick green curve represents the experimentally observed values of the baryon asymmetry $Y_B^{\rm obs} = 8.66 \times 10^{-11}$ [59].

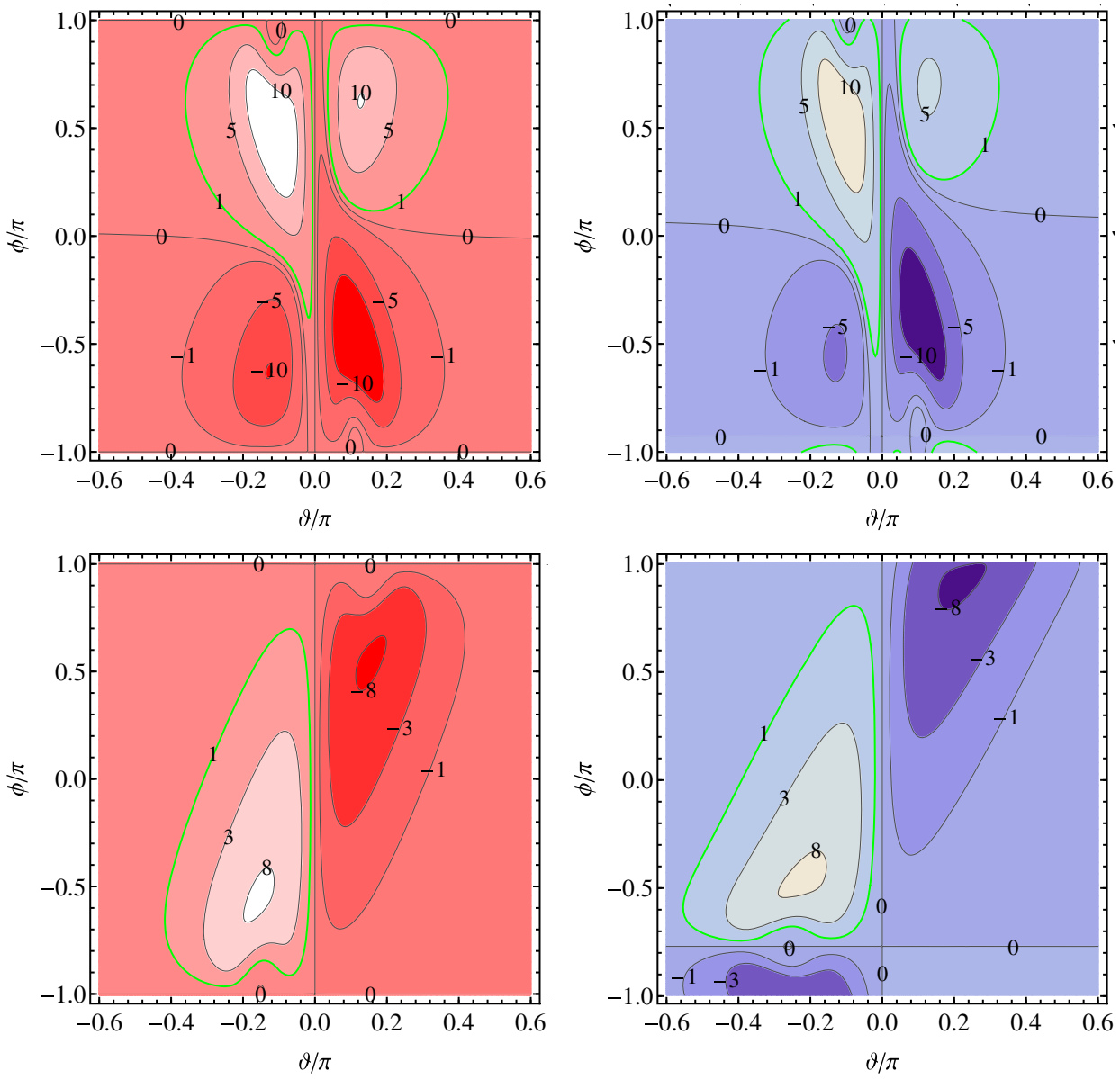

FIG. 2. The contour plots of $Y_B/Y_B^{\rm obs}$ in the $\vartheta-\phi$ plane for the case of R-2nd. Here we choose $M_1 = 5\times 10^{11}$ GeV, so that only the tau Yukawa couplings are in equilibrium. The first row and the second row are for the NO and IO spectra, respectively, and the Dirac *CP* phase δ is taken to be 0 in the left panels and $-\pi/2$ in the right panels. The neutrino oscillation parameters θ_{12}, θ_{13}, θ_{23}, δm^2, and Δm^2 are fixed at their best fit values [4]. The thick green curve represents the experimentally observed values of the baryon asymmetry $Y_B^{\rm obs} = 8.66\times 10^{-11}$ [59].

the Dirac *CP* phase δ is not constrained at the 3σ level at present, we display the regions in the $\delta-\phi$ plane in Fig. 4, where successful leptogenesis ($Y_B/Y_B^{\rm obs}=1$) can be realized for certain values of ϑ. We notice that the observed baryon asymmetry can be generated in quite large regions of the $\delta-\phi$ plane. For the cases of IO:R-1st and NO:R-3rd with $M_1 = 5\times 10^{11}$ GeV, the baryon asymmetry Y_B is too small to be in accordance with experimental data. Equations (2.9) and (2.14) imply that Y_B increases with M_1. The maximal value of M_1 is 10^{12} GeV in the flavored leptogenesis regime; accordingly we find that the maximum of $Y_B/Y_B^{\rm obs}$ is 0.226 and 0.968 for IO:R-1st and NO:R-3rd, respectively, when δ, ϕ, and ϑ are treated as free parameters. Therefore these two cases cannot lead to successful leptogenesis in our setup even if δ and M_1 are not fixed to the above example values. From Fig. 4, we can easily see whether the minimal seesaw model plus a residual *CP* symmetry is capable of explaining the matter/antimatter asymmetry or not for each possible experimental outcome of δ and ϕ.

The $0\nu\beta\beta$ decay process is an important probe for the Majorana nature of neutrinos. If it were observed in the

future, then neutrinos must be Majorana particles. The amplitude of the $0\nu\beta\beta$ decay is proportional to the effective Majorana neutrino mass m_{ee}, which is defined as [58]

$$m_{ee} = \left|\sum_i m_i U_{1i}^2\right| = |m_1 c_{12}^2 c_{13}^2 + m_2 s_{12}^2 c_{13}^2 e^{i\phi} + m_3 s_{13}^2 e^{-2i\delta}|. \tag{3.21}$$

In the 2RNH model, the lightest neutrino is massless with $m_1 = 0$ for NO and $m_3 = 0$ for IO. Consequently the expression of m_{ee} can be reduced to

$$m_{ee} = \begin{cases} \left|\sqrt{\delta m^2} s_{12}^2 c_{13}^2 e^{i(\phi+2\delta)} + \sqrt{\Delta m^2 + \delta m^2/2} s_{13}^2\right|, & \text{for NO,} \\ \left|\sqrt{-\Delta m^2 - \delta m^2/2} c_{12}^2 c_{13}^2 + \sqrt{-\Delta m^2 + \delta m^2/2} s_{12}^2 c_{13}^2 e^{i\phi}\right|, & \text{for IO,} \end{cases} \tag{3.22}$$

where the light neutrino masses in Eq. (2.1) are used. We see that the effective mass m_{ee} depends on the combination $\phi + 2\delta$ for the NO and on the phase ϕ for the IO case. From the panels in the first row of Fig. 4, we find that the phase $\phi + 2\delta$ can take any value between $-\pi$ and π when sufficient baryon asymmetries are generated for the NO case. Similarly the panels in the second row of Fig. 4 imply that the phase ϕ can vary in the range of $[-\pi, \pi]$ if the observed baryon asymmetry is generated for IO. Thus the effective Majorana mass m_{ee} reaches the maximal value when $\phi + 2\delta = 0$ $(\phi = 0)$ and the minimal value when $\phi + 2\delta = \pi (\phi = \pi)$ for the NO (IO) spectrum. Therefore in the parameter space of successful leptogenesis, the effective mass m_{ee} varies in the interval

$$\begin{aligned} &0.000717 \text{ eV} \leq m_{ee} \leq 0.00449 \text{ eV} \quad \text{for NO,} \\ &0.0130 \text{ eV} \leq m_{ee} \leq 0.0478 \text{ eV} \quad \text{for IO.} \end{aligned} \tag{3.23}$$

The predictions of the IO case can be tested in future $0\nu\beta\beta$ decay experiments.

IV. LEPTOGENESIS WITH TWO RESIDUAL *CP* TRANSFORMATIONS OR A CYCLIC RESIDUAL FLAVOR SYMMETRY

In this section, we shall proceed to discuss the predictions for leptogenesis in the case that two residual CP transformations or a cyclic residual flavor symmetry is preserved by the seesaw Lagrangian in the 2RHN model.

A. Two residual *CP* transformations preserved

Following the same method as in Sec. III, we investigate what we could learn if the parent CP symmetry at a high energy scale is broken down to two residual CP transformations in the neutrino sectors. The lepton fields transform as

$$\begin{aligned} &\nu_L \overset{\text{CP}_1}{\mapsto} iX_{\nu 1}\gamma_0 C\bar{\nu}_L^T, \qquad N_R \overset{\text{CP}_1}{\mapsto} i\hat{X}_{N1}\gamma_0 C\bar{N}_R^T, \\ &\nu_L \overset{\text{CP}_2}{\mapsto} iX_{\nu 2}\gamma_0 C\bar{\nu}_L^T, \qquad N_R \overset{\text{CP}_2}{\mapsto} i\hat{X}_{N2}\gamma_0 C\bar{N}_R^T, \end{aligned} \tag{4.1}$$

with $X_{\nu 1} \neq X_{\nu 2}$ and $\hat{X}_{N1} \neq \hat{X}_{N2}$. The invariance of λ and M under the action of the above CP transformations $X_{\nu i}$ and $\hat{X}_{Ni}$ implies

$$\hat{X}_{N1}^\dagger \lambda X_{\nu 1} = \lambda^*, \qquad \hat{X}_{N1}^\dagger M \hat{X}_{N1}^* = M^*, \tag{4.2a}$$

$$\hat{X}_{N2}^\dagger \lambda X_{\nu 2} = \lambda^*, \qquad \hat{X}_{N2}^\dagger M \hat{X}_{N2}^* = M^*. \tag{4.2b}$$

Notice that $-X_{\nu i}$, $-\hat{X}_{Ni}$ leads to the same constraints as $X_{\nu i}$, $\hat{X}_{Ni}$; hence they are identified as the same residual CP transformation. Because the RH neutrino fields N_{1R} and N_{2R} are assumed to be in the mass eigenstates, $\hat{X}_{N1}$ and $\hat{X}_{N2}$ must be diagonal with elements $+1$ or -1, i.e.,

$$\hat{X}_{N1}, \qquad \hat{X}_{N2} = \text{diag}(\pm 1, \pm 1). \tag{4.3}$$

The light neutrino mass matrix m_ν is given by the seesaw relation. We can straightforwardly check that the residual CP transformations lead to the following two constraints on m_ν,

$$X_{\nu 1}^T m_\nu X_{\nu 1} = m_\nu^*, \qquad X_{\nu 2}^T m_\nu X_{\nu 2} = m_\nu^*. \tag{4.4}$$

This is exactly the condition that m_ν is invariant under the residual CP transformations $X_{\nu 1}$ and $X_{\nu 2}$. From Eq. (4.4) we can derive that the unitary transformation U_ν which diagonalizes m_ν should satisfy

$$U_\nu^\dagger X_{\nu 1} U_\nu^* = \hat{X}_{\nu 1}, \qquad U_\nu^\dagger X_{\nu 2} U_\nu^* = \hat{X}_{\nu 2}, \tag{4.5}$$

with

$$\begin{aligned} &\hat{X}_{\nu 1}, \hat{X}_{\nu 2} = \text{diag}(e^{i\alpha_{1,2}}, \pm 1, \pm 1) \quad \text{for NO,} \\ &\hat{X}_{\nu 1}, \hat{X}_{\nu 2} = \text{diag}(\pm 1, \pm 1, e^{i\alpha_{1,2}}) \quad \text{for IO,} \end{aligned} \tag{4.6}$$

where α_1 and α_2 are arbitrary real parameters. Equation (4.5) indicates that both residual CP

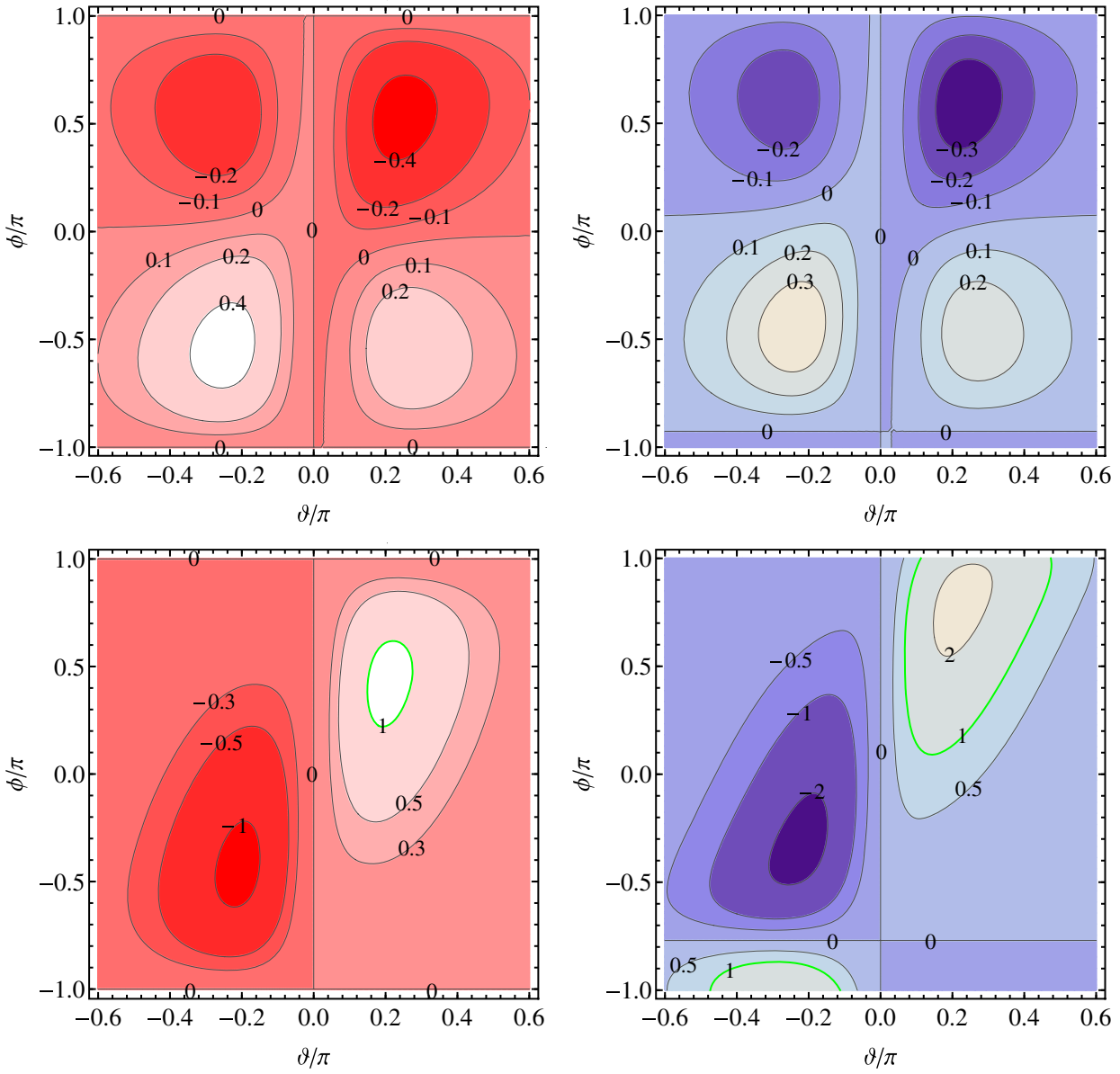

FIG. 3. The contour plots of $Y_B/Y_B^{\rm obs}$ in the $\vartheta-\phi$ plane for the case of R-3rd. Here we choose $M_1 = 5\times 10^{11}$ GeV, so that only the tau Yukawa couplings are in equilibrium. The first row and the second row are for the NO and IO spectra, respectively, and the Dirac *CP* phase δ is taken to be 0 in the left panels and $-\pi/2$ in the right panels. The neutrino oscillation parameters θ_{12}, θ_{13}, θ_{23}, δm^2, and Δm^2 are fixed at their best fit values [4]. The thick green curve represents the experimentally observed values of the baryon asymmetry $Y_B^{\rm obs} = 8.66\times 10^{-11}$ [59].

transformations $X_{\nu 1}$ and $X_{\nu 2}$ must be symmetric unitary matrices. Using the symmetry properties of λ, M, and U_ν shown in Eqs. (4.2), (4.2b), and (4.4), we find that the R-matrix is subject to the following constraints,

$$\hat{X}_{N1} R^* \hat{X}_{\nu 1}^{-1} = R, \qquad \hat{X}_{N2} R^* \hat{X}_{\nu 2}^{-1} = R, \tag{4.7}$$

which imply

$$R = \hat{X}_{N1}\hat{X}_{N2} R \hat{X}_{\nu 1}\hat{X}_{\nu 2}^{-1}. \tag{4.8}$$

Because the residual *CP* transformations $X_{\nu 1}$, $\hat{X}_{N1}$ are distinct from $X_{\nu 2}$, $\hat{X}_{N2}$, the combinations $\hat{X}_{N1}\hat{X}_{N2}$ and $\hat{X}_{\nu 1}\hat{X}_{\nu 2}^{-1}$ should take the form[3]

$$\begin{aligned} &\hat{X}_{N1}\hat{X}_{N2} = {\rm diag}(1,-1), \\ &\hat{X}_{\nu 1}\hat{X}_{\nu 2}^{-1} = P_\nu {\rm diag}(e^{i(\alpha_1-\alpha_2)},1,-1)P_\nu^T, \end{aligned} \tag{4.9}$$

[3]The same results for the R-matrix would be obtained in the case of $\hat{X}_{N1}\hat{X}_{N2} = -{\rm diag}(1,-1)$, $\hat{X}_{\nu 1}\hat{X}_{\nu 2}^{-1} = P_\nu {\rm diag}(e^{i(\alpha_1-\alpha_2)},1,-1)P_\nu^T$.

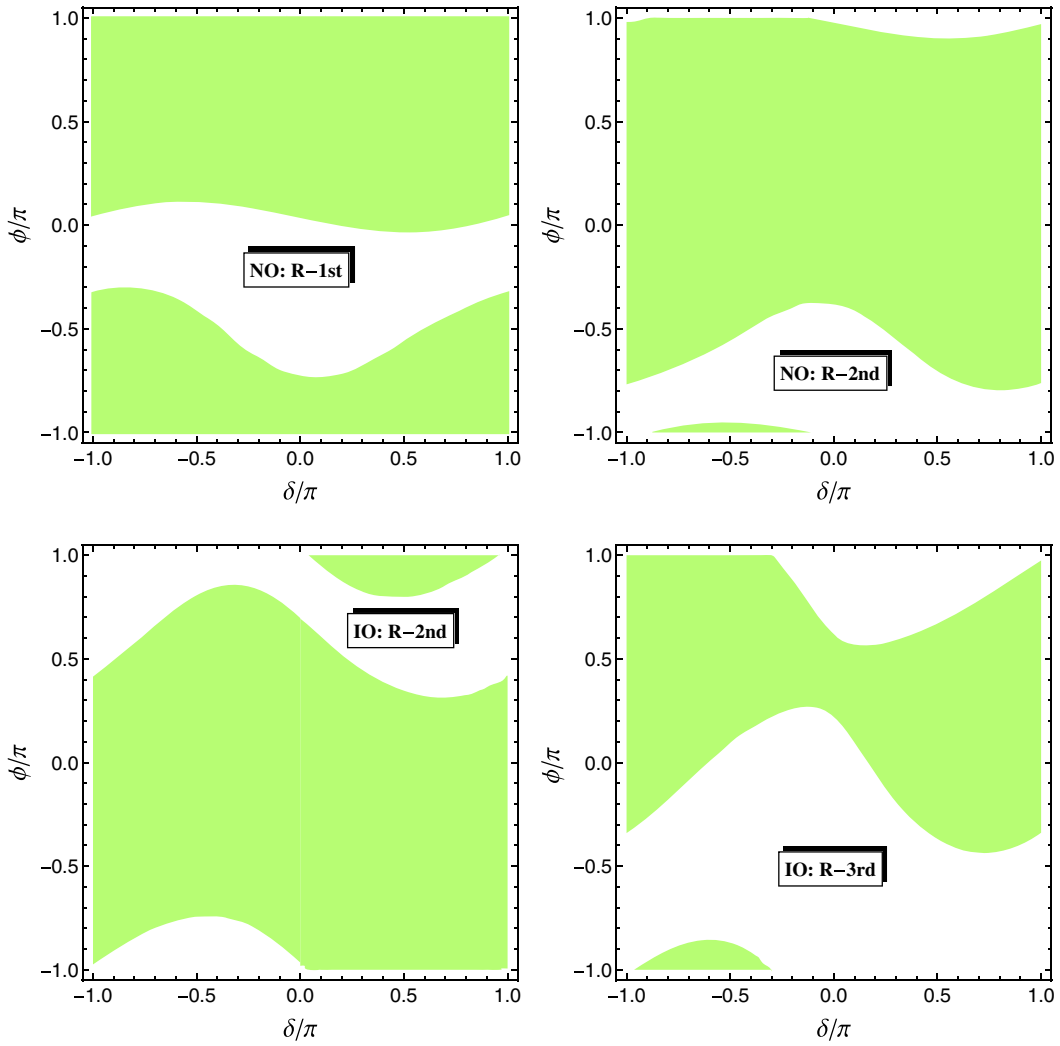

FIG. 4. The viable regions in the $\delta-\phi$ plane where the cosmological matter/antimatter asymmetry can be generated for certain values of ϑ. For the cases of IO:R-1st and NO:R-3rd, the baryon asymmetry Y_B is smaller than its observed value for any value of δ, ϕ, and ϑ.

where P_ν is a permutation matrix with $P_\nu = P_{123}, P_{132}$ for NO and $P_\nu = P_{231}, P_{321}$ for IO. Here the six 3×3 permutation matrices are denoted as

$$P_{123}=\begin{pmatrix}1&0&0\\0&1&0\\0&0&1\end{pmatrix},\quad P_{132}=\begin{pmatrix}1&0&0\\0&0&1\\0&1&0\end{pmatrix},$$
$$P_{213}=\begin{pmatrix}0&1&0\\1&0&0\\0&0&1\end{pmatrix},\quad P_{231}=\begin{pmatrix}0&1&0\\0&0&1\\1&0&0\end{pmatrix},$$
$$P_{312}=\begin{pmatrix}0&0&1\\1&0&0\\0&1&0\end{pmatrix},\quad P_{321}=\begin{pmatrix}0&0&1\\0&1&0\\1&0&0\end{pmatrix}. \quad (4.10)$$

Inserting Eq. (4.9) into Eq. (4.8) we obtain

$$RP_\nu = \mathrm{diag}(1,-1)RP_\nu\mathrm{diag}(e^{i(\alpha_1-\alpha_2)},1,-1). \quad (4.11)$$

Consequently the (13) and (22) elements of the matrix RP_ν are vanishing. The explicit forms of the R-matrix for all possible values of P_ν are summarized in Table III. It is easy to check that all the flavored CP symmetry ϵ_α is vanishing, i.e.,

TABLE III. The explicit form of the R-matrix for different possible values P_ν, where ξ is either $+1$ or -1.

Mass ordering	P_ν	$\hat{\theta}$	R
NO	P_{123}	$0,\pi$	$R=\begin{pmatrix}0&\pm1&0\\0&0&\pm\xi\end{pmatrix}$
	P_{132}	$\pm\frac{\pi}{2}$	$R=\begin{pmatrix}0&0&\pm\xi\\0&\mp1&0\end{pmatrix}$
IO	P_{231}	$0,\pi$	$R=\begin{pmatrix}\pm1&0&0\\0&\pm\xi&0\end{pmatrix}$
	P_{321}	$\pm\frac{\pi}{2}$	$R=\begin{pmatrix}0&\pm\xi&0\\\mp1&0&0\end{pmatrix}$

$$\epsilon_e = \epsilon_\mu = \epsilon_\tau = 0. \tag{4.12}$$

As a result, a net baryon asymmetry cannot be generated at leading order in this case, and moderate high order corrections are necessary in order to make leptogenesis viable. We would like to emphasize that this result is quite general and it is independent of the explicit form of the residual *CP* transformations $X_{\nu i}$ and $\hat{X}_{Ni}$.

B. A cyclic residual flavor symmetry preserved

In this section we shall proceed to discuss the implications of the residual flavor symmetry (without residual *CP*) for leptogenesis. We assume that the flavor symmetry group is broken down to a cyclic Z_n subgroup in the neutrino sector, where the subscript n denotes the order of the cyclic group. Under the action of the generator of the residual flavor symmetry Z_n, the neutrino fields transform as

$$\nu_L \overset{Z_n}{\mapsto} G_\nu \nu_L, \qquad N_R \overset{Z_n}{\mapsto} \hat{G}_N N_R, \tag{4.13}$$

where G_ν is a 3×3 unitary matrix with $G_\nu^n = 1_{3\times 3}$ and $\hat{G}_N = \mathrm{diag}(\pm 1, \pm 1)$ in our working basis. For this residual symmetry to hold, the Yukawa coupling λ and the RH neutrino mass matrix $M \equiv \mathrm{diag}(M_1, M_2)$ have to fulfill

$$\hat{G}_N^\dagger \lambda G_\nu = \lambda, \qquad \hat{G}_N^\dagger M \hat{G}_N^* = M. \tag{4.14}$$

Subsequently we can check that the light neutrino mass matrix is invariant under the residual flavor symmetry

$$G_\nu^T m_\nu G_\nu = m_\nu. \tag{4.15}$$

From this condition we find that the neutrino diagonalization matrix U_ν can diagonalize the residual flavor symmetry transformation G_ν as well,

$$U_\nu^\dagger G_\nu U_\nu = \hat{G}_\nu, \quad \text{with} \quad \hat{G}_\nu = \begin{cases} \mathrm{diag}(e^{i\alpha}, \pm 1, \pm 1) & \text{for NO} \\ \mathrm{diag}(\pm 1, \pm 1, e^{i\alpha}) & \text{for IO} \end{cases}, \tag{4.16}$$

where $\alpha = 2\pi k/n$ with k coprime to n is a rational multiple of π. Notice that the maximal invariance group of the neutrino mass matrix is $U(1)\times Z_2 \times Z_2$, not a Klein group $Z_2 \times Z_2$, because one light neutrino mass is zero in this case. From Eqs. (4.14) and (4.16), we can determine that the residual flavor symmetry gives rise to the following constraint on the R-matrix,

$$R = \hat{G}_N R \hat{G}_\nu. \tag{4.17}$$

The explicit forms of the R-matrix for all possible values of $\hat{G}_\nu$ and $\hat{G}_N$ are listed in Table IV. We see that there is only one nonzero element in each row of the R-matrix; consequently all the flavored *CP* asymmetries are zero:

$$\epsilon_e = \epsilon_\mu = \epsilon_\tau = 0. \tag{4.18}$$

Hence the baryon asymmetry Y_B would be generally vanishing in the 2RHN model with a remnant Z_n flavor symmetry in the neutrino sector. In a concrete model, one could take into account the nonleading corrections arising from loop effects and higher dimensional operators to explain the correct size of matter/antimatter asymmetry [21].

TABLE IV. The explicit form of the R-matrix for different possible values of $\hat{G}_N$ and $\hat{G}_\nu$. The notation ✗ means that the solution for the R-matrix does not exist, and $\mathcal{D}(x,y)$ with $x, y = \pm 1$ refers to $\mathrm{diag}(e^{i\alpha}, x, y)$ and $\mathrm{diag}(x, y, e^{i\alpha})$ for NO and IO, respectively. Note that the residual flavor symmetry gives no constraint on the R-matrix for $\hat{G}_N = -\mathrm{diag}(1,1)$ and $\hat{G}_\nu = \mathcal{D}(-1,-1)$.

$\hat{G}_N$	$\hat{G}_\nu$	R (NO)	R (IO)
$\mathrm{diag}(1,-1)$	$\mathcal{D}(1,1)$	✗	✗
$\mathrm{diag}(1,-1)$	$\mathcal{D}(1,-1)$	$\begin{pmatrix} 0 & \pm 1 & 0 \\ 0 & 0 & \pm\xi \end{pmatrix}$	$\begin{pmatrix} \pm 1 & 0 & 0 \\ 0 & \pm\xi & 0 \end{pmatrix}$
$\mathrm{diag}(1,-1)$	$\mathcal{D}(-1,1)$	$\begin{pmatrix} 0 & 0 & \pm\xi \\ 0 & \mp 1 & 0 \end{pmatrix}$	$\begin{pmatrix} 0 & \pm\xi & 0 \\ \mp 1 & 0 & 0 \end{pmatrix}$
$\mathrm{diag}(1,-1)$	$\mathcal{D}(-1,-1)$	✗	✗
$\mathrm{diag}(-1,1)$	$\mathcal{D}(1,1)$	✗	✗
$\mathrm{diag}(-1,1)$	$\mathcal{D}(1,-1)$	$\begin{pmatrix} 0 & 0 & \pm\xi \\ 0 & \mp 1 & 0 \end{pmatrix}$	$\begin{pmatrix} 0 & \pm\xi & 0 \\ \mp 1 & 0 & 0 \end{pmatrix}$
$\mathrm{diag}(-1,1)$	$\mathcal{D}(-1,1)$	$\begin{pmatrix} 0 & \pm 1 & 0 \\ 0 & 0 & \pm\xi \end{pmatrix}$	$\begin{pmatrix} \pm 1 & 0 & 0 \\ 0 & \pm\xi & 0 \end{pmatrix}$
$\mathrm{diag}(1,1)$	$\mathcal{D}(-1,-1)$	✗	✗
$-\mathrm{diag}(1,1)$	$\mathcal{D}(1,1)$	✗	✗
$-\mathrm{diag}(1,1)$	$\mathcal{D}(1,-1)$	✗	✗
$-\mathrm{diag}(1,1)$	$\mathcal{D}(-1,1)$	✗	✗

V. EXAMPLES IN $\Delta(6n^2)$ FLAVOR SYMMETRY AND *CP*

In Sec. III, we have presented the general results for leptogenesis in the scenario that one residual *CP* transformation is preserved in the neutrino sector. In order to show concrete examples, we shall study the case that the single residual *CP* transformation arises from the breaking of the generalized *CP* symmetry compatible with the $\Delta(6n^2)$ flavor group.

$\Delta(6n^2)$ as the flavor symmetry group and the resulting phenomenological consequence for lepton flavor mixing have been discussed in the literature [28–30,60]. In the present work, we shall adopt the conventions and notations of Ref. [30] for the $\Delta(6n^2)$ group. The $\Delta(6n^2)$ group is isomorphic to $(Z_n \times Z_n)\rtimes S_3$, where the index n is a generic integer. The $\Delta(6n^2)$ group can be generated by four generators, a, b, c, and d, which obey the following relations [30,61]:

$$a^3 = b^2 = (ab)^2 = c^n = d^n = 1, \qquad cd = dc,$$
$$aca^{-1} = c^{-1}d^{-1}, \qquad ada^{-1} = c, \qquad bcb^{-1} = d^{-1},$$
$$bdb^{-1} = c^{-1}. \tag{5.1}$$

The $\Delta(6n^2)$ group has $6n^2$ elements, which can be expressed as

$$g = a^\alpha b^\beta c^\gamma d^\delta, \qquad \alpha = 0, 1, 2, \qquad \beta = 0, 1,$$
$$\gamma, \delta = 0, 1, \ldots, n-1. \tag{5.2}$$

The group $\Delta(6n^2)$ has one-dimensional, two-dimensional, three-dimensional, and six-dimensional irreducible representations [30,61]. It has been shown that $\Delta(6n^2)$ has $2(n-1)$ three-dimensional irreducible representations denoted by $\mathbf{3}_{k,l}$ in which the explicit form of the four generators can be chosen as

$$\mathbf{3}_{k,l}: \; a = \begin{pmatrix} 0 & 1 & 0 \\ 0 & 0 & 1 \\ 1 & 0 & 0 \end{pmatrix}, \qquad b = (-1)^k \begin{pmatrix} 0 & 0 & 1 \\ 0 & 1 & 0 \\ 1 & 0 & 0 \end{pmatrix},$$
$$c = \begin{pmatrix} \eta^l & 0 & 0 \\ 0 & \eta^{-l} & 0 \\ 0 & 0 & 1 \end{pmatrix}, \qquad d = \begin{pmatrix} 1 & 0 & 0 \\ 0 & \eta^l & 0 \\ 0 & 0 & \eta^{-l} \end{pmatrix}, \tag{5.3}$$

where $\eta \equiv e^{2\pi i/n}$; $k = 1, 2$; and $l = 1, 2, \ldots, n-1$. In the following, without loss of generality, we shall embed the three generations of left-handed lepton doublets into the faithful triplet $\mathbf{3}_{1,1}$, which is denoted by 3 for simplicity, while the two right-handed neutrinos are assumed to transform as a doublet of $\Delta(6n^2)$. As has been shown in Ref. [30], the most general CP transformation consistent with the $\Delta(6n^2)$ flavor symmetry is of the same form as the flavor symmetry transformation in the basis of Eq. (5.3), i.e.,

$$X_{\mathbf{r}} = \rho_{\mathbf{r}}(g), \qquad g \in \Delta(6n^2), \tag{5.4}$$

where $\rho_{\mathbf{r}}(g)$ denotes the representation matrix of the element g in the irreducible representation $\mathbf{r}$ of the $\Delta(6n^2)$ group. Moreover, we assume that the $\Delta(6n^2)$ flavor symmetry is broken down to an Abelian subgroup G_l in the charged lepton sector and G_l is capable of distinguishing among the three generations of the charged leptons. As a result, the charged lepton mass matrix is invariant under the action of the generator g_l of G_l,

$$\rho^\dagger_{\mathbf{3}}(g_l) m_l^\dagger m_l \rho_{\mathbf{3}}(g_l) = m_l^\dagger m_l, \tag{5.5}$$

where the charged lepton mass matrix m_l is given in the right-left basis. The matrix $\rho_{\mathbf{3}}(g_l)$ can be diagonalized by a unitary transformation U_l,

$$U_l^\dagger \rho_{\mathbf{3}}(g_l) U_l = \rho^{\mathrm{diag}}_{\mathbf{3}}(g_l). \tag{5.6}$$

Then Eq. (5.5) implies that U_l also diagonalizes the charged lepton mass matrix $m_l^\dagger m_l$. Notice that U_l is uniquely determined up to permutations and phases of their column vectors. All possible residual subgroup G_l and the corresponding diagonalization matrices U_l are summarized in Table V, where G_l is assumed to be generated by a single generator. If we further take into account the case that G_l is a product of several cyclic groups, the constraints on the parameters s and t in Table V would be removed, yet no new additional form of U_l is generated [62]. In the neutrino sector, a single remnant CP transformation X_ν is preserved by the neutrino mass matrix such that the neutrino mixing matrix U_ν is of the form of Eq. (3.13), as shown in Sec. III. Hence the lepton mixing matrix is determined to be given by

$$U = P_l U_l^\dagger \Sigma_\nu O_{3\times 3} \hat{X}_\nu^{-\frac{1}{2}}, \tag{5.7}$$

where P_l is a generic 3×3 permutation matrix since the charged lepton masses cannot be predicted in this approach. One can straightforwardly check that two pairs of subgroups $\{G_l, X_\nu\}$ and $\{G_l', X_\nu'\}$ would yield the same results for the Pontecorvo-Maki-Nakagawa-Sakata (PMNS) mixing matrix [34], if they are related by a similarity transformation Ω,

$$\rho_{\mathbf{3}}(g_l') = \Omega \rho_{\mathbf{3}}(g_l) \Omega^\dagger, \qquad X_\nu' = \Omega X_\nu \Omega^T, \tag{5.8}$$

where g_l and g_l' denote the generator of G_l and G_l', respectively. Moreover generally, we denote the mixing matrices predicted by two generic residual symmetries $\{G_l, X_\nu\}$ and $\{G_l', X_\nu'\}$ as

$$U = P_l U_l^\dagger \Sigma_\nu O_{3\times 3} \hat{X}_\nu^{-\frac{1}{2}}, \quad U' = P_l' U_l'^\dagger \Sigma_\nu' O_{3\times 3}' \hat{X}_\nu'^{-\frac{1}{2}}. \tag{5.9}$$

The condition under which U and U' essentially lead to the same mixing pattern is found to be [34]

$$\Sigma \Sigma^T = Q_L P_L \Sigma' \Sigma'^T P_L^T Q_L, \tag{5.10}$$

where $\Sigma \equiv U_l^\dagger \Sigma_\nu$, $\Sigma' \equiv U_l'^\dagger \Sigma_\nu'$, $P_L \equiv P_l^T P_l'$, and Q_L is a diagonal phase matrix. As stated above, we assume that the concerned $\Delta(6n^2)$ flavor group and CP symmetry are broken to an Abelian subgroup in the charged lepton sector and to a single remnant CP transformation X_ν in the neutrino sector. Thus X_ν has to be a symmetric unitary matrix and it can be

$$X_\nu = \rho_{\mathbf{3}}(c^x d^y), \qquad \rho_{\mathbf{3}}(bc^x d^{-x}), \qquad \rho_{\mathbf{3}}(abc^x d^{2x}),$$
$$\rho_{\mathbf{3}}(a^2 bc^{2x} d^x), \qquad x, y = 0, 1, \ldots, n-1, \tag{5.11}$$

which are related to each other by a similarity transformation as follows:

TABLE V. The unitary transformation U_l for the possible remnant subgroup G_l. Here the notation $\langle g\rangle$ denotes a group generated by the element g. The allowed values of the parameters s and t are $s, t = 0, 1, \ldots, n-1$, and $\omega = e^{2\pi i/3}$ is the cube root of the unit. Note that the identity $(ac^t d^{t-s})^2 = a^2 c^s d^t$ is fulfilled; consequently the unitary matrix U_l for $G_l = \langle a^2 c^s d^t\rangle$ can be obtained from the corresponding one of $G_l = \langle ac^s d^t\rangle$ through the replacement $s \to t$ and $t \to t - s$. The constraints on the parameters s and t are to eliminate the degeneracy among the eigenvalues of the generator of G_l, and they can be completely relaxed by extending G_l to be the direct product of several cyclic groups [62].

G_l	U_l	Constraints
$\langle c^s d^t\rangle$	$\begin{pmatrix} 1 & 0 & 0 \\ 0 & 1 & 0 \\ 0 & 0 & 1 \end{pmatrix}$	$s+t \neq 0 \mod (n)$ $s-2t \neq 0 \mod (n)$ $t-2s \neq 0 \mod (n)$
$\langle bc^s d^t\rangle$	$\frac{1}{\sqrt{2}}\begin{pmatrix} e^{-i\pi\frac{s+t}{2n}} & 0 & e^{-i\pi\frac{s+t}{2n}} \\ 0 & \sqrt{2} & 0 \\ -e^{i\pi\frac{s+t}{2n}} & 0 & e^{i\pi\frac{s+t}{2n}} \end{pmatrix}$	$s-t \neq 0, \frac{n}{3}, \frac{2n}{3} \mod (n)$
$\langle ac^s d^t\rangle$	$\frac{1}{\sqrt{3}}\begin{pmatrix} e^{-2i\pi\frac{s}{n}} & \omega^2 e^{-2i\pi\frac{s}{n}} & \omega e^{-2i\pi\frac{s}{n}} \\ e^{-2i\pi\frac{t}{n}} & \omega e^{-2i\pi\frac{t}{n}} & \omega^2 e^{-2i\pi\frac{t}{n}} \\ 1 & 1 & 1 \end{pmatrix}$	$\cdots$
$\langle a^2 c^s d^t\rangle$	$\frac{1}{\sqrt{3}}\begin{pmatrix} e^{-2i\pi\frac{t}{n}} & \omega^2 e^{-2i\pi\frac{t}{n}} & \omega e^{-2i\pi\frac{t}{n}} \\ e^{2i\pi\frac{s-t}{n}} & \omega e^{2i\pi\frac{s-t}{n}} & \omega^2 e^{2i\pi\frac{s-t}{n}} \\ 1 & 1 & 1 \end{pmatrix}$	$\cdots$
$\langle abc^s d^t\rangle$	$\frac{1}{\sqrt{2}}\begin{pmatrix} e^{i\pi\frac{t-2s}{2n}} & e^{i\pi\frac{t-2s}{2n}} & 0 \\ -e^{-i\pi\frac{t-2s}{2n}} & e^{-i\pi\frac{t-2s}{2n}} & 0 \\ 0 & 0 & \sqrt{2} \end{pmatrix}$	$t \neq 0, \frac{n}{3}, \frac{2n}{3}$
$\langle a^2 bc^s d^t\rangle$	$\frac{1}{\sqrt{2}}\begin{pmatrix} \sqrt{2} & 0 & 0 \\ 0 & e^{i\pi\frac{s-2t}{2n}} & e^{i\pi\frac{s-2t}{2n}} \\ 0 & -e^{-i\pi\frac{s-2t}{2n}} & e^{-i\pi\frac{s-2t}{2n}} \end{pmatrix}$	$s \neq 0, \frac{n}{3}, \frac{2n}{3}$

$$\begin{aligned}\rho_{\mathbf{3}}(b)\rho_{\mathbf{3}}(bc^x d^{-x})\rho_{\mathbf{3}}^T(b) &= \rho_{\mathbf{3}}(bc^x d^{-x}),\\ \rho_{\mathbf{3}}(a^2)\rho_{\mathbf{3}}(bc^x d^{-x})\rho_{\mathbf{3}}^T(a^2) &= \rho_{\mathbf{3}}(abc^x d^{2x}),\\ \rho_{\mathbf{3}}(ad^{2x})\rho_{\mathbf{3}}(bc^x d^{-x})\rho_{\mathbf{3}}^T(ad^{2x}) &= \rho_{\mathbf{3}}(a^2 bc^{2x} d^x).\end{aligned} \tag{5.12}$$

Hence it is sufficient to consider the choices of $X_\nu = \rho_{\mathbf{3}}(c^x d^y)$ and $X_\nu = \rho_{\mathbf{3}}(bc^x d^{-x})$ with $x, y = 0, 1, \ldots, n-1$. The corresponding Takagi factorization matrix can be read out as

$$\begin{aligned} X_\nu &= \rho_{\mathbf{3}}(c^x d^y),\\ \Sigma_\nu &= \mathrm{diag}(e^{\frac{x\pi i}{n}}, e^{\frac{(y-x)\pi i}{n}}, e^{-\frac{y\pi i}{n}}),\end{aligned} \tag{5.13}$$

$$X_\nu = \rho_{\mathbf{3}}(bc^x d^{-x}), \qquad \Sigma_\nu = \begin{pmatrix} 0 & -ie^{\frac{x\pi i}{n}} & e^{\frac{x\pi i}{n}} \\ \sqrt{2}e^{-\frac{2x\pi i}{n}} & 0 & 0 \\ 0 & ie^{\frac{x\pi i}{n}} & e^{\frac{x\pi i}{n}} \end{pmatrix}. \tag{5.14}$$

Furthermore taking into account the following conjugate relations,

$$\begin{aligned} b(abc^s d^t)b^{-1} &= a^2 bc^{-t} d^{-s},\\ \rho_{\mathbf{3}}(b)\rho_{\mathbf{3}}(c^x d^y)\rho_{\mathbf{3}}^T(b) &= \rho_{\mathbf{3}}(c^{-y} d^{-x}),\\ \rho_{\mathbf{3}}(b)\rho_{\mathbf{3}}(bc^x d^{-x})\rho_{\mathbf{3}}^T(b) &= \rho_{\mathbf{3}}(bc^x d^{-x}),\end{aligned} \tag{5.15}$$

we only need to consider eight possible remnant symmetries constituted by $G_l = \langle c^s d^t\rangle$, $\langle bc^s d^t\rangle$, $\langle ac^s d^t\rangle$, $\langle abc^s d^t\rangle$ and $X_\nu = \rho_{\mathbf{3}}(c^x d^y)$, $X_\nu = \rho_{\mathbf{3}}(bc^x d^{-x})$. In this section, we shall investigate the predictions for lepton flavor mixing and matter-antimatter asymmetry via leptogenesis for each possible case. The explicit form of the lepton mixing matrix and the expressions of the mixing parameters and rephasing bilinear invariants are given in Appendix C.

For the first case, the lepton mixing matrix is given by Eq. (C1), and both Dirac and Majorana *CP* violation phases are trivial. The *CP* asymmetries ϵ_α are found to be vanishing; therefore nonzero baryon asymmetry cannot be generated, although the experimental data on lepton mixing angles can be accommodated. Freely varying the parameters $\theta_{1,2,3}$ and requiring the three mixing angles in the experimentally preferred 3σ ranges [4], we find that the effective Majorana neutrino mass m_{ee} takes values in the following intervals,

$$\begin{aligned} \text{NO:}\ & 0.000717\ \text{eV} \leq m_{ee} \leq 0.00219\ \text{eV} \quad \text{and}\\ & 0.00308\ \text{eV} \leq m_{ee} \leq 0.00449\ \text{eV},\\ \text{IO:}\ & 0.0130\ \text{eV} \leq m_{ee} \leq 0.0227\ \text{eV} \quad \text{and}\\ & 0.0471\ \text{eV} \leq m_{ee} \leq 0.0478\ \text{eV}.\end{aligned} \tag{5.16}$$

Here the two different regimes for both NO and IO arise from the *CP* parity matrix $\hat{X}_\nu$. In other words, the *CP* parities of the two massive light neutrinos can be identical or opposite, and accordingly two distinct values of m_{ee} are obtained.

The second kind of residual symmetry gives rise to the lepton mixing pattern of Eq. (C6). Three independent mixing patterns can be obtained from the six row permutations, yet only the mixing matrix $U_{II,3}$ is viable. Equation (C9) indicates that both the Dirac *CP* phase δ and the atmospheric mixing angle θ_{23} are maximal, while the values of θ_{12} and θ_{13} are not constrained for the mixing matrix $U_{II,3}$. The best fitting values $(\sin^2\theta_{13})^{\mathrm{bf}} = 0.0234$ $[(\sin^2\theta_{13})^{\mathrm{bf}} = 0.0240]$ and $(\sin^2\theta_{12})^{\mathrm{bf}} = 0.308$ [4] for NO (IO) can be reproduced for certain values of the

parameters $\theta_{1,2,3}$, as shown in Table VI. Since the lepton mixing angles in Eq. (C9) are invariant under the transformations $(\theta_2,\theta_3)\to(\pi-\theta_2,\theta_3)$, $(\theta_2,\theta_3)\to(\theta_2,\pi-\theta_3)$, and $(\theta_2,\theta_3)\to(\pi-\theta_2,\pi-\theta_3)$, four best fitting values for $\theta_{2,3}$ can be found. Recently T2K and NOνA have reported a slight preference for δ close to $3\pi/2$, while maximal θ_{23} is favored by T2K and disfavored by NOνA [9–13]. T2K and NOνA are expected to be able to exclude maximal θ_{23} at a 90% confidence level after their full period of data taking. These two experiments can also contribute to the measurement of the Dirac phase δ, if running in both the neutrino and the antineutrino modes. They can possibly

TABLE VI. Results of the χ^2 analysis for some representative mixing patterns which arise from the breaking of the $\Delta(6n^2)$ flavor group and CP to an Abelian subgroup in the charged lepton sector and a single remnant CP transformation in the neutrino sector. The χ^2 function has a global minimum $\chi^2_{\rm min}$ at the best fit values $\theta_1^{\rm bf}$, $\theta_2^{\rm bf}$, and $\theta_3^{\rm bf}$ for θ_1, θ_2, and θ_3. We display the values of the mixing angles as well as $|\sin\delta|$ and $|\sin\phi|$ at the given $\theta^{\rm bf}_{1,2,3}$. We also present the value of the effective Majorana neutrino mass m_{ee} at the best fit points $\theta^{\rm bf}_{1,2,3}$. Notice that m_{ee} can take two distinct values due to the CP parity matrix $\hat{X}_\nu$.

	ϱ_i		$\theta_1^{\rm bf}/\pi$	$\theta_2^{\rm bf}/\pi$	$\theta_3^{\rm bf}/\pi$	$\chi^2_{\rm min}$	$\sin^2\theta_{13}$	$\sin^2\theta_{12}$	$\sin^2\theta_{23}$	$\lvert\sin\delta\rvert$	$\lvert\sin\phi\rvert$	m_{ee}/eV
$U_{II,3}$	$\cdots$	NO	$\cdots$	0.049	0.187 0.813	3.645	0.0234	0.308	0.5	1	0	0.00377 or 0.00145
				0.951	0.187 0.813							
		IO	$\cdots$	0.050	0.187 0.813	0.105	0.024					0.0475 or 0.0179
				0.950	0.187 0.813							
$U_{III,1}$	$\varrho_1=\frac{\pi}{6}$	NO	0.322	0.155	0.614 0.977	27.205	0.0295	0.308	0.577	0.985	0.253	0.00162 or 0.00389
			0.678	0.845	0.386 0.023							
		IO	0.340	0.143	0.606 0.968	2.143	0.0251		0.641	0.983	0.789	0.0433 or 0.0263
			0.660	0.857	0.394 0.032							
$U_{III,2}$	$\varrho_1=\frac{\pi}{6}$	NO	0.329	0.150	0.611 0.974	7.674	0.0278	0.308	0.398	0.984	0.829	0.00168 or 0.00381
			0.671	0.850	0.389 0.026							
		IO	0.331	0.149	0.610 0.973	7.281	0.0274		0.393	0.984	0.773	0.0434 or 0.0259
			0.669	0.851	0.390 0.027							
$U_{III,3}$	$\varrho_1=\frac{\pi}{3}$	NO	0.049	0.040	0.306 0.681	0	0.0234	0.308	0.437	0.873	0.852	0.00377 or 0.00145
			0.951	0.960	0.319 0.694							
			0.281	0.437	0.035 0.409							
			0.719	0.563	0.591 0.965							
		IO	0.050	0.028	0.308 0.683		0.024		0.455	0.870	0	0.0475 or 0.0179
			0.950	0.972	0.317 0.692							
			0.334	0.443	0.356 0.981							
			0.666	0.557	0.019 0.644							

(Table continued)

TABLE VI. *(Continued)*

	ϱ_i		$\theta_1^{\rm bf}/\pi$	$\theta_2^{\rm bf}/\pi$	$\theta_3^{\rm bf}/\pi$	$\chi^2_{\rm min}$	$\sin^2\theta_{13}$	$\sin^2\theta_{12}$	$\sin^2\theta_{23}$	$\lvert\sin\delta\rvert$	$\lvert\sin\phi\rvert$	m_{ee}/eV
$U_{V,1}$	$\varrho_3=0,\ \varrho_4=\frac{\pi}{2}$	NO	0.454	0.694	0.028	3.327	0.0233	0.339	0.433	0.931	0.072	0.00210 or 0.00385
			0.468	0.808								
		IO	0.465	0.692	0.021	3.599	0.0238	0.340	0.449	0.961	0	0.0149 or 0.0475
			0.476	0.809								
$U_{V,1}$	$\varrho_3=0,\ \varrho_4=\frac{\pi}{3}$	NO	0.448	0.684	0.017	0	0.0234	0.308	0.437	0.899	0.929	0.00153 or 0.00374
					0.746					0.703	0.848	0.00366 or 0.00173
			0.465	0.798	0.003					0.984	0.892	0.00274 or 0.00298
					0.740					0.097	0.999	0.00259 or 0.00310
		IO	0.463	0.684	0.004		0.024		0.455	0.936	0.826	0.0272 or 0.0428
					0.736					0.623		
			0.475	0.803	0.731					0.191	0.806	0.0267 or 0.0431
					0.995					0.997		
U_{VI}	$\varrho_5=\frac{\pi}{2}$	NO	0.530	0.075	0.487	0.854	0.0235	0.323	0.448	0.894	0.016	0.00355 or 0.00226
				0.925								
		IO	0.508	0.086	0.496	0.349	0.0240	0.317	0.487	0.994	0	0.0170 or 0.0475
				0.914								
$U_{\rm VIII,1}$	$\cdots$	NO	1	0.862	0.106	18.549	0.0244	0.308	0.578	0.667	0.580	0.00228 or 0.00337
					0.894							
			0	0.138	0.106							
					0.894							
		IO	1	0.861	0.106	0.794	0.024		0.579	0.668	0.616	0.0229 or 0.0453
					0.894							
			0	0.139	0.106							
					0.894							
$U_{\rm VIII,2}$	$\cdots$	NO	1	0.861	0.106	0.537	0.0236	0.308	0.420	0.389	0.616	0.00228 or 0.00334
					0.894							
			0	0.139	0.106							
					0.894							
		IO	0	0.138	0.894	1.182	0.0242		0.422	0.667	0.615	0.0229 or 0.0453
					0.106							
			1	0.862	0.894							
					0.106							

exclude certain ranges of δ, especially the values around $\delta=\pm\pi/2$, depending on θ_{23} and the neutrino mass hierarchy. Future long-baseline experiments DUNE [63], T2HK [64], and T2HKK [65] will allow for a measurement of the Dirac phase and atmospheric mixing angle with significantly improved sensitivities and thus can fully test the maximal-maximal predictions. Note that the next-generation neutrino experiments [63,64] are capable of testing the predictions for maximal δ and θ_{23}. Furthermore, we plot the numerical results of the baryon asymmetry Y_B with respect to the free parameter ϑ in Fig. 5, where the parameters $\theta_{1,2,3}$ are set to their best fit values. Obviously the observed matter-antimatter asymmetry in the Universe can be obtained for particular values of ϑ except the cases of NO:R-3rd and IO:R-1st. This conclusion is consistent with the general results of Sec. III. In addition, the allowed regions of the effective Majorana mass m_{ee} are found to be the same as case I, and they are given in Eq. (5.16). The reason is because m_{ee} is independent of θ_{23}, as shown in Eq. (3.22). We also present the value of m_{ee} at the best fitting points $\theta^{\rm bf}_{1,2,3}$ in Table VI.

For case III, three independent lepton mixing patterns can be obtained as shown in Eq. (C16). The predictions of the mixing parameters for mixing matrix $U_{III,1}$ are given in Eq. (C17). The parameter value of $\varrho_1=0$ is always admissible, and the resulting lepton mixing matrix is the same as U_I if the possible shifts in $\theta_{1,2,3}$ are taken into account. Consequently the lepton mixing angles in the experimentally preferred range can be achieved for appropriate choices of the parameters $\theta_{1,2,3}$. However, both Dirac phase δ and Majorana phase ϕ would be determined to be trivial, such that successful leptogenesis cannot be achieved. The smallest value of the index n which is

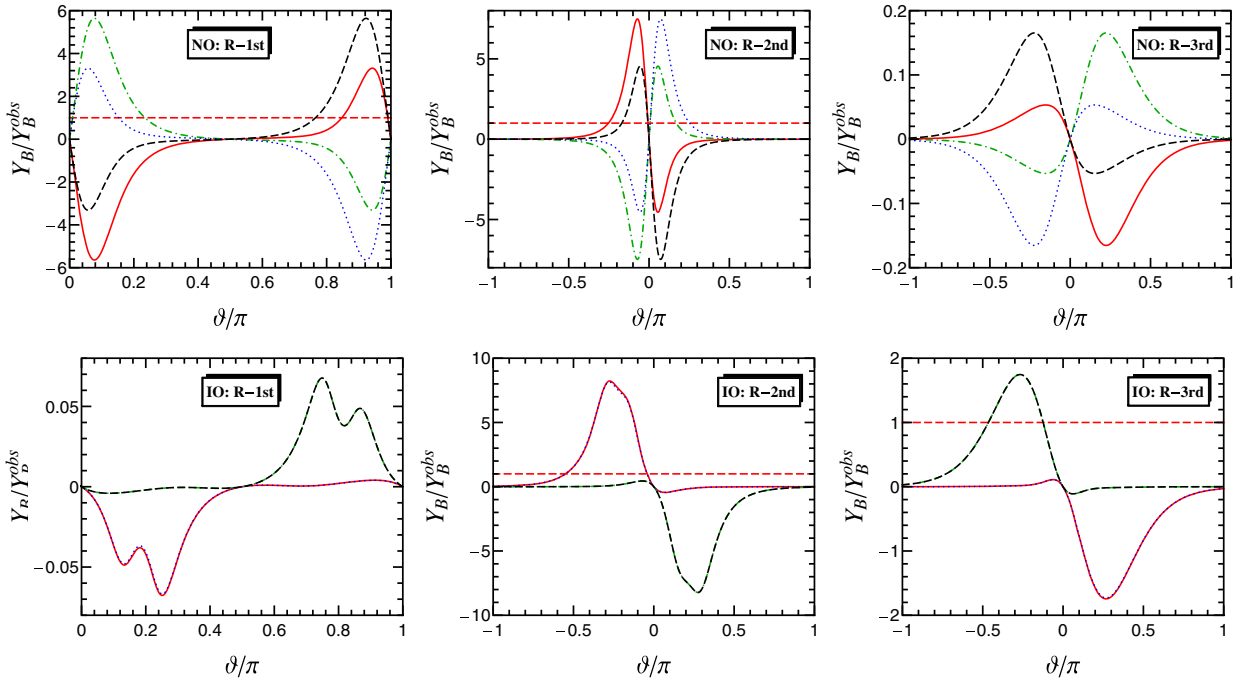

FIG. 5. $Y_B/Y_B^{\rm obs}$ as a function of the parameter ϑ in case II, where we choose the RH neutrino mass $M_1 = 5 \times 10^{11}$ GeV. The red solid, green dashed-dotted, blue dotted, and black dashed lines correspond to the four best fitting points as shown in Table VI. The horizontal red dashed line represents the experimental measured value $Y_B^{\rm obs}$. The neutrino mass spectrum is NO and IO in the first row and the second row, respectively. The panels in the left, middle, and right columns are for the three admissible forms of the R-matrix such as R-1st, R-2nd, and R-3rd, respectively.

capable of accommodating the experimental data and nontrivial CP violating phases is $n = 6$, with $\varrho_1 = \pi/6$ up to the symmetry transformations shown in Eq. (C14). Please see Table VI for the corresponding results of the χ^2 analysis. We notice that the atmospheric mixing angle deviates from maximal mixing with $\sin^2\theta_{23} = 0.577$ (0.641) for NO (IO) at the best fit point where the χ^2 function reaches a global minimum, and the Dirac CP phase is approximately maximal with $|\sin\delta| = 0.985$ (0.983). This result is consistent with the weak evidence of maximal Dirac CP violation reported by T2K [9–11] and NOνA [12,13] and global data fitting [4–8], and it can be tested in forthcoming neutrino oscillation experiments [63–65]. The numerical results of Y_B versus ϑ for $\varrho_1 = \pi/6$ are shown in Fig. 6. We see that the correct value of the baryon asymmetry can be obtained for particular values of ϑ except in the case of R-3rd with the NO spectrum and R-1st with the IO. Moreover, we find that the effective mass m_{ee} varies in the intervals,

$$\begin{aligned} &\text{NO}: \ 0.000723\ \text{eV} \leq m_{ee} \leq 0.00449\ \text{eV}, \\ &\text{IO}: \ 0.0223\ \text{eV} \leq m_{ee} \leq 0.0297\ \text{eV} \quad \text{and} \\ &\qquad 0.0430\ \text{eV} \leq m_{ee} \leq 0.0436\ \text{eV}. \end{aligned} \tag{5.17}$$

The mixing parameters for $U_{III,2}$ are given by Eq. (C19). As shown in Table VI, agreement with the experimental data can be achieved for both $\varrho_1 = 0$ and $\varrho_1 = \pi/6$. The CP asymmetries fulfill $\epsilon_2 = \epsilon_\tau = 0$ in this case; therefore the baryon asymmetry Y_B is predicted to be zero. Regarding the third mixing pattern $U_{III,3}$, the expressions of mixing parameters and the rephase invariants are shown in Eqs. (C21) and (C22), respectively. For the smallest group index $n = 2$, the parameter ϱ_1 can be either 0 or $\pi/2$. We find that the experimental data on lepton mixing angles can be accommodated well for both $\varrho_1 = 0$ and $\varrho_1 = \pi/2$. The mixing pattern $U_{III,3}$ with $\varrho_1 = 0$ is equivalent to U_I in Eq. (C1), the Dirac as well as Majorana CP phases are trivial, and consequently a nonzero baryon asymmetry cannot be generated. The mixing matrix $U_{III,3}$ for $\varrho_1 = \pi/2$ is related to $U_{II,3}$ as follows:

$$U_{III,3}(\varrho_1 = \pi/2, \theta_1, \theta_2, \theta_3) = U_{II,3}(\theta_1', \theta_2', \theta_3'), \tag{5.18}$$

where $\theta_{1,2,3}'$ are defined through $O_{3\times3}(\theta_1', \theta_2', \theta_3') = P_{231} O_{3\times3}(\theta_1, \theta_2, \theta_3)$. Hence $U_{III,3}$ with $\varrho_1 = \pi/2$ and $U_{II,3}$ lead to the same predictions for lepton mixing parameters and Y_B. Furthermore, the new mixing pattern can be obtained from the $\Delta(6 \cdot 3^2) = \Delta(54)$ group for $\varrho_1 = \pi/3$. Note that $\varrho_1 = 2\pi/3$ leads to the same mixing matrix as $\varrho_1 = \pi/3$ after the shift of $\theta_{1,2,3}$ is considered. As shown in Table VI, the best fit values [4] of the three mixing angles can be achieved for certain values of the parameters $\theta_{1,2,3}$. The corresponding predictions for Y_B as a function of

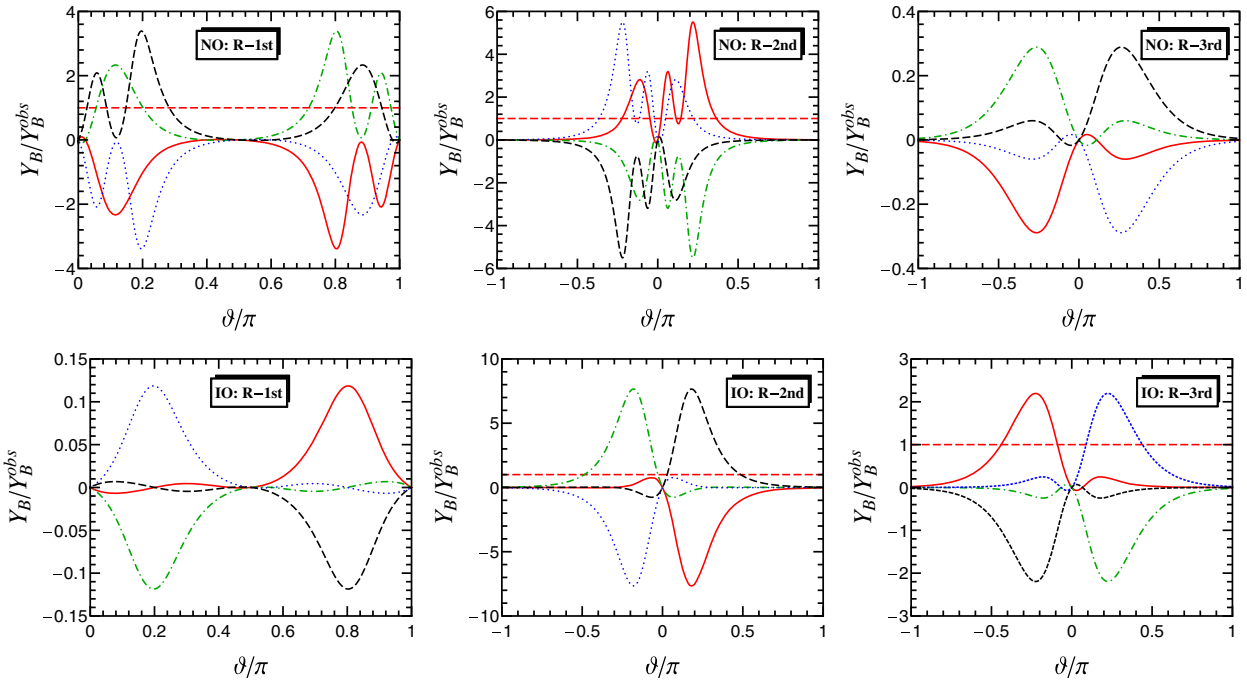

FIG. 6. $Y_B/Y_B^{\rm obs}$ as a function of the parameter ϑ for the mixing pattern $U_{III,1}$ with $\varrho_1 = \pi/6$, where we choose the RH neutrino mass $M_1 = 5 \times 10^{11}$ GeV. The red solid, green dashed-dotted, blue dotted, and black dashed lines correspond to the four best fitting points as shown in Table VI. The horizontal red dashed line represents the experimental measured value $Y_B^{\rm obs}$. The neutrino mass spectrum is NO and IO in the first row and the second row, respectively. The panels in the left, middle, and right columns are for the three admissible forms of the R-matrix such as R-1st, R-2nd, and R-3rd, respectively.

ϑ are plotted in Fig. 7. The observed matter-antimatter asymmetry could be reproduced except for the cases of NO: R-3rd and IO:R-1st. Furthermore, we obtain the effective mass m_{ee} of the $0\nu\beta\beta$ decay is

$$\begin{aligned} &\text{NO:}\ 0.000717\ \text{eV} \leq m_{ee} \leq 0.00219\ \text{eV} \quad \text{and} \\ &\qquad 0.00308\ \text{eV} \leq m_{ee} \leq 0.00449\ \text{eV}, \\ &\text{IO:}\ 0.0130\ \text{eV} \leq m_{ee} \leq 0.0227\ \text{eV} \quad \text{and} \\ &\qquad 0.0471\ \text{eV} \leq m_{ee} \leq 0.0478\ \text{eV}. \end{aligned} \tag{5.19}$$

For case IV, the resulting lepton mixing matrix U_{IV} is equivalent to U_I. Hence we get the same predictions for lepton flavor mixing, $0\nu\beta\beta$ decay, and leptogenesis as those of case I.

Similarly three mixing matrices can be obtained in case V. For the mixing matrix $U_{V,1}$, the results of the mixing parameters are given by Eq. (C32), the *CP* invariants $I^{\alpha}_{\rm NO}$ and $I^{\alpha}_{\rm IO}$ are shown in Eq. (C33). For the smallest $\Delta(6n^2)$ group with $n = 2$, the values of ϱ_3 and ϱ_4 can be 0 and $\pi/2$ in the fundamental interval. Utilizing the equivalence condition of Eq. (5.10), we find two independent mixing patterns with $\varrho_3 = \varrho_4 = 0$ and $\varrho_3 = 0, \varrho_4 = \pi/2$. Moreover, the mixing matrix $U_{V,1}$ for $\varrho_3 = \varrho_4 = 0$ is the same as $U_{II,3}$ if the possible shifts of $\theta_{1,2,3}$ are considered. In the case of $\varrho_3 = 0$ and $\varrho_4 = \pi/2$, the results of the χ^2 analysis are summarized in Table VI, and the predictions for Y_B are plotted in Fig. 8. The effective Majorana neutrino mass m_{ee} is determined to take values in the intervals

$$\begin{aligned} &\text{NO:}\ 0.00143\ \text{eV} \leq m_{ee} \leq 0.00449\ \text{eV}, \\ &\text{IO:}\ 0.0144\ \text{eV} \leq m_{ee} \leq 0.0161\ \text{eV} \quad \text{and} \\ &\qquad 0.0464\ \text{eV} \leq m_{ee} \leq 0.0478\ \text{eV}. \end{aligned} \tag{5.20}$$

For the flavor group $\Delta(6 \cdot 3^2) = \Delta(54)$, the possible values of ϱ_3 and ϱ_4 are 0, $\pi/3$, and $2\pi/3$. We can obtain three phenomenologically viable mixing patterns corresponding to $(\varrho_3, \varrho_4) = (0, 0), (0, \pi/3), (0, 2\pi/3)$. Note that $U_{V,1}$ for $(\varrho_3, \varrho_4) = (0, 2\pi/3)$ is equivalent to the complex conjugate of $U_{V,1}$ with $(\varrho_3, \varrho_4) = (0, \pi/3)$. The best fit values of the three lepton mixing angles can be reproduced for particular values of $\theta_{1,2,3}$ in the case of $(\varrho_3, \varrho_4) = (0, \pi/3)$, the resulting predictions for *CP* violation phases are listed in Table VI, and the variation of Y_B with respect to ϑ is plotted in Fig. 9. In addition, we find that the effective mass m_{ee} is

$$\begin{aligned} &\text{NO:}\ 0.000717\ \text{eV} \leq m_{ee} \leq 0.00449\ \text{eV}, \\ &\text{IO:}\ 0.0264\ \text{eV} \leq m_{ee} \leq 0.0285\ \text{eV} \quad \text{and} \\ &\qquad 0.0399\ \text{eV} \leq m_{ee} \leq 0.0455\ \text{eV}. \end{aligned} \tag{5.21}$$

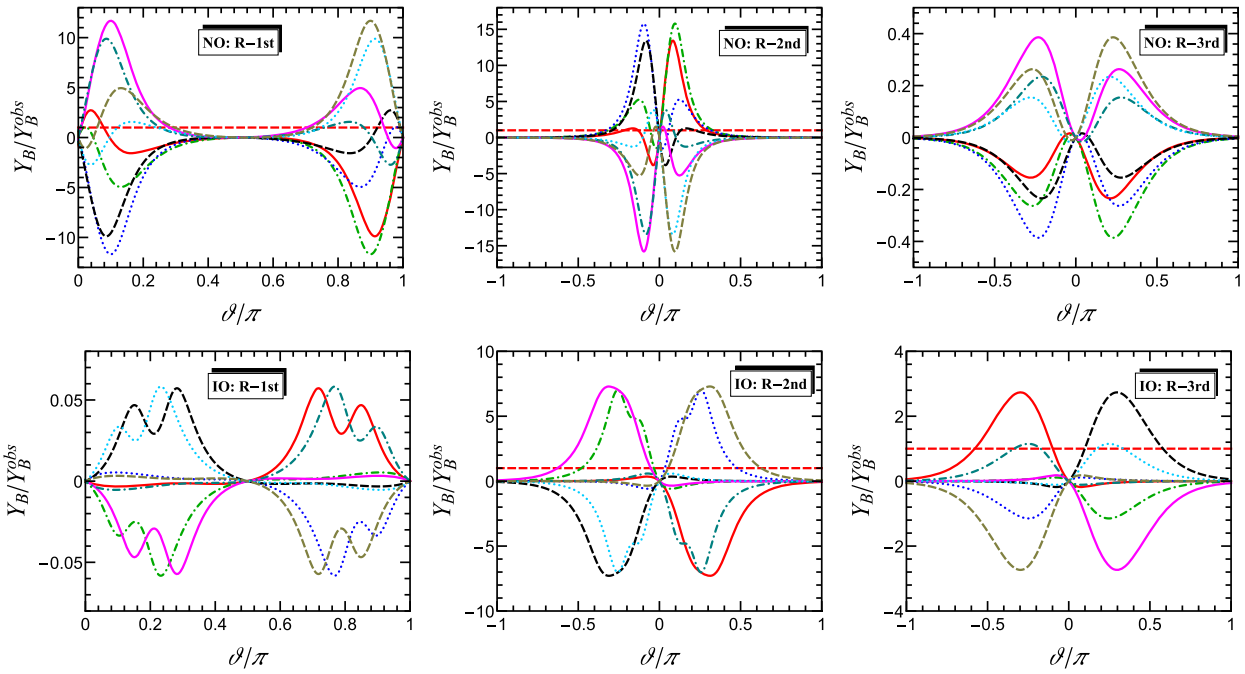

FIG. 7. $Y_B/Y_B^{\rm obs}$ as a function of the parameter ϑ for the mixing pattern $U_{III,3}$ with $\varrho_1 = \pi/3$, where we choose the RH neutrino mass $M_1 = 5 \times 10^{11}$ GeV. The red solid, green dashed-dotted, blue dotted, black dashed, pink solid, cyan dashed-dotted, dark green dotted, and brown dashed lines correspond to the eight best fitting points as shown in Table VI. The horizontal red dashed line represents the experimental measured value $Y_B^{\rm obs}$. The neutrino mass spectrum is NO and IO in the first row and the second row, respectively. The panels in the left, middle, and right columns are for the three admissible forms of the R-matrix such as R-1st, R-2nd, and R-3rd, respectively.

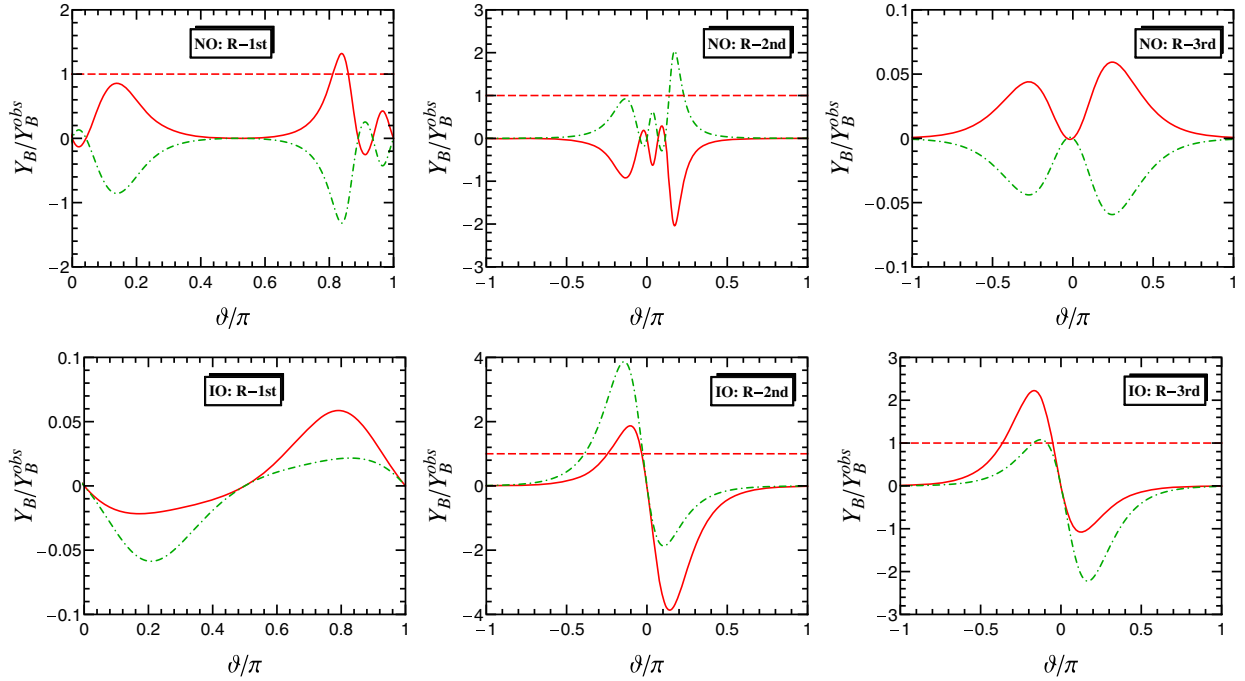

FIG. 8. $Y_B/Y_B^{\rm obs}$ as a function of the parameter ϑ for the mixing pattern $U_{V,1}$ with $\varrho_3 = 0$ and $\varrho_4 = \pi/2$, where we choose the RH neutrino mass $M_1 = 5 \times 10^{11}$ GeV. The red solid and green dashed-dotted lines correspond to the two best fitting points as shown in Table VI. The horizontal red dashed line represents the experimental measured value $Y_B^{\rm obs}$. The neutrino mass spectrum is NO and IO in the first row and the second row, respectively. The panels in the left, middle, and right columns are for the three admissible forms of the R-matrix such as R-1st, R-2nd, and R-3rd, respectively.

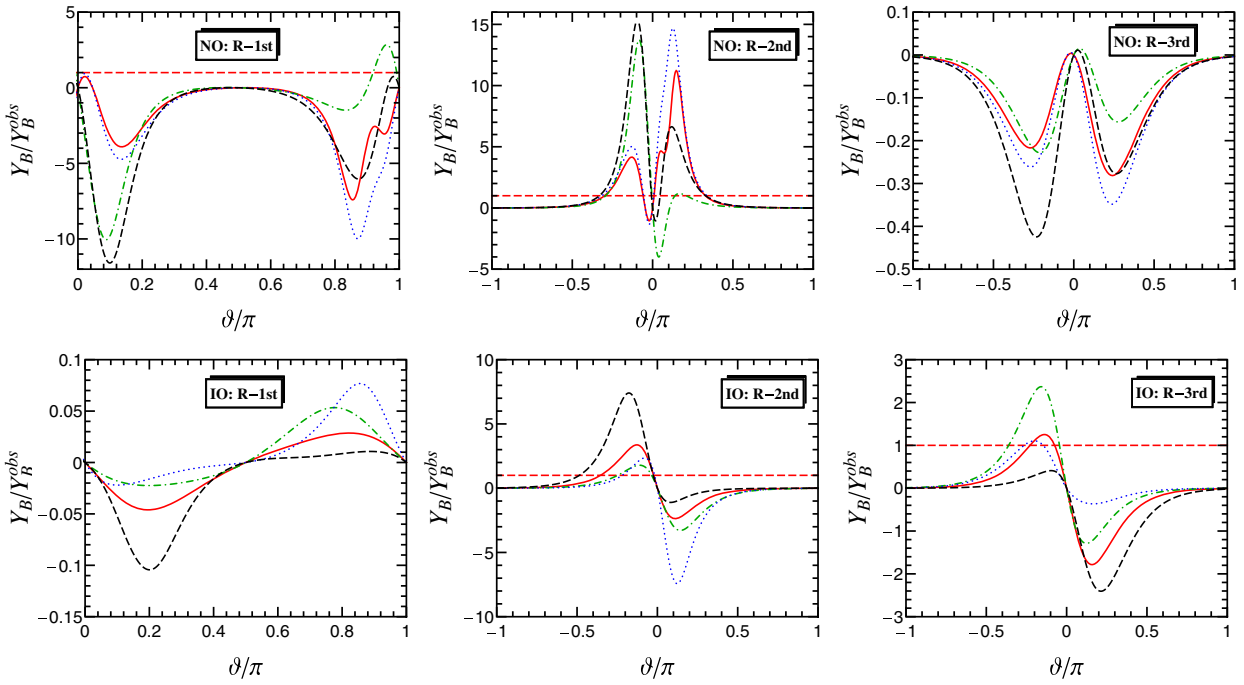

FIG. 9. $Y_B/Y_B^{\rm obs}$ as a function of the parameter ϑ for the mixing pattern $U_{V,1}$ with $\varrho_3 = 0$ and $\varrho_4 = \pi/3$, where we choose the RH neutrino mass $M_1 = 5 \times 10^{11}$ GeV. The red solid, green dashed-dotted, blue dotted, and black dashed lines correspond to the four best fitting points as shown in Table VI. The horizontal red dashed line represents the experimental measured value $Y_B^{\rm obs}$. The neutrino mass spectrum is NO and IO in the first row and the second row, respectively. The panels in the left, middle, and right columns are for the three admissible forms of the R-matrix such as R-1st, R-2nd, and R-3rd, respectively.

The other two mixing matrices $U_{V,2}$ and $U_{V,3}$ cannot accommodate the experimental data on the lepton mixing angles for $n = 2$, and they give rise to the same mixing patterns as $U_{V,1}$ in the case of $n = 3$.

The symmetry breaking pattern in case VI leads to only one independent mixing matrix, which is given in Eq. (C35). The predictions for the mixing parameters and the rephasing invariants are reported in Eqs. (C40) and (C41), respectively. For the $\Delta(6 \cdot 2^2) \cong S_4$ flavor group, the value of ϱ_5 is either 0 or $\pi/2$ in the fundamental region. Notice that U_{VI} for $\varrho_5 = 0$ is equivalent to U_I. Hence the three lepton mixing angles are not subject to any constraint, and the Dirac as well as Majorana *CP* phases are trivial. The results of the χ^2 analysis for $\varrho_5 = \pi/2$ are collected in Table VI. We display the variation of Y_B with respect to ϑ in Fig. 10. The observed baryon asymmetry can be generated for certain values of ϑ except in the case of NO:R-3rd and IO:R-1st. Moreover, we find the effective Majorana neutrino mass m_{ee} is in the intervals

$$\begin{aligned}&\text{NO}: 0.00117\ \text{eV} \leq m_{ee} \leq 0.00449\ \text{eV},\\ &\text{IO}: 0.0144\ \text{eV} \leq m_{ee} \leq 0.0174\ \text{eV} \quad \text{and}\\ &\qquad 0.0458\ \text{eV} \leq m_{ee} \leq 0.0478\ \text{eV}.\end{aligned} \tag{5.22}$$

As shown in Appendix C, case VII leads to the same predictions for lepton mixing, neutrinoless double decay, and matter/antimatter asymmetry via leptogenesis as case III.

At the end of this section, we proceed to discuss the last case, case VIII. After considering all possible row permutations, we can obtain three independent mixing matrices, which are given by Eq. (C46). The mixing parameters and *CP* invariants for the mixing pattern $U_{\rm VIII,1}$ are summarized in Eqs. (C48) and (C49), respectively. Our numerical results for this case are summarized in Table VI, and the variation of Y_B as a function of ϑ is shown in Fig. 11. From the expressions of the *CP* asymmetry ϵ_α and the washout mass $\tilde{m}_\alpha$, we can see that the final baryon asymmetry Y_B has the following symmetry properties:

$$\begin{aligned}&Y_B(\vartheta, \theta_1 = \pi, \theta_2, \theta_3)\\ &\quad = -Y_B(\vartheta, \theta_1 = \pi, \theta_2, \pi - \theta_3)\\ &\quad = Y_B(-\vartheta, \theta_1 = 0, \pi - \theta_2, \theta_3)\\ &\quad = -Y_B(-\vartheta, \theta_1 = 0, \pi - \theta_2, \pi - \theta_3), \quad \text{for NO},\end{aligned} \tag{5.23}$$

$$\begin{aligned}&Y_B(\vartheta, \theta_1 = \pi, \theta_2, \theta_3)\\ &\quad = -Y_B(-\vartheta, \theta_1 = \pi, \theta_2, \pi - \theta_3)\\ &\quad = Y_B(\vartheta, \theta_1 = 0, \pi - \theta_2, \theta_3)\\ &\quad = -Y_B(-\vartheta, \theta_1 = 0, \pi - \theta_2, \pi - \theta_3), \quad \text{for IO}.\end{aligned} \tag{5.24}$$

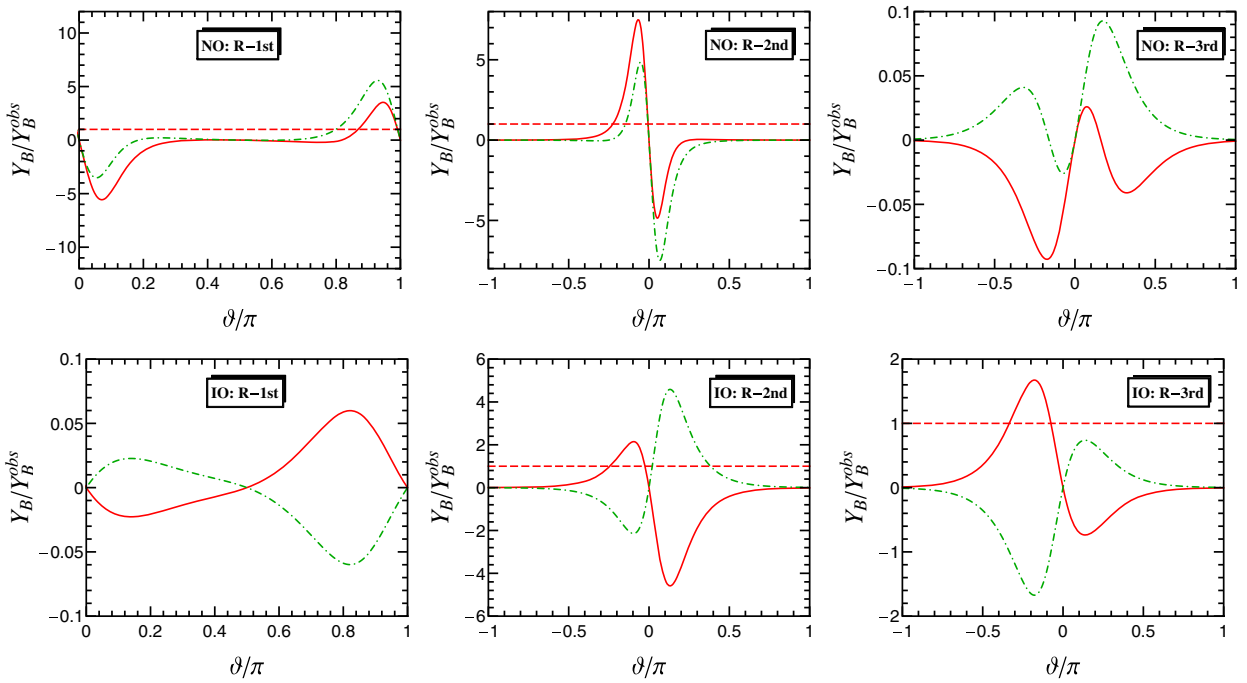

FIG. 10. $Y_B/Y_B^{\rm obs}$ as a function of the parameter ϑ for the mixing pattern U_{VI} with $\varrho_5 = \pi/2$, where we choose the RH neutrino mass $M_1 = 5 \times 10^{11}$ GeV. The red solid and green dashed-dotted lines correspond to the two best fitting points as shown in Table VI. The horizontal red dashed line represents the experimental measured value $Y_B^{\rm obs}$. The neutrino mass spectrum is NO and IO in the first row and the second row, respectively. The panels in the left, middle, and right columns are for the three admissible forms of the R-matrix such as R-1st, R-2nd, and R-3rd, respectively.

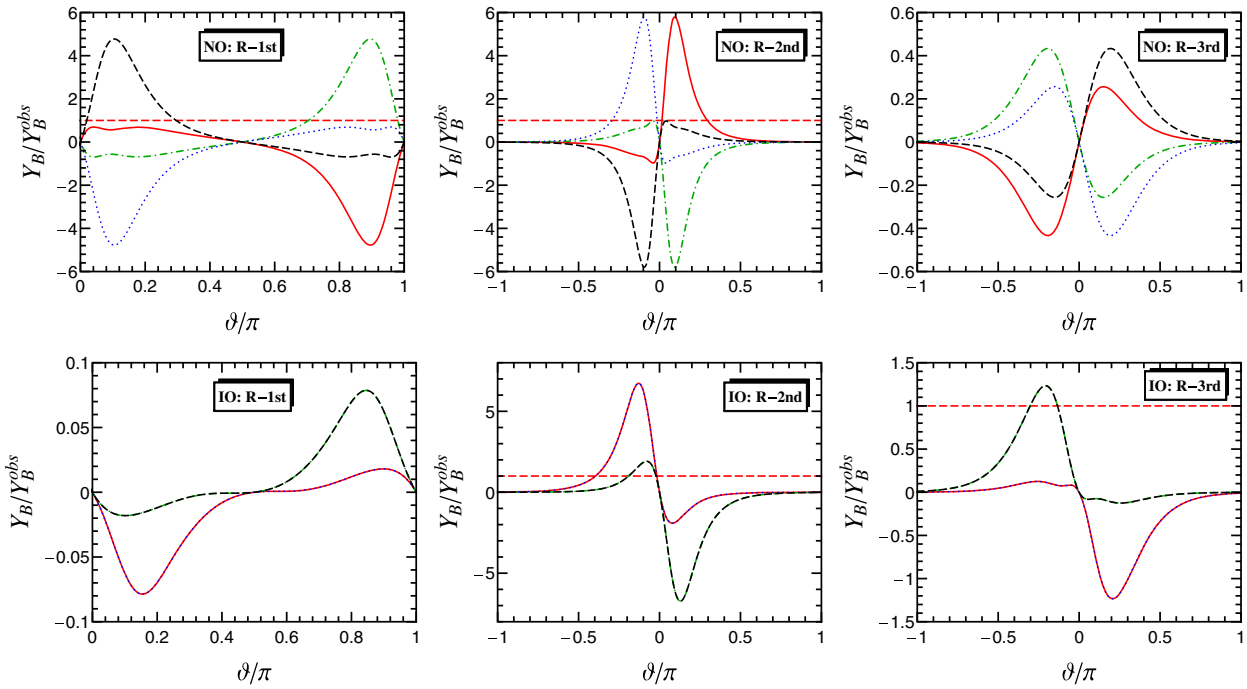

FIG. 11. $Y_B/Y_B^{\rm obs}$ as a function of the parameter ϑ for the mixing pattern $U_{\rm VIII,1}$, where we choose the RH neutrino mass $M_1 = 5 \times 10^{11}$ GeV. The red solid, green dashed-dotted, blue dotted, and black dashed lines correspond to the four best fitting points as shown in Table VI. The horizontal red dashed line represents the experimental measured value $Y_B^{\rm obs}$. The neutrino mass spectrum is NO and IO in the first row and the second row, respectively. The panels in the left, middle, and right columns are for the three admissible forms of the R-matrix such as R-1st, R-2nd, and R-3rd, respectively.

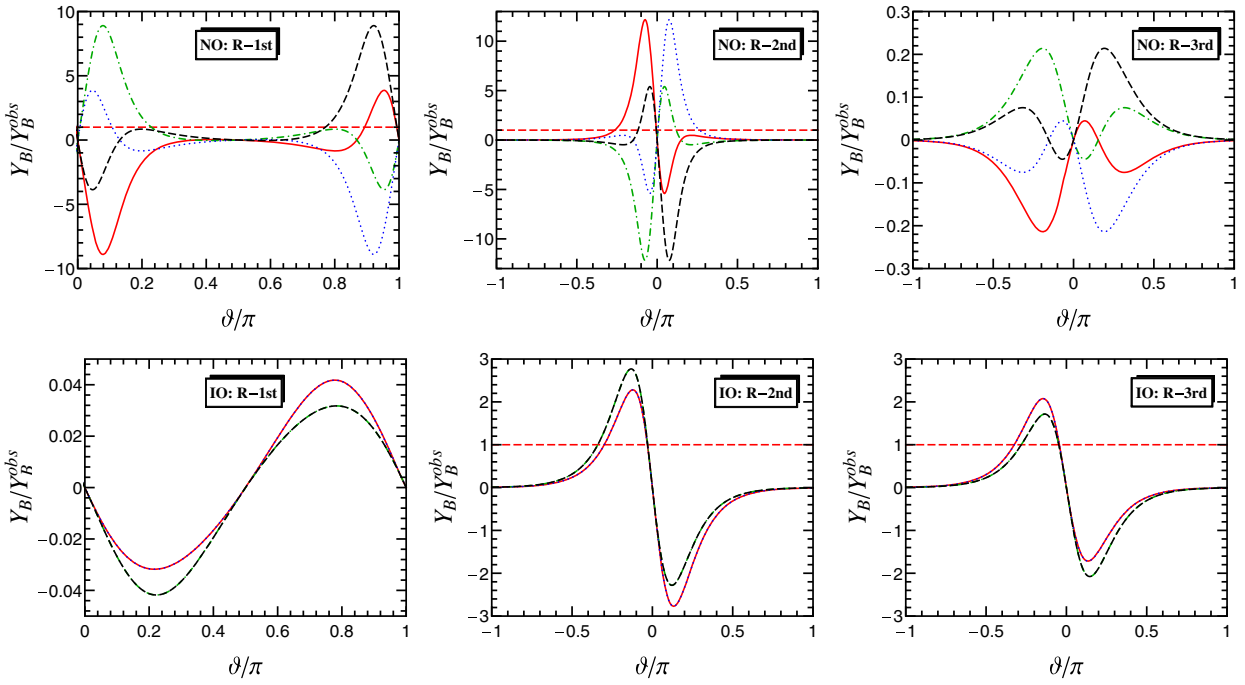

FIG. 12. $Y_B/Y_B^{\rm obs}$ as a function of the parameter ϑ for the mixing pattern $U_{\rm VIII,2}$, where we choose the RH neutrino mass $M_1 = 5 \times 10^{11}$ GeV. The red solid, green dashed-dotted, blue dotted, and black dashed lines correspond to the four best fitting points as shown in Table VI. The horizontal red dashed line represents the experimental measured value $Y_B^{\rm obs}$. The neutrino mass spectrum is NO and IO in the first row and the second row, respectively. The panels in the left, middle, and right columns are for the three admissible forms of the R-matrix such as R-1st, R-2nd, and R-3rd, respectively.

Thus the coincidence of two pairs of curves in the IO case can be easily understood from Eq. (5.24). The second mixing matrix $U_{\rm VIII,2}$ is related to $U_{\rm VIII,1}$ through the exchange of the second and third rows. Therefore they lead to the same reactor and solar mixing angles, while the atmospheric angle changes from θ_{23} to $\pi/2 - \theta_{23}$ and the Dirac phase changes from δ to $\pi + \delta$. The corresponding results of the χ^2 analysis are listed in Table VI, and the predictions for the matter-antimatter asymmetry Y_B are displayed in Fig. 12. $U_{\rm VIII,1}$ and $U_{\rm VIII,2}$ give the same prediction for the effective mass m_{ee} as follows:

$$\begin{aligned} &\text{NO}: \ 0.000717 \text{ eV} \leq m_{ee} \leq 0.00449 \text{ eV}, \\ &\text{IO}: \ 0.0226 \text{ eV} \leq m_{ee} \leq 0.0256 \text{ eV} \quad \text{and} \\ &\qquad 0.0417 \text{ eV} \leq m_{ee} \leq 0.0475 \text{ eV}. \end{aligned} \tag{5.25}$$

Lastly, the third mixing matrix $U_{\rm VIII,3}$ cannot describe the measured values of θ_{13} and θ_{12} simultaneously because of the sum rule shown in Eq. (C52).

The above predicted lepton mixing patterns can be tested in various ways. The upcoming reactor neutrino oscillation experiments such as JUNO [66] will be able to make very precise subpercent measurements of the solar mixing angle θ_{12}. The current experiments T2K and NOνA have the potential to exclude maximal θ_{23} and maximal Dirac phase δ. The next generation of long-baseline experiments DUNE [63], T2HK [64], and T2HKK [65] will be able to place important constraints on the parameters θ_{23} and δ; in particular the sensitivity to the CP phase δ would be improved significantly. In short, future neutrino facilities would be able to improve our knowledge of the mixing parameters in a number of ways. This could allow many of the presented mixing patterns to be excluded. Moreover, forthcoming $0\nu\beta\beta$ experiments are expected to probe the full region of parameter space associated with the IO neutrino mass spectrum. Thus all our models for the IO mass spectrum can be tested independently of oscillation physics.

VI. CONCLUSIONS

The smallness of neutrino masses can be naturally explained by the seesaw mechanism in which two or three RH neutrinos are added in the SM. The 2RHN model can be regarded as the limiting case of the three RH neutrino model in which one of the RH neutrinos is very heavy. The 2RHN model is more predictive than the three RH neutrino model because the number of parameters is greatly reduced. One remarkable feature is that the lightest neutrino is massless in the 2RHN model. Leptogenesis is a natural cosmological consequence of the seesaw mechanism, and it provides a simple explanation for the matter-antimatter asymmetry of the Universe.

Finite discrete flavor symmetry and CP symmetry, which are broken to distinct subgroups in the charged

lepton and neutrino sectors, are a quite powerful approach to explain the lepton mixing angles and CP violation phases. Other phenomena involving CP phases, such as neutrinoless double beta decay and leptogenesis, are also subject to strong constraints in this approach. In the present work, we study the interplay between residual symmetry and leptogenesis in the 2RHN model, and we assume that the scale of flavor symmetry breaking is above the leptogenesis scale. In our method, only the residual symmetry is assumed, and we do not need to consider the possible dynamics which realizes the residual symmetry.

Without loss of generality we work in the basis in which both the charged lepton and RH neutrino mass matrices are diagonal. If two residual CP transformations or a cyclic residual flavor symmetry arising from the original flavor and CP symmetries are preserved by the seesaw Lagrangian, we find that each row of the R-matrix would have only one nonzero entry, which is equal to ± 1. Hence the baryon asymmetry would be zero at leading order. Successful leptogenesis is possible only if the remnant symmetry is appropriately broken by subleading order contributions in concrete models [21].

If a single residual CP transformation is preserved in the neutrino sector, then the lepton mixing matrix contains three real free parameters $\theta_{1,2,3}$ in the range of $[0, \pi)$, the R-matrix is found to depend on only one real parameter ϑ, and it can take three viable forms as summarized in Eq. (3.9). Each entry of the R-matrix is real or purely imaginary in this case; consequently the total CP asymmetry ϵ_1 vanishes unless the nonleading contributions are taken into account in a concrete model. Hence in this paper we discuss the flavored thermal leptogenesis in which the interactions mediated by the τ lepton Yukawa couplings are in equilibrium, and the lightest RH neutrino mass is typically in the interval of $10^9\ \mathrm{GeV} \leq M_1 \leq 10^{12}\ \mathrm{GeV}$. Then the baryon asymmetry is generated uniquely by the CP phases in the PMNS mixing matrix in this scenario. Therefore the observation of low energy leptonic CP violating phases would imply the existence of a baryon asymmetry. Moreover, we have performed a general analysis of leptogenesis in the 2RHN model with a residual CP transformation. For illustration, the numerical results of Y_B for $\delta = 0, -\pi/2$ are presented, as shown in Figs. 1, 2, and 3.

We have performed a comprehensive study in which the single remnant CP transformation originates from the CP symmetry compatible with the $\Delta(6n^2)$ flavor group, which is broken to an Abelian subgroup in the charged lepton sector. All possible residual symmetries and the resulting predictions for lepton flavor mixing and leptogenesis are studied. We find there are in total eight possible cases (from case I to case VIII). Cases I and IV give rise to the same lepton mixing pattern and the same results for leptogenesis. Cases III and VII are also the same after the shift of the free parameters $\theta_{1,2,3}$ is taken into account. The PMNS matrix in cases I and IV is real up to the CP parity of the neutrino states. As a consequence, although the experimental data on mixing angles can be accommodated in these cases, all the leptogenesis CP asymmetries are vanishing and a net baryon asymmetry cannot be generated without corrections. For the remaining cases, the observed matter/antimatter asymmetry could be reproduced except for R-3rd with a NO spectrum and R-1st with an IO spectrum. Moreover, we find that the small $\Delta(6n^2)$ group (e.g., $n = 2$, 3, 4, etc.) can describe the experimentally measured values of the mixing angles for certain choices of the parameter values. Our approach is very general and model independent, and the results of this paper should be helpful to discuss the phenomenology of leptogenesis in a specific 2RHN model based on flavor and CP symmetries.

ACKNOWLEDGMENTS

G.-J. D. acknowledges the support of the National Natural Science Foundation of China under Grant No. 11522546. C.-C. L. is supported by CPSF-CAS Joint Foundation for Excellent Postdoctoral Fellows No. 2017LH0003.

APPENDIX A: BASIS INDEPENDENCE

In this paper, we have worked in the leptogenesis basis in which both the charged lepton mass matrix and the RH neutrino mass matrix are diagonal. However, the conclusions of this paper do not depend on the basis. In a large class of models, the charged lepton mass matrix is diagonal, while the RH neutrino mass matrix is not diagonal. Then the Lagrangian for the lepton masses is written as

$$\mathcal{L}^{\mathrm{mod}} = -y_\alpha \bar{L}_\alpha H l_{\alpha R} - \lambda^{\mathrm{mod}}_{i\alpha} \bar{N}_{iR} \tilde{H}^\dagger L_\alpha - \frac{1}{2} M^{\mathrm{mod}}_{ij} \bar{N}_{iR} N^c_{jR} + \mathrm{H.c.}, \tag{A1}$$

where M^{mod}_{ij} is a complex symmetric 2×2 matrix, and it can be diagonalized by a unitary transformation U_N,

$$U_N^\dagger M^{\mathrm{mod}} U_N^* = \mathrm{diag}(M_1, M_2) \equiv M. \tag{A2}$$

Similar to Sec. III, we consider the scenario that the neutrino sector preserves one CP transformation, i.e.,

$$\nu_L \overset{\mathrm{CP}}{\mapsto} i X_\nu \gamma_0 C \bar{\nu}_L^T, \qquad N_R \overset{\mathrm{CP}}{\mapsto} i X_N \gamma_0 C \bar{N}_R^T, \tag{A3}$$

where the CP transformation matrix X_N is not diagonal for nondiagonal M^{mod}. The invariance of λ^{mod} and M^{mod} under the above residual CP transformation implies

$$X_N^\dagger \lambda^{\mathrm{mod}} X_\nu = (\lambda^{\mathrm{mod}})^*, \qquad X_N^\dagger M^{\mathrm{mod}} X_N^* = (M^{\mathrm{mod}})^*. \tag{A4}$$

Inserting Eq. (A2) into Eq. (A4) we obtain

$$U_N^T X_N^\dagger U_N = \mathrm{diag}(\pm 1, \pm 1) \equiv \hat{X}_N. \tag{A5}$$

In the leptogenesis basis, the neutrino Yukawa coupling λ takes the form

$$\lambda = U_N^{\dagger}\lambda^{\rm mod}. \tag{A6}$$

From Eqs. (A4)–(A6) we can check that λ and M are subject to the following constraint,

$$\hat{X}_N^{\dagger}\lambda X_\nu = \lambda^*, \qquad \hat{X}_N^{\dagger} M \hat{X}_N^{*} = M^*, \tag{A7}$$

which exactly coincides with Eq. (3.2). Therefore the same predictions for leptogenesis are obtained as in Sec. III, and the results do not change with the working basis.

APPENDIX B: GENERAL RESULTS OF ϵ_α AND $\tilde{m}_\alpha$

In this Appendix we shall present the explicit expressions of the *CP* asymmetry parameter ϵ_α and the washout mass $\tilde{m}_\alpha$ for the three viable forms of the R-matrix shown in Eq. (3.9). Here we shall perform a general analysis, and the lepton mixing matrix is parametrized in the standard convention of Eq. (3.20).

(i) R-1st

In this case, the *CP* asymmetry parameter ϵ_α for the NO case is given by

$$\begin{aligned}
\epsilon_e &= \frac{3M_1}{16\pi v^2} W_{\rm NO} s_{12} c_{13} s_{13} \sin\left(\delta + \frac{\phi}{2}\right), \\
\epsilon_\mu &= -\frac{3M_1}{16\pi v^2} W_{\rm NO} c_{13} s_{23} \left[s_{12} s_{13} s_{23} \sin\left(\delta + \frac{\phi}{2}\right) - c_{12} c_{23} \sin\frac{\phi}{2} \right], \\
\epsilon_\tau &= -\frac{3M_1}{16\pi v^2} W_{\rm NO} c_{13} c_{23} \left[s_{12} s_{13} c_{23} \sin\left(\delta + \frac{\phi}{2}\right) + c_{12} s_{23} \sin\frac{\phi}{2} \right],
\end{aligned} \tag{B1}$$

where the expression of $W_{\rm NO}$ has been listed in Table II. It is easy to check that the identity $\epsilon_e + \epsilon_\mu + \epsilon_\tau = 0$ is fulfilled. Notice that the *CP* asymmetry ϵ_α is closely related to the lower energy *CP* phases. If both the Dirac phase δ and the Majorana phase ϕ are trivially zero, all the asymmetry parameters ϵ_e, ϵ_μ, and ϵ_τ would be vanishing such that a nonzero baryon asymmetry cannot be generated. The washout mass $\tilde{m}_\alpha$ for NO takes the form

$$\begin{aligned}
\tilde{m}_e &= \left| \sqrt{m_2} s_{12} c_{13} e^{\frac{i\phi}{2}} \cos\vartheta + \xi \sqrt{m_3} s_{13} e^{-i\delta} \sin\vartheta \right|^2, \\
\tilde{m}_\mu &= \left| \sqrt{m_2} (c_{12} c_{23} - s_{12} s_{13} s_{23} e^{i\delta}) e^{\frac{i\phi}{2}} \cos\vartheta + \xi \sqrt{m_3} c_{13} s_{23} \sin\vartheta \right|^2, \\
\tilde{m}_\tau &= \left| \sqrt{m_2} (c_{12} s_{23} + s_{12} s_{13} c_{23} e^{i\delta}) e^{\frac{i\phi}{2}} \cos\vartheta - \xi \sqrt{m_3} c_{13} c_{23} \sin\vartheta \right|^2.
\end{aligned} \tag{B2}$$

In the same manner, we find that ϵ_α for the IO spectrum is

$$\begin{aligned}
\epsilon_e &= -\frac{3M_1}{16\pi v^2} W_{\rm IO} c_{12} s_{12} c_{13}^2 \sin\frac{\phi}{2}, \\
\epsilon_\mu &= \frac{-3M_1}{16\pi v^2} W_{\rm IO} \left[s_{13} c_{23} s_{23} \left(c_{12}^2 \sin\left(\delta - \frac{\phi}{2}\right) + s_{12}^2 \sin\left(\delta + \frac{\phi}{2}\right) \right) - c_{12} s_{12} (c_{23}^2 - s_{13}^2 s_{23}^2) \sin\frac{\phi}{2} \right], \\
\epsilon_\tau &= \frac{3M_1}{16\pi v^2} W_{\rm IO} \left[s_{13} c_{23} s_{23} \left(c_{12}^2 \sin\left(\delta - \frac{\phi}{2}\right) + s_{12}^2 \sin\left(\delta + \frac{\phi}{2}\right) \right) + c_{12} s_{12} (s_{23}^2 - s_{13}^2 c_{23}^2) \sin\frac{\phi}{2} \right]
\end{aligned} \tag{B3}$$

and for the washout mass $\tilde{m}_\alpha$ we get

$$\begin{aligned}
\tilde{m}_e &= c_{13}^2 \left| \sqrt{m_1} c_{12} \cos\vartheta + \xi \sqrt{m_2} s_{12} e^{\frac{i\phi}{2}} \sin\vartheta \right|^2, \\
\tilde{m}_\mu &= \left| \sqrt{m_1} (s_{12} c_{23} + c_{12} s_{13} s_{23} e^{i\delta}) \cos\vartheta - \xi \sqrt{m_2} (c_{12} c_{23} - s_{12} s_{13} s_{23} e^{i\delta}) e^{\frac{i\phi}{2}} \sin\vartheta \right|^2, \\
\tilde{m}_\tau &= \left| \sqrt{m_1} (s_{12} s_{23} - c_{12} s_{13} c_{23} e^{i\delta}) \cos\vartheta - \xi \sqrt{m_2} (c_{12} s_{23} + s_{12} s_{13} c_{23} e^{i\delta}) e^{\frac{i\phi}{2}} \sin\vartheta \right|^2.
\end{aligned} \tag{B4}$$

We see that both ϵ_α and $\tilde{m}_\alpha$ depend on the *CP* violating phases δ, ϕ and the free parameter ϑ.

(ii) R-2nd

In this case, ϵ_α for NO is found to be

$$\begin{aligned}
\epsilon_e &= -\frac{3M_1}{16\pi v^2} W_{\rm NO} s_{12} c_{13} s_{13} \cos\left(\delta + \frac{\phi}{2}\right), \\
\epsilon_\mu &= -\frac{3M_1}{16\pi v^2} W_{\rm NO} c_{13} s_{23} \left[c_{12} c_{23} \cos\frac{\phi}{2} - s_{12} s_{13} s_{23} \cos\left(\delta + \frac{\phi}{2}\right)\right], \\
\epsilon_\tau &= \frac{3M_1}{16\pi v^2} W_{\rm NO} c_{13} c_{23} \left[c_{12} s_{23} \cos\frac{\phi}{2} + s_{12} s_{13} c_{23} \cos\left(\delta + \frac{\phi}{2}\right)\right].
\end{aligned} \tag{B5}$$

The washout mass $\tilde{m}_\alpha$ is of the following form:

$$\begin{aligned}
\tilde{m}_e &= |\sqrt{m_2} s_{12} c_{13} e^{\frac{i\phi}{2}} \cosh\vartheta - i\xi\sqrt{m_3} s_{13} e^{-i\delta} \sinh\vartheta|^2, \\
\tilde{m}_\mu &= |\sqrt{m_2}(c_{12} c_{23} - s_{12} s_{13} s_{23} e^{i\delta}) e^{\frac{i\phi}{2}} \cosh\vartheta - i\xi\sqrt{m_3} c_{13} s_{23} \sinh\vartheta|^2, \\
\tilde{m}_\tau &= |\sqrt{m_2}(c_{12} s_{23} + s_{12} s_{13} c_{23} e^{i\delta}) e^{\frac{i\phi}{2}} \cosh\vartheta + i\xi\sqrt{m_3} c_{13} c_{23} \sinh\vartheta|^2.
\end{aligned} \tag{B6}$$

Similarly for the IO mass spectrum, we have

$$\begin{aligned}
\epsilon_e &= -\frac{3M_1}{16\pi v^2} W_{\rm IO} c_{12} s_{12} c_{13}^2 \cos\frac{\phi}{2}, \\
\epsilon_\mu &= \frac{3M_1}{16\pi v^2} W_{\rm IO} \left[s_{13} c_{23} s_{23} \left(c_{12}^2 \cos\left(\delta - \frac{\phi}{2}\right) - s_{12}^2 \cos\left(\delta + \frac{\phi}{2}\right)\right) + c_{12} s_{12} (c_{23}^2 - s_{13}^2 s_{23}^2) \cos\frac{\phi}{2}\right], \\
\epsilon_\tau &= -\frac{3M_1}{16\pi v^2} W_{\rm IO} \left[s_{13} c_{23} s_{23} \left(c_{12}^2 \cos\left(\delta - \frac{\phi}{2}\right) - s_{12}^2 \cos\left(\delta + \frac{\phi}{2}\right)\right) + c_{12} s_{12} (s_{13}^2 c_{23}^2 - s_{23}^2) \cos\frac{\phi}{2}\right].
\end{aligned} \tag{B7}$$

and

$$\begin{aligned}
\tilde{m}_e &= c_{13}^2 |\sqrt{m_1} c_{12} \cosh\vartheta - i\xi\sqrt{m_2} s_{12} e^{\frac{i\phi}{2}} \sinh\vartheta|^2, \\
\tilde{m}_\mu &= |\sqrt{m_1}(s_{12} c_{23} + c_{12} s_{13} s_{23} e^{i\delta}) \cosh\vartheta + i\xi\sqrt{m_2}(c_{12} c_{23} - s_{12} s_{13} s_{23} e^{i\delta}) e^{\frac{i\phi}{2}} \sinh\vartheta|^2, \\
\tilde{m}_\tau &= |\sqrt{m_1}(s_{12} s_{23} - c_{12} s_{13} c_{23} e^{i\delta}) \cosh\vartheta + i\xi\sqrt{m_2}(c_{12} s_{23} + s_{12} s_{13} c_{23} e^{i\delta}) e^{\frac{i\phi}{2}} \sinh\vartheta|^2.
\end{aligned} \tag{B8}$$

(iii) R-3rd

In the case of NO, we find that the flavored CP asymmetry ϵ_α is

$$\begin{aligned}
\epsilon_e &= \frac{3M_1}{16\pi v^2} W_{\rm NO} s_{12} c_{13} s_{13} \cos\left(\delta + \frac{\phi}{2}\right), \\
\epsilon_\mu &= \frac{3M_1}{16\pi v^2} W_{\rm NO} c_{13} s_{23} \left[c_{12} c_{23} \cos\frac{\phi}{2} - s_{12} s_{13} s_{23} \cos\left(\delta + \frac{\phi}{2}\right)\right], \\
\epsilon_\tau &= -\frac{3M_1}{16\pi v^2} W_{\rm NO} c_{13} c_{23} \left[c_{12} s_{23} \cos\frac{\phi}{2} + s_{12} s_{13} c_{23} \cos\left(\delta + \frac{\phi}{2}\right)\right].
\end{aligned} \tag{B9}$$

It is easy to check that the equality $\epsilon_2 \equiv \epsilon_e + \epsilon_\mu = -\epsilon_\tau$ is satisfied. The washout mass $\tilde{m}_\alpha$ takes the form

$$\begin{aligned}
\tilde{m}_e &= |i\sqrt{m_2} s_{12} c_{13} e^{\frac{i\phi}{2}} \sinh\vartheta + \xi\sqrt{m_3} s_{13} e^{-i\delta} \cosh\vartheta|^2, \\
\tilde{m}_\mu &= |i\sqrt{m_2}(c_{12} c_{23} - s_{12} s_{13} s_{23} e^{i\delta}) e^{\frac{i\phi}{2}} \sinh\vartheta + \xi\sqrt{m_3} c_{13} s_{23} \cosh\vartheta|^2, \\
\tilde{m}_\tau &= |i\sqrt{m_2}(c_{12} s_{23} + s_{12} s_{13} c_{23} e^{i\delta}) e^{\frac{i\phi}{2}} \sinh\vartheta - \xi\sqrt{m_3} c_{13} c_{23} \cosh\vartheta|^2.
\end{aligned} \tag{B10}$$

For the IO case, we can read out ϵ_α as

$$\begin{aligned}
\epsilon_e &= \frac{3M_1}{16\pi v^2} W_{\rm IO} c_{12}s_{12}c_{13}^2 \cos\frac{\phi}{2}, \\
\epsilon_\mu &= \frac{-3M_1}{16\pi v^2} W_{\rm IO}\left(s_{13}c_{23}s_{23}\left(c_{12}^2\cos\left(\delta-\frac{\phi}{2}\right)-s_{12}^2\cos\left(\delta+\frac{\phi}{2}\right)\right)+c_{12}s_{12}(c_{23}^2-s_{13}^2s_{23}^2)\cos\frac{\phi}{2}\right), \\
\epsilon_\tau &= \frac{3M_1}{16\pi v^2} W_{\rm IO}\left(s_{13}c_{23}s_{23}\left(c_{12}^2\cos\left(\delta-\frac{\phi}{2}\right)-s_{12}^2\cos\left(\delta+\frac{\phi}{2}\right)\right)-c_{12}s_{12}(s_{23}^2-s_{13}^2c_{23}^2)\cos\frac{\phi}{2}\right).
\end{aligned} \tag{B11}$$

Furthermore the washout mass $\tilde{m}_\alpha$ for IO turns out to be

$$\begin{aligned}
\tilde{m}_e &= c_{13}^2\left|i\sqrt{m_1}c_{12}\sinh\vartheta+\xi\sqrt{m_2}s_{12}e^{\frac{i\phi}{2}}\cosh\vartheta\right|^2, \\
\tilde{m}_\mu &= \left|i\sqrt{m_1}(s_{12}c_{23}+c_{12}s_{13}s_{23}e^{i\delta})\sinh\vartheta-\xi\sqrt{m_2}(c_{12}c_{23}-s_{12}s_{13}s_{23}e^{i\delta})e^{\frac{i\phi}{2}}\cosh\vartheta\right|^2, \\
\tilde{m}_\tau &= \left|i\sqrt{m_1}(s_{12}s_{23}-c_{12}s_{13}c_{23}e^{i\delta})\sinh\vartheta-\xi\sqrt{m_2}(c_{12}s_{23}+s_{12}s_{13}c_{23}e^{i\delta})e^{\frac{i\phi}{2}}\cosh\vartheta\right|^2.
\end{aligned} \tag{B12}$$

APPENDIX C: LEPTON MIXING PATTERNS AND LEPTOGENESIS FROM $\Delta(6n^2)$ AND *CP*

As shown in Sec. V, it is sufficient to consider only eight possible residual symmetries in the scenario that the discrete flavor group $\Delta(6n^2)$ and *CP* symmetry are broken down to an Abelian subgroup G_l in the charged lepton sector and to a single remnant *CP* transformation X_ν in the neutrino sector. In the following, we shall investigate the predictions for lepton flavor mixing and matter-antimatter asymmetry via leptogenesis in each possible case.

(I) $G_l = \langle c^s d^t\rangle$, $X_\nu = \rho_{\mathbf{3}}(c^x d^y)$

From Table V and Eq. (5.13) we find that the lepton mixing matrix is given by

$$U_I = P_l O_{3\times3}(\theta_1,\theta_2,\theta_3)\hat{X}_\nu^{-\frac{1}{2}}. \tag{C1}$$

The permutation matrix P_l can be absorbed into the orthogonal matrix $O_{3\times3}$; hence we can choose $P_l = P_{123} = 1_{3\times3}$ without loss of generality. Thus the three lepton mixing angles read

$$\sin^2\theta_{12}=\sin^2\theta_3,\quad \sin^2\theta_{13}=\sin^2\theta_2,\quad \sin^2\theta_{23}=\sin^2\theta_1 \tag{C2}$$

and the Jarlskog invariant J_{CP} is vanishing,

$$J_{CP}=0, \tag{C3}$$

where J_{CP} is defined as [67]

$$\begin{aligned}
J_{CP} &= \Im(U_{11}U_{33}U_{13}^*U_{31}^*) \\
&= \frac{1}{8}\sin2\theta_{12}\sin2\theta_{13}\sin2\theta_{23}\cos\theta_{13}\sin\delta.
\end{aligned} \tag{C4}$$

Consequently the Dirac *CP* phase δ is either 0 or π. Moreover, we can easily check that both the rephase invariants $I_{\rm NO}^\alpha$, $I_{\rm IO}^\alpha$ and the *CP* asymmetry ϵ_α in leptogenesis are vanishing as well:

$$I_{\rm NO}^\alpha = I_{\rm IO}^\alpha = \epsilon_\alpha = 0. \tag{C5}$$

Therefore a net baryon asymmetry cannot be generated in this case, and moderate subleading corrections are necessary in order to make the leptogenesis viable.

(II) $G_l = \langle c^s d^t\rangle$, $X_\nu = \rho_{\mathbf{3}}(bc^x d^{-x})$

In this case, the PMNS mixing matrix is determined to be of the form

$$\begin{aligned}
U_{II} &= \frac{1}{\sqrt{2}}\begin{pmatrix}0 & -i & 1\\ \sqrt{2} & 0 & 0\\ 0 & i & 1\end{pmatrix} O_{3\times3}(\theta_1,\theta_2,\theta_3)\hat{X}_\nu^{-\frac{1}{2}} \\
&= \mathrm{diag}(e^{-i\theta_1},1,e^{i\theta_1})\frac{1}{\sqrt{2}}\begin{pmatrix}0 & -i & 1\\ \sqrt{2} & 0 & 0\\ 0 & i & 1\end{pmatrix} \\
&\quad\times O_{3\times3}(0,\theta_2,\theta_3)\hat{X}_\nu^{-\frac{1}{2}}
\end{aligned} \tag{C6}$$

up to possible permutations of rows. The diagonal phase matrix $\mathrm{diag}(e^{-i\theta_1},1,e^{i\theta_1})$ can be absorbed into the charged lepton fields. Moreover, it is easy to check that the following identity is fulfilled:

$$\begin{aligned}
&P_{321}U_{II}(\theta_1,\theta_2,\theta_3) \\
&\quad = U_{II}(-\theta_1,\theta_2,-\theta_3)\mathrm{diag}(1,-1,1).
\end{aligned} \tag{C7}$$

Consequently the six possible row permutations lead to three independent mixing patterns,

$$U_{II,1}=U_{II},\quad U_{II,2}=P_{132}U_{II},\quad U_{II,3}=P_{213}U_{II}. \tag{C8}$$

We find that $U_{II,1}$ and $U_{II,2}$ predict $\tan\theta_{13}=\cos\theta_{23}$ and $\tan\theta_{13}=\sin\theta_{23}$, respectively, such that the experimental data [4] of the mixing angles θ_{13} and θ_{23} cannot be accommodated simultaneously. For the mixing matrix $U_{II,3}$, the lepton mixing parameters are given by

$$\sin^2\theta_{13}=\sin^2\theta_2,\quad \sin^2\theta_{12}=\sin^2\theta_3,\quad \sin^2\theta_{23}=\frac{1}{2},$$
$$J_{CP}=\frac{1}{8}\cos\theta_2\sin 2\theta_2\sin 2\theta_3,\quad |\sin\delta|=1. \tag{C9}$$

Furthermore, we find that the rephasing bilinear invariants take the form

$$I^e_{\rm NO}=0,\qquad I^\mu_{\rm NO}=-I^\tau_{\rm NO}=\frac{1}{2}\cos\theta_2\cos\theta_3,$$
$$I^e_{\rm IO}=0,\qquad I^\mu_{\rm IO}=-I^\tau_{\rm IO}=\frac{1}{2}\sin\theta_2. \tag{C10}$$

Hence only the muon and tau flavored asymmetries in heavy neutrino decay contribute to the leptogenesis.

(III) $G_l=\langle bc^s d^t\rangle$, $X_\nu=\rho_{\mathbf{3}}(c^x d^y)$

Using Table V and Eq. (5.13), we find that the lepton mixing matrix up to possible permutations of rows is fixed to be

$$U_{III}=\frac{1}{\sqrt{2}}\begin{pmatrix}1&0&-e^{i\varrho_1}\\0&\sqrt{2}&0\\1&0&e^{i\varrho_1}\end{pmatrix}O_{3\times3}(\theta_1,\theta_2,\theta_3)\hat{X}_\nu^{-\frac{1}{2}}, \tag{C11}$$

with

$$\varrho_1=-\frac{(s+t+x+y)}{n}\pi, \tag{C12}$$

which can take the following values:

$$\varrho_1(\mathrm{mod}\ 2\pi)=0,\frac{1}{n}\pi,\frac{2}{n}\pi,\ldots,\frac{2n-1}{n}\pi. \tag{C13}$$

We can easily check that the mixing matrix U_{III} has the properties

$$U_{III}(\varrho_1+\pi,\theta_1,\theta_2,\theta_3)=U_{III}(\varrho_1,-\theta_1,-\theta_2,\theta_3)\mathrm{diag}(1,1,-1),$$
$$U_{III}(\pi-\varrho_1,\theta_1,\theta_2,\theta_3)=\mathrm{diag}(-e^{-i\varrho_1},1,e^{-i\varrho_1})U_{III}(\varrho_1,\theta_1',\theta_2',\theta_3')\mathrm{diag}(1,1,-1), \tag{C14}$$

where the parameters $\theta'_{1,2,3}$ fulfill $O_{3\times3}(\theta_1',\theta_2',\theta_3')=P_{321}O_{3\times3}(-\theta_1,-\theta_2,\theta_3)$. As a consequence, the fundamental interval of the parameter ϱ_1 can be chosen to be $0\le\varrho_1\le\frac{\pi}{2}$. The mixing pattern arising from the multiplication of the permutation matrix P_{321} from the left-hand side is related to U_{III} through shifts of the continuous parameters $\theta_{1,2,3}$ and redefining $\hat{X}_\nu$ as follows:

$$P_{321}U_{III}(\varrho_1,\theta_1,\theta_2,\theta_3)=U_{III}(\varrho_1,-\theta_1,-\theta_2,\theta_3)\mathrm{diag}(1,1,-1). \tag{C15}$$

Hence three mixing patterns are obtained after all six row permutations are considered:

$$U_{III,1}=U_{III},\qquad U_{III,2}=P_{132}U_{III},\qquad U_{III,3}=P_{213}U_{III}. \tag{C16}$$

For the mixing matrix $U_{III,1}$, we can extract the mixing parameters in the usual way and find

$$\sin^2\theta_{13}=\frac{1}{2}(\sin^2\theta_2+\cos^2\theta_1\cos^2\theta_2-\cos\theta_1\sin 2\theta_2\cos\varrho_1),$$
$$\sin^2\theta_{12}=\sin^2\theta_3+\frac{\sin 2\theta_3(2\sin\theta_1\cos\theta_2\cos\varrho_1+\sin 2\theta_1\sin\theta_2)+2\sin^2\theta_1\cos 2\theta_3}{2-\sin^2\theta_2-\cos^2\theta_1\cos^2\theta_2+\cos\theta_1\sin 2\theta_2\cos\varrho_1},$$
$$\sin^2\theta_{23}=\frac{2\sin^2\theta_1\cos^2\theta_2}{2-\sin^2\theta_2-\cos^2\theta_1\cos^2\theta_2+\cos\theta_1\sin 2\theta_2\cos\varrho_1},$$
$$J_{CP}=\frac{1}{16}\sin\theta_1\cos\theta_2\sin\varrho_1[4\sin 2\theta_1\sin\theta_2\cos 2\theta_3+(1+3\cos 2\theta_1+2\sin^2\theta_1\cos 2\theta_2)\sin 2\theta_3], \tag{C17}$$

which have the symmetry transformation $(\theta_1,\theta_2,\theta_3)\to(\pi-\theta_1,\pi-\theta_2,\pi-\theta_3)$. As regards the leptogenesis, the relevant *CP* invariants are of the form

$$I^e_{\rm NO}=-I^\tau_{\rm NO}=-\frac{1}{2}(\cos\theta_1\sin\theta_3+\sin\theta_1\sin\theta_2\cos\theta_3)\sin\varrho_1,\qquad I^\mu_{\rm NO}=0,$$
$$I^e_{\rm IO}=-I^\tau_{\rm IO}=\frac{1}{2}\sin\theta_1\cos\theta_2\sin\varrho_1,\qquad I^\mu_{\rm IO}=0. \tag{C18}$$

One sees that the lepton asymmetry ϵ_α would be vanishing for $\varrho_1=0$ such that the cosmological baryon asymmetry cannot be generated. For the second mixing pattern $U_{III,2}$, the three lepton mixing angles and Jarlskog invariant are determined to be

$$\sin^2\theta_{13}=\frac{1}{2}(\sin^2\theta_2+\cos^2\theta_1\cos^2\theta_2-\cos\theta_1\sin 2\theta_2\cos\varrho_1),$$
$$\sin^2\theta_{12}=\sin^2\theta_3+\frac{\sin 2\theta_3(2\sin\theta_1\cos\theta_2\cos\varrho_1+\sin 2\theta_1\sin\theta_2)+2\sin^2\theta_1\cos 2\theta_3}{2-\sin^2\theta_2-\cos^2\theta_1\cos^2\theta_2+\cos\theta_1\sin 2\theta_2\cos\varrho_1},$$
$$\sin^2\theta_{23}=\frac{1-\sin^2\theta_1\cos^2\theta_2+\cos\theta_1\sin 2\theta_2\cos\varrho_1}{2-\sin^2\theta_2-\cos^2\theta_1\cos^2\theta_2+\cos\theta_1\sin 2\theta_2\cos\varrho_1},$$
$$J_{CP}=-\frac{1}{16}\sin\theta_1\cos\theta_2\sin\varrho_1[4\sin 2\theta_1\sin\theta_2\cos 2\theta_3+(1+3\cos 2\theta_1+2\sin^2\theta_1\cos 2\theta_2)\sin 2\theta_3]. \tag{C19}$$

Regarding the *CP* invariants in leptogenesis, we get

$$I^e_{\rm NO}=-I^\mu_{\rm NO}=-\frac{1}{2}(\cos\theta_1\sin\theta_3+\sin\theta_1\sin\theta_2\cos\theta_3)\sin\varrho_1,\qquad I^\tau_{\rm NO}=0,$$
$$I^e_{\rm IO}=-I^\mu_{\rm IO}=\frac{1}{2}\sin\theta_1\cos\theta_2\sin\varrho_1,\qquad I^\tau_{\rm IO}=0, \tag{C20}$$

which implies $I^e_{\rm NO}+I^\mu_{\rm NO}=0$ and $I^e_{\rm IO}+I^\mu_{\rm IO}=0$. Hence the summation of the *CP* asymmetry in the electron and muon flavors would vanish, i.e., $\epsilon_2\equiv\epsilon_e+\epsilon_\mu=0$. As a consequence, Y_B would be predicted to be zero in the mass window $10^9\ {\rm GeV}\le M_1\le 10^{12}\ {\rm GeV}$ unless the postulated residual symmetry is broken by nonleading order corrections arising from higher dimensional operators. For the third possible PMNS mixing matrix $U_{\rm III,3}$, the lepton mixing parameters read as

$$\sin^2\theta_{13}=\sin^2\theta_1\cos^2\theta_2,$$
$$\sin^2\theta_{12}=\frac{(\cos\theta_1\cos\theta_3-\sin\theta_1\sin\theta_2\sin\theta_3)^2}{1-\sin^2\theta_1\cos^2\theta_2},$$
$$\sin^2\theta_{23}=\frac{1}{2}-\frac{\cos\theta_1\sin 2\theta_2\cos\varrho_1}{2-2\sin^2\theta_1\cos^2\theta_2},$$
$$J_{CP}=-\frac{1}{16}\sin\theta_1\cos\theta_2\sin\varrho_1[4\sin 2\theta_1\sin\theta_2\cos 2\theta_3+(1+3\cos 2\theta_1+2\sin^2\theta_1\cos 2\theta_2)\sin 2\theta_3]. \tag{C21}$$

The rephase invariants $I^\alpha_{\rm NO}$ and $I^\alpha_{\rm IO}$ are of the following form:

$$I^\mu_{\rm NO}=-I^\tau_{\rm NO}=-\frac{1}{2}(\cos\theta_1\sin\theta_3+\sin\theta_1\sin\theta_2\cos\theta_3)\sin\varrho_1,\qquad I^e_{\rm NO}=0,$$
$$I^\mu_{\rm IO}=-I^\tau_{\rm IO}=\frac{1}{2}\sin\theta_1\cos\theta_2\sin\varrho_1,\qquad I^e_{\rm IO}=0. \tag{C22}$$

(IV) $G_l=\langle bc^sd^t\rangle$, $X_\nu=\rho_{\mathbf{3}}(bc^xd^{-x})$

In the same manner as previous cases, we find the lepton mixing matrix is given by

$$U_{IV}=P_l\begin{pmatrix}0&\cos\varrho_2&\sin\varrho_2\\1&0&0\\0&-\sin\varrho_2&\cos\varrho_2\end{pmatrix}O_{3\times3}(\theta_1,\theta_2,\theta_3)\hat{X}_\nu^{-\frac{1}{2}}=P_lP_{213}O_{3\times3}(\theta_1+\varrho_2,\theta_2,\theta_3)\hat{X}_\nu^{-\frac{1}{2}}, \tag{C23}$$

where P_l is a generic 3×3 permutation matrix, and the contributions of P_l and P_{213} can be absorbed into the real orthogonal matrix $O_{3\times 3}$. The parameter ϱ_2 is fixed by the chosen residual symmetry as

$$\varrho_2 = -\frac{s+t}{2n}\pi, \tag{C24}$$

whose possible values are

$$\varrho_2(\text{mod } 2\pi) = 0, \frac{1}{2n}\pi, \frac{2}{2n}\pi, \ldots, \frac{4n-1}{2n}\pi. \tag{C25}$$

After the relabeling of $P_l P_{213} \to P_l$ and $\theta_1 + \varrho_1 \to \theta_1$ is taken into account, the mixing matrix U_{IV} would coincide with U_I, as shown in Eq. (C1). As a result, the predictions for mixing parameters and leptogenesis are exactly the same as case I. The experimentally preferred values of the lepton mixing angles can be accommodated, the Dirac CP phase δ is trivial, and the cosmic baryon asymmetry Y_B is predicted to be vanishing without higher order corrections.

(V) $G_l = \langle ac^s d^t\rangle$, $X_\nu = \rho_{\mathbf{3}}(c^x d^y)$

Combining the unitary transformations U_l for $G_l = \langle ac^s d^t\rangle$ shown in Table V and U_ν in Eq. (5.13), we find that the PMNS mixing matrix is of the form

$$U_V = \frac{1}{\sqrt{3}}\begin{pmatrix} e^{i\varrho_3} & 1 & e^{i\varrho_4} \\ \omega^2 e^{i\varrho_3} & 1 & \omega e^{i\varrho_4} \\ \omega e^{i\varrho_3} & 1 & \omega^2 e^{i\varrho_4} \end{pmatrix} O_{3\times 3}(\theta_1,\theta_2,\theta_3)\hat{X}_\nu^{-\frac{1}{2}}, \tag{C26}$$

up to permutations of rows, where ϱ_3 and ϱ_4 are determined by residual symmetry,

$$\varrho_3 = \frac{2s-2t+2x-y}{n}\pi, \quad \varrho_4 = \frac{-2t+x-2y}{n}\pi, \tag{C27}$$

which can independently take the values

$$\varrho_3, \varrho_4(\text{mod } 2\pi) = 0, \frac{1}{n}\pi, \frac{2}{n}\pi, \ldots, \frac{2n-1}{n}\pi. \tag{C28}$$

We observe that the mixing matrix U_V has the following properties:

$$\begin{aligned} &U_V(\varrho_3+\pi,\varrho_4,\theta_1,\theta_2,\theta_3) \\ &\quad = U_V(\varrho_3,\varrho_4,\theta_1,-\theta_2,-\theta_3)\text{diag}(-1,1,1), \\ &U_V(\varrho_3,\varrho_4+\pi,\theta_1,\theta_2,\theta_3) \\ &\quad = U_V(\varrho_3,\varrho_4,-\theta_1,-\theta_2,\theta_3)\text{diag}(1,1,-1). \end{aligned} \tag{C29}$$

Consequently the fundamental regions of the parameters ϱ_3 and ϱ_4 can be taken to be $[0,\pi)$. Exchanging the second and third rows of U_V leads to the same mixing pattern as swapping ϱ_3 and ϱ_4, i.e.,

$$P_{132}U_V(\varrho_3,\varrho_4,\theta_1,\theta_2,\theta_3) = U_V(\varrho_4,\varrho_3,\theta_1',\theta_2',\theta_3'), \tag{C30}$$

where $\theta'_{1,2,3}$ fulfill $O_{3\times 3}(\theta_1',\theta_2',\theta_3') = P_{321}O_{3\times 3}(\theta_1,\theta_2,\theta_3)$. Hence it is enough to only consider three out of the six possible row permutations if all possible values of ϱ_3 and ϱ_4 are considered,

$$U_{V,1} = U_V, \quad U_{V,2} = P_{213}U_V, \quad U_{V,3} = P_{231}U_V. \tag{C31}$$

For the case of $U_{V,1}$, we can obtain the following expressions for the mixing angles and the Jarlskog invariant,

$$\begin{aligned} \sin^2\theta_{13} &= \frac{1}{3}[\sin 2\theta_2(\cos\theta_1\cos(\varrho_3-\varrho_4)+\sin\theta_1\cos\varrho_3)+\sin 2\theta_1\cos^2\theta_2\cos\varrho_4+1], \\ \sin^2\theta_{12} &= \sin^2\theta_3 + \frac{\sin 2\theta_3(\cos\theta_1\cos\theta_2\cos\varrho_3-\sin\theta_1\cos\theta_2\cos(\varrho_3-\varrho_4)-\cos 2\theta_1\sin\theta_2\cos\varrho_4)}{2-\sin 2\theta_2(\cos\theta_1\cos(\varrho_3-\varrho_4)+\sin\theta_1\cos\varrho_3)-\sin 2\theta_1\cos^2\theta_2\cos\varrho_4} \\ &\quad + \frac{\cos 2\theta_3(1-\sin 2\theta_1\cos\varrho_4)}{2-\sin 2\theta_2(\cos\theta_1\cos(\varrho_3-\varrho_4)+\sin\theta_1\cos\varrho_3)-\sin 2\theta_1\cos^2\theta_2\cos\varrho_4}, \\ \sin^2\theta_{23} &= \frac{\sin 2\theta_2(\cos\theta_1\sin(\varrho_3-\varrho_4+\frac{\pi}{6})+\sin\theta_1\cos(\varrho_3+\frac{\pi}{3}))+\cos^2\theta_2\sin 2\theta_1\cos(\varrho_4-\frac{\pi}{3})-1}{\sin 2\theta_2(\cos\theta_1\cos(\varrho_3-\varrho_4)+\sin\theta_1\cos\varrho_3)+\sin 2\theta_1\cos^2\theta_2\cos\varrho_4-2}, \\ J_{CP} &= \frac{1}{6\sqrt{3}}[\cos 2\theta_1\cos 2\theta_2\cos 2\theta_3+\sin 2\theta_1\sin\theta_2(1-3/2\cos^2\theta_2)\sin 2\theta_3 \\ &\quad + \cos\theta_2(\sin 2\theta_3(\cos^2\theta_1-\sin^2\theta_1\sin^2\theta_2)+\sin 2\theta_1\sin\theta_2\cos 2\theta_3)[\sin\theta_1\cos(\varrho_3+\varrho_4) \\ &\quad - \cos\theta_1\cos(\varrho_3-2\varrho_4)]+\cos^3\theta_2\sin 2\theta_3(\cos\theta_1\cos(\varrho_3-2\varrho_4)-\tan\theta_2\cos(2\varrho_3-\varrho_4))]. \end{aligned} \tag{C32}$$

Moreover, the *CP* invariants $I^{\alpha}_{\rm NO}$ and $I^{\alpha}_{\rm IO}$ are given by

$$
\begin{aligned}
I^{e}_{\rm NO} &= \frac{1}{3}[\sin(\varrho_4-\varrho_3)(\sin\theta_1\sin\theta_2\cos\theta_3+\cos\theta_1\sin\theta_3)+\cos\theta_2\cos\theta_3\sin\varrho_4 \\
&\quad +\sin\varrho_3(\cos\theta_1\sin\theta_2\cos\theta_3-\sin\theta_1\sin\theta_3)], \\
I^{\mu}_{\rm NO} &= \frac{1}{3}\left[\sin\left(\varrho_3-\varrho_4-\frac{\pi}{3}\right)(\sin\theta_1\sin\theta_2\cos\theta_3+\cos\theta_1\sin\theta_3)+\cos\theta_2\cos\theta_3\sin\left(\frac{\pi}{3}-\varrho_4\right)\right. \\
&\quad \left.+\sin\left(\varrho_3+\frac{\pi}{3}\right)(\sin\theta_1\sin\theta_3-\cos\theta_1\sin\theta_2\cos\theta_3)\right], \\
I^{e}_{\rm IO} &= \frac{1}{3}(\sin\theta_1\cos\theta_2\sin(\varrho_3-\varrho_4)-\cos\theta_1\cos\theta_2\sin\varrho_3+\sin\theta_2\sin\varrho_4), \\
I^{\mu}_{\rm IO} &= \frac{1}{3}\left(\sin\theta_1\cos\theta_2\sin\left(\frac{\pi}{3}-\varrho_3+\varrho_4\right)+\cos\theta_1\cos\theta_2\sin\left(\varrho_3+\frac{\pi}{3}\right)+\sin\theta_2\sin\left(\frac{\pi}{3}-\varrho_4\right)\right), \\
I^{\tau}_{\rm NO} &= -(I^{e}_{\rm NO}+I^{\mu}_{\rm NO}), \qquad I^{\tau}_{\rm IO} = -(I^{e}_{\rm IO}+I^{\mu}_{\rm IO}).
\end{aligned}
\tag{C33}
$$

Then we proceed to discuss the second permutation $U_{V,2}$. We can straightforwardly extract the mixing parameters and find

$$
\begin{aligned}
\sin^2\theta_{13} &= \frac{1}{3}\left[1-\sin 2\theta_2\left(\cos\theta_1\cos\left(\varrho_3-\varrho_4-\frac{\pi}{3}\right)+\sin\theta_1\cos\left(\varrho_3+\frac{\pi}{3}\right)\right)-\sin 2\theta_1\cos^2\theta_2\cos\left(\varrho_4-\frac{\pi}{3}\right)\right], \\
\sin^2\theta_{12} &= \sin^2\theta_3+\frac{\cos 2\theta_3(\sin 2\theta_1\cos(\varrho_4-\frac{\pi}{3})+1)}{2+\sin 2\theta_2(\cos\theta_1\cos(\varrho_3-\varrho_4-\frac{\pi}{3})+\sin\theta_1\cos(\varrho_3+\frac{\pi}{3}))+\sin 2\theta_1\cos^2\theta_2\cos(\varrho_4-\frac{\pi}{3})}, \\
&\quad +\frac{\sin 2\theta_3(\sin\theta_1\cos\theta_2\cos(\varrho_3-\varrho_4-\frac{\pi}{3})-\cos\theta_1\cos\theta_2\cos(\varrho_3+\frac{\pi}{3})+\cos 2\theta_1\sin\theta_2\cos(\varrho_4-\frac{\pi}{3}))}{2+\sin 2\theta_2(\cos\theta_1\cos(\varrho_3-\varrho_4-\frac{\pi}{3})+\sin\theta_1\cos(\varrho_3+\frac{\pi}{3}))+\sin 2\theta_1\cos^2\theta_2\cos(\varrho_4-\frac{\pi}{3})}, \\
\sin^2\theta_{23} &= \frac{\sin 2\theta_2(\cos\theta_1\cos(\varrho_3-\varrho_4)+\sin\theta_1\cos\varrho_3)+\sin 2\theta_1\cos^2\theta_2\cos\varrho_4+1}{2+\sin 2\theta_2(\cos\theta_1\cos(\varrho_3-\varrho_4-\frac{\pi}{3})+\sin\theta_1\cos(\varrho_3+\frac{\pi}{3}))+\sin 2\theta_1\cos^2\theta_2\cos(\varrho_4-\frac{\pi}{3})}, \\
J_{CP} &= -\frac{1}{6\sqrt{3}}[\cos 2\theta_1\cos 2\theta_2\cos 2\theta_3+\sin 2\theta_1\sin\theta_2(1-3/2\cos^2\theta_2)\sin 2\theta_3 \\
&\quad +\cos\theta_2(\sin 2\theta_3(\cos^2\theta_1-\sin^2\theta_1\sin^2\theta_2)+\sin 2\theta_1\sin\theta_2\cos 2\theta_3)[\sin\theta_1\cos(\varrho_3+\varrho_4) \\
&\quad -\cos\theta_1\cos(\varrho_3-2\varrho_4)]+\cos^3\theta_2\sin 2\theta_3(\cos\theta_1\cos(\varrho_3-2\varrho_4)-\tan\theta_2\cos(2\varrho_3-\varrho_4))].
\end{aligned}
\tag{C34}
$$

Since $U_{V,2}$ and $U_{V,1}$ are related through the permutation of the first and second rows, the rephasing invariants $I^{\alpha}_{\rm NO,IO}$ for $U_{V,2}$ can be obtained from Eq. (C33) by interchanging the expressions of $I^{e}_{\rm NO,IO}$ and $I^{\mu}_{\rm NO,IO}$. The third mixing matrix $U_{V,3}$ can be easily obtained by exchanging the second and third rows of $U_{V,2}$. As a consequence, $U_{V,2}$ and $U_{V,3}$ lead to the same reactor and solar mixing angles, while the atmospheric one changes from θ_{23} to $\pi/2-\theta_{23}$, i.e., $\sin^2\theta_{23}$ is replaced by $\cos^2\theta_{23}$ in Eq. (C34), and the Dirac phase changes from δ to $\pi+\delta$ such that the overall sign of the Jarlskog invariant J_{CP} becomes opposite. Furthermore, the *CP* invariants can be obtained from Eq. (C33) by replacing $I^{e}_{\rm NO,IO}\to I^{\tau}_{\rm NO,IO}$, $I^{\mu}_{\rm NO,IO}\to I^{e}_{\rm NO,IO}$, and $I^{\tau}_{\rm NO,IO}\to I^{\mu}_{\rm NO,IO}$.

(VI) $G_l=\langle ac^s d^t\rangle$, $X_\nu=\rho_{\mathbf{3}}(bc^x d^{-x})$

In this case, the PMNS mixing matrix takes the following form,

$$
\begin{aligned}
U_{VI} &= \sqrt{\frac{2}{3}}\begin{pmatrix} \frac{e^{i\varrho_5}}{\sqrt{2}} & \sin\varrho_6 & \cos\varrho_6 \\ -\frac{e^{i\varrho_5}}{\sqrt{2}} & \cos(\frac{\pi}{6}-\varrho_6) & \sin(\frac{\pi}{6}-\varrho_6) \\ \frac{e^{i\varrho_5}}{\sqrt{2}} & \cos(\varrho_6+\frac{\pi}{6}) & -\sin(\varrho_6+\frac{\pi}{6}) \end{pmatrix} O_{3\times 3}(\theta_1,\theta_2,\theta_3)\hat{X}_\nu^{-\frac{1}{2}} \\
&= \sqrt{\frac{2}{3}}\begin{pmatrix} \frac{e^{i\varrho_5}}{\sqrt{2}} & 0 & 1 \\ -\frac{e^{i\varrho_5}}{\sqrt{2}} & \cos\frac{\pi}{6} & \sin\frac{\pi}{6} \\ \frac{e^{i\varrho_5}}{\sqrt{2}} & \cos\frac{\pi}{6} & -\sin\frac{\pi}{6} \end{pmatrix} O_{3\times 3}(\theta_1-\varrho_6,\theta_2,\theta_3)\hat{X}_\nu^{-\frac{1}{2}},
\end{aligned}
\tag{C35}
$$

where the discrete parameters ϱ_5 and ϱ_6 depend on the choice of the residual symmetry as

$$\varrho_5 = \frac{-s+2t-3x}{n}\pi, \qquad \varrho_6 = \frac{s}{n}\pi, \tag{C36}$$

whose values can be

$$\varrho_5, \varrho_6 (\mathrm{mod}\ 2\pi) = 0, \frac{1}{n}\pi, \frac{2}{n}\pi, \ldots, \frac{2n-1}{n}\pi. \tag{C37}$$

From Eq. (C35) we can see that the parameter ϱ_6 is irrelevant since it can be absorbed into the free parameter θ_1. Furthermore we find that U_{VI} has several symmetry properties,

$$\begin{aligned}
P_{132}U_{VI}(\varrho_5,\varrho_6,\theta_1,\theta_2,\theta_3) &= \mathrm{diag}(1,-1,-1)U_{VI}(\varrho_5,-\varrho_6,-\theta_1,\theta_2,-\theta_3)\mathrm{diag}(1,-1,1),\\
P_{312}U_{VI}(\varrho_5,\varrho_6,\theta_1,\theta_2,\theta_3) &= \mathrm{diag}(1,-1,-1)U_{VI}\left(\varrho_5,\varrho_6+\frac{2\pi}{3},\theta_1,\theta_2,\theta_3\right),\\
P_{231}U_{VI}(\varrho_5,\varrho_6,\theta_1,\theta_2,\theta_3) &= \mathrm{diag}(-1,-1,1)U_{VI}\left(\varrho_5,\varrho_6-\frac{2\pi}{3},\theta_1,\theta_2,\theta_3\right),
\end{aligned} \tag{C38}$$

and

$$U_{VI}(\varrho_5+\pi,\varrho_6,\theta_1,\theta_2,\theta_3) = U_{VI}(\varrho_5,\varrho_6,\theta_1,-\theta_2,-\theta_3)\mathrm{diag}(-1,1,1). \tag{C39}$$

Equation (C38) implies that the six possible row permutations lead to the same mixing pattern, and Eq. (C39) indicates that the fundamental region of ϱ_5 is $[0,\pi)$. We can read off the mixing parameters from the mixing matrix U_{VI} in Eq. (C35) as follows:

$$\begin{aligned}
\sin^2\theta_{13} &= \frac{1}{3}(1+\cos 2\theta_1\cos^2\theta_2+\sqrt{2}\cos\theta_1\sin 2\theta_2\cos\varrho_5),\\
\sin^2\theta_{12} &= \sin^2\theta_3+\frac{\sin\theta_1(2\sin\theta_1\cos 2\theta_3-\sin 2\theta_3(\sqrt{2}\cos\theta_2\cos\varrho_5-2\cos\theta_1\sin\theta_2))}{2-\cos 2\theta_1\cos^2\theta_2-\sqrt{2}\cos\theta_1\sin 2\theta_2\cos\varrho_5},\\
\sin^2\theta_{23} &= \frac{1-\cos(2\theta_1+\pi/3)\cos^2\theta_2-\sqrt{2}\sin(\theta_1+\pi/6)\sin 2\theta_2\cos\varrho_5}{2-\cos 2\theta_1\cos^2\theta_2-\sqrt{2}\cos\theta_1\sin 2\theta_2\cos\varrho_5},\\
J_{CP} &= \frac{\cos\theta_2\sin 2\theta_3\sin\varrho_5[4\sin 3\theta_1\sin\theta_2\cot 2\theta_3-\cos 3\theta_1(\cos 2\theta_2-3)-2\sqrt{2}\sin 2\theta_2\cos\varrho_5]}{12\sqrt{6}},
\end{aligned} \tag{C40}$$

where the redefinition of $\theta_1 \to \theta_1+\varrho_6$ is used. Moreover, the rephasing invariants involved in leptogenesis are found to be of the form

$$\begin{aligned}
I^e_{\mathrm{NO}} &= -\frac{\sqrt{2}}{3}\sin\varrho_5(\cos\theta_1\sin\theta_3+\sin\theta_1\sin\theta_2\cos\theta_3),\\
I^\mu_{\mathrm{NO}} &= \frac{\sqrt{2}}{3}\sin\varrho_5[\sin(\theta_1+\pi/6)\sin\theta_3+\sin(\theta_1-\pi/3)\sin\theta_2\cos\theta_3]\\
I^e_{\mathrm{IO}} &= \frac{\sqrt{2}}{3}\sin\theta_1\cos\theta_2\sin\varrho_5,\\
I^\mu_{\mathrm{IO}} &= -\frac{\sqrt{2}}{3}\sin(\theta_1-\pi/3)\cos\theta_2\sin\varrho_5,\\
I^\tau_{\mathrm{NO}} &= -(I^e_{\mathrm{NO}}+I^\mu_{\mathrm{NO}}), I^\tau_{\mathrm{IO}} = -(I^e_{\mathrm{IO}}+I^\mu_{\mathrm{IO}}).
\end{aligned} \tag{C41}$$

(VII) $G_l = \langle abc^s d^t\rangle$, $X_\nu = \rho_{\mathbf{3}}(c^x d^y)$

Similar to the previous cases, the lepton mixing matrix is given by, up to permutations of rows and unphysical phases,

$$U_{VII} = \frac{1}{\sqrt{2}}\begin{pmatrix} e^{i\varrho_7} & -1 & 0 \\ e^{i\varrho_7} & 1 & 0 \\ 0 & 0 & \sqrt{2} \end{pmatrix} O_{3\times 3}(\theta_1,\theta_2,\theta_3)\hat{X}_\nu^{-\frac{1}{2}},$$
$$= \mathrm{diag}(-1,1,1)P_{132}\frac{1}{\sqrt{2}}\begin{pmatrix} 1 & 0 & -e^{i\varrho_7} \\ 0 & \sqrt{2} & 0 \\ 1 & 0 & e^{i\varrho_7} \end{pmatrix}[P_{231}O_{3\times 3}(\theta_1,\theta_2,\theta_3)]\hat{X}_\nu^{-\frac{1}{2}}, \tag{C42}$$

with

$$\varrho_7 = \frac{2s-t+2x-y}{n}\pi. \tag{C43}$$

Comparing Eq. (C42) with Eq. (C11), we can see that this case gives rise to the same mixing pattern and the baryon asymmetry Y_B as case III if all possible row permutations are taken into account.

(VIII) $G_l = \langle abc^s d^t\rangle$, $X_\nu = \rho_{\mathbf{3}}(bc^x d^{-x})$

In this case, we find that the PMNS mixing matrix takes the form

$$U_{\mathrm{VIII}} = \frac{1}{2}\begin{pmatrix} -\sqrt{2} & -ie^{i\varrho_8} & e^{i\varrho_8} \\ \sqrt{2} & -ie^{i\varrho_8} & e^{i\varrho_8} \\ 0 & i\sqrt{2}e^{-i\varrho_8} & \sqrt{2}e^{-i\varrho_8} \end{pmatrix} O_{3\times 3}(\theta_1,\theta_2,\theta_3)\hat{X}_\nu^{-\frac{1}{2}}$$
$$= \frac{1}{2}\begin{pmatrix} -\sqrt{2} & -i & 1 \\ \sqrt{2} & -i & 1 \\ 0 & i\sqrt{2} & \sqrt{2} \end{pmatrix} O_{3\times 3}(\theta_1-\varrho_8,\theta_2,\theta_3)\hat{X}_\nu^{-\frac{1}{2}}, \tag{C44}$$

with

$$\varrho_8 = \frac{2s-t+3x}{n}\pi. \tag{C45}$$

Obviously the value of ϱ_8 is irrelevant since it can be absorbed into the free parameter θ_1. Furthermore, the six possible row permutations lead to three independent mixing patterns, which can be chosen as

$$U_{\mathrm{VIII},1} = U_{\mathrm{VIII}}, \qquad U_{\mathrm{VIII},2} = P_{132}U_{\mathrm{VIII}}, \qquad U_{\mathrm{VIII},3} = P_{312}U_{\mathrm{VIII}}. \tag{C46}$$

The reason is because U_{VIII} fulfills the equality

$$P_{213}U_{\mathrm{VIII}}(\varrho_8,\theta_1,\theta_2,\theta_3) = U_{\mathrm{VIII}}(\varrho_8,\theta_1,-\theta_2,-\theta_3)\mathrm{diag}(-1,1,1). \tag{C47}$$

For the mixing matrix $U_{\mathrm{VIII},1}$, after the parameter θ_1 is shifted into $\theta_1+\varrho_8$, we can read off the mixing parameters as

$$\sin^2\theta_{13} = \frac{1}{8}(3-\cos 2\theta_2 - 2\sqrt{2}\cos\theta_1\sin 2\theta_2),$$
$$\sin^2\theta_{12} = \sin^2\theta_3 + \frac{2(\cos 2\theta_3 + \sqrt{2}\sin\theta_1\cos\theta_2\sin 2\theta_3)}{5+\cos 2\theta_2 + 2\sqrt{2}\cos\theta_1\sin 2\theta_2},$$
$$\sin^2\theta_{23} = \frac{3-\cos 2\theta_2 + 2\sqrt{2}\cos\theta_1\sin 2\theta_2}{5+\cos 2\theta_2 + 2\sqrt{2}\cos\theta_1\sin 2\theta_2},$$
$$J_{CP} = \frac{1}{32\sqrt{2}}[4\sin\theta_1\sin 2\theta_2\cos 2\theta_3 - \cos\theta_1(\cos\theta_2 + 3\cos 3\theta_2)\sin 2\theta_3]. \tag{C48}$$

The CP invariants $I^{\alpha}_{\rm NO,IO}$ ($\alpha = e, \mu, \tau$) turn out to take the form

$$
\begin{aligned}
I^{e}_{\rm NO} &= \frac{1}{4}[\cos\theta_2\cos\theta_3 + \sqrt{2}(\sin\theta_1\sin\theta_3 - \cos\theta_1\sin\theta_2\cos\theta_3)],\\
I^{\mu}_{\rm NO} &= \frac{1}{4}[\cos\theta_2\cos\theta_3 - \sqrt{2}(\sin\theta_1\sin\theta_3 - \cos\theta_1\sin\theta_2\cos\theta_3)]\\
I^{e}_{\rm IO} &= \frac{1}{4}(\sin\theta_2 + \sqrt{2}\cos\theta_1\cos\theta_2), \qquad I^{\mu}_{\rm IO} = \frac{1}{4}(\sin\theta_2 - \sqrt{2}\cos\theta_1\cos\theta_2),\\
I^{\tau}_{\rm NO} &= -(I^{e}_{\rm NO} + I^{\mu}_{\rm NO}) = -\frac{1}{2}\cos\theta_2\cos\theta_3, \qquad I^{\tau}_{\rm IO} = -(I^{e}_{\rm IO} + I^{\mu}_{\rm IO}) = -\frac{1}{2}\sin\theta_2.
\end{aligned}
\tag{C49}
$$

The second mixing matrix $U_{\rm VIII,2}$ is related to $U_{\rm VIII,1}$ through the permutation of the second and third rows. As a consequence, the expressions for θ_{12} and θ_{13} coincide with Eq. (C48), the overall sign of J_{CP} is reversed, and the atmospheric mixing angle θ_{23} changes into

$$
\sin^2\theta_{23} = \frac{4\cos^2\theta_2}{5 + \cos 2\theta_2 + 2\sqrt{2}\cos\theta_1\sin 2\theta_2}. \tag{C50}
$$

Moreover the rephase invariants can be obtained from Eq. (C49) by interchanging $I^{\mu}_{\rm NO,IO}$ and $I^{\tau}_{\rm NO,IO}$. Finally we proceed to the third mixing matrix $U_{\rm VIII,3}$. We can extract the following results for the mixing angles,

$$
\sin^2\theta_{13} = \frac{1}{2}\cos^2\theta_2, \qquad \sin^2\theta_{12} = \frac{1}{2} + \frac{\cos^2\theta_2\cos 2\theta_3}{3 - \cos 2\theta_2}, \qquad \sin^2\theta_{23} = \frac{1}{2} - \frac{\sqrt{2}\cos\theta_1\sin 2\theta_2}{3 - \cos 2\theta_2}, \tag{C51}
$$

which implies

$$
\left|\sin^2\theta_{12} - \frac{1}{2}\right| \leq \frac{1}{2}\tan^2\theta_{13}, \qquad \left|\sin^2\theta_{23} - \frac{1}{2}\right| \leq \tan\theta_{13}\sqrt{1 - \tan^2\theta_{13}}. \tag{C52}
$$

Hence the experimental data [4] on θ_{13} and θ_{12} cannot be accommodated simultaneously without higher order corrections for this mixing matrix.

[1] T. Kajita, Rev. Mod. Phys. **88**, 030501 (2016).
[2] A. B. McDonald, Rev. Mod. Phys. **88**, 030502 (2016).
[3] *Special Issue on "Neutrino Oscillations: Celebrating the Nobel Prize in Physics 2015,"* edited by T. Ohlsson [*Nucl. Phys.* B908, 1 (2016)], http://www.sciencedirect.com/science/journal/05503213/908/supp/C.
[4] F. Capozzi, G. L. Fogli, E. Lisi, A. Marrone, D. Montanino, and A. Palazzo, Phys. Rev. D **89**, 093018 (2014).
[5] D. V. Forero, M. Tortola, and J. W. F. Valle, Phys. Rev. D **90**, 093006 (2014).
[6] M. C. Gonzalez-Garcia, M. Maltoni, and T. Schwetz, J. High Energy Phys. 11 (2014) 052.
[7] F. Capozzi, E. Lisi, A. Marrone, D. Montanino, and A. Palazzo, Nucl. Phys. **B908**, 218 (2016).
[8] I. Esteban, M. C. Gonzalez-Garcia, M. Maltoni, I. Martinez-Soler, and T. Schwetz, J. High Energy Phys. 01 (2017) 087.
[9] K. Abe *et al.* (T2K Collaboration), Phys. Rev. D **91**, 072010 (2015).
[10] K. Iwamoto (T2K Collaboration), in *Proceedings of 38th International Conference on High Energy Physics, Chicago, USA 2016* (2016), http://indico.cern.ch/event/432527/contributions/2143636/.
[11] K. Abe *et al.* (T2K Collaboration), Phys. Rev. Lett. **118**, 151801 (2017).
[12] J. Bian (NOνA Collaboration), in *Proceedings of 38th International Conference on High Energy Physics* (Chicago, 2016), http://indico.cern.ch/event/432527/contributions/2144798/.
[13] P. Adamson *et al.* (NOνA Collaboration), Phys. Rev. Lett. **118**, 231801 (2017).
[14] C. S. Lam, Phys. Lett. B **656**, 193 (2007); Phys. Rev. Lett. **101**, 121602 (2008); R. de Adelhart Toorop, F. Feruglio, and C. Hagedorn, Nucl. Phys. **B858**, 437 (2012); M. Holthausen, K. S. Lim, and M. Lindner, Phys. Lett. B

721, 61 (2013); C. Y. Yao and G. J. Ding, Phys. Rev. D **92**, 096010 (2015).
[15] G. Altarelli and F. Feruglio, Rev. Mod. Phys. **82**, 2701 (2010).
[16] H. Ishimori, T. Kobayashi, H. Ohki, Y. Shimizu, H. Okada, and M. Tanimoto, Prog. Theor. Phys. Suppl. **183**, 1 (2010).
[17] S. F. King and C. Luhn, Rep. Prog. Phys. **76**, 056201 (2013); S. F. King, A. Merle, S. Morisi, Y. Shimizu, and M. Tanimoto, New J. Phys. **16**, 045018 (2014); S. F. King, J. Phys. G **42**, 123001 (2015); Prog. Part. Nucl. Phys. **94**, 217 (2017).
[18] P. Minkowski, Phys. Lett. **67B**, 421 (1977); M. Gell-Mann, P. Ramond, and R. Slansky, *Proceedings of the Supergravity Stony Brook Workshop, New York 1979*, edited by P. Van Nieuwenhuizen and D. Freedman; T. Yanagida, *Proceedings of the Workshop on Unified Theories and Baryon Number in the Universe, Tsukuba, Japan 1979*, edited by A. Sawada and A. Sugamoto; R. N. Mohapatra and G. Senjanovic, Phys. Rev. Lett. **44**, 912 (1980); J. Schechter and J. W. F. Valle, Phys. Rev. D **22**, 2227 (1980).
[19] M. Fukugita and T. Yanagida, Phys. Lett. B **174**, 45 (1986).
[20] A. Abada, S. Davidson, F. X. Josse-Michaux, M. Losada, and A. Riotto, J. Cosmol. Astropart. Phys. 04 (2006) 004; E. Nardi, Y. Nir, E. Roulet, and J. Racker, J. High Energy Phys. 01 (2006) 164; A. Abada, S. Davidson, A. Ibarra, F.-X. Josse-Michaux, M. Losada, and A. Riotto, J. High Energy Phys. 09 (2006) 010; S. Pascoli, S. T. Petcov, and A. Riotto, Phys. Rev. D **75**, 083511 (2007); Nucl. Phys. **B774**, 1 (2007); E. Molinaro, S. T. Petcov, T. Shindou, and Y. Takanishi, Nucl. Phys. **B797**, 93 (2008); E. Molinaro and S. T. Petcov, Eur. Phys. J. C **61**, 93 (2009); Phys. Lett. B **671**, 60 (2009).
[21] E. E. Jenkins and A. V. Manohar, Phys. Lett. B **668**, 210 (2008); E. Bertuzzo, P. Di Bari, F. Feruglio, and E. Nardi, J. High Energy Phys. 11 (2009) 036; C. Hagedorn, E. Molinaro, and S. T. Petcov, J. High Energy Phys. 09 (2009) 115.
[22] P. Chen, G. J. Ding, and S. F. King, J. High Energy Phys. 03 (2016) 206.
[23] F. Feruglio, C. Hagedorn, and R. Ziegler, J. High Energy Phys. 07 (2013) 027; M. Holthausen, M. Lindner, and M. A. Schmidt, J. High Energy Phys. 04 (2013) 122; G. J. Ding, S. F. King, C. Luhn, and A. J. Stuart, J. High Energy Phys. 05 (2013) 084; F. Feruglio, C. Hagedorn, and R. Ziegler, Eur. Phys. J. C **74**, 2753 (2014); C. C. Li and G. J. Ding, Nucl. Phys. **B881**, 206 (2014); J. High Energy Phys. 08 (2015) 017.
[24] G. J. Ding, S. F. King, and A. J. Stuart, J. High Energy Phys. 12 (2013) 006; C. C. Nishi, Phys. Rev. D **93**, 093009 (2016); C. C. Li, J. N. Lu, and G. J. Ding, Nucl. Phys. **B913**, 110 (2016).
[25] C. C. Li and G. J. Ding, J. High Energy Phys. 05 (2015) 100; A. Di Iura, C. Hagedorn, and D. Meloni, J. High Energy Phys. 08 (2015) 037; P. Ballett, S. Pascoli, and J. Turner, Phys. Rev. D **92**, 093008 (2015); J. Turner, Phys. Rev. D **92**, 116007 (2015).
[26] G. C. Branco, I. de Medeiros Varzielas, and S. F. King, Phys. Rev. D **92**, 036007 (2015); Nucl. Phys. **B899**, 14 (2015).
[27] G. J. Ding and Y. L. Zhou, Chin. Phys. C **39**, 021001 (2015); J. High Energy Phys. 06 (2014) 023.
[28] S. F. King and T. Neder, Phys. Lett. B **736**, 308 (2014).
[29] C. Hagedorn, A. Meroni, and E. Molinaro, Nucl. Phys. **B891**, 499 (2015).
[30] G. J. Ding, S. F. King, and T. Neder, J. High Energy Phys. 12 (2014) 007.
[31] G. J. Ding and S. F. King, Phys. Rev. D **89**, 093020 (2014).
[32] G. J. Ding and S. F. King, Phys. Rev. D **93**, 025013 (2016); C. C. Li, C. Y. Yao, and G. J. Ding, J. High Energy Phys. 05 (2016) 007.
[33] C. Y. Yao and G. J. Ding, Phys. Rev. D **94**, 073006 (2016).
[34] J. N. Lu and G. J. Ding, Phys. Rev. D **95**, 015012 (2017); S. j. Rong, Phys. Rev. D **95**, 076014 (2017).
[35] P. Chen, C. C. Li, and G. J. Ding, Phys. Rev. D **91**, 033003 (2015); L. L. Everett, T. Garon, and A. J. Stuart, J. High Energy Phys. 04 (2015) 069; P. Chen, C. Y. Yao, and G. J. Ding, Phys. Rev. D **92**, 073002 (2015); L. L. Everett and A. J. Stuart, Phys. Rev. D **96**, 035030 (2017).
[36] C. Hagedorn and E. Molinaro, Nucl. Phys. **B919**, 404 (2017).
[37] S. F. King, Nucl. Phys. **B576**, 85 (2000).
[38] P. H. Frampton, S. L. Glashow, and T. Yanagida, Phys. Lett. B **548**, 119 (2002).
[39] M. Raidal and A. Strumia, Phys. Lett. B **553**, 72 (2003).
[40] S. Pascoli, S. T. Petcov, and W. Rodejohann, Phys. Rev. D **68**, 093007 (2003).
[41] J. A. Casas and A. Ibarra, Nucl. Phys. **B618**, 171 (2001).
[42] A. Ibarra and G. G. Ross, Phys. Lett. B **575**, 279 (2003); **591**, 285 (2004); A. Ibarra, J. High Energy Phys. 01 (2006) 064.
[43] M. Flanz, E. A. Paschos, U. Sarkar, and J. Weiss, Phys. Lett. B **389**, 693 (1996); A. Pilaftsis, Phys. Rev. D **56**, 5431 (1997); A. Pilaftsis and T. E. J. Underwood, Nucl. Phys. **B692**, 303 (2004).
[44] F. Vissani, Phys. Rev. D **57**, 7027 (1998); J. D. Clarke, R. Foot, and R. R. Volkas, Phys. Rev. D **91**, 073009 (2015); G. Bambhaniya, P. S. B. Dev, S. Goswami, S. Khan, and W. Rodejohann, Phys. Rev. D **95**, 095016 (2017).
[45] Leptogenesis in the seesaw mechanism with two right-handed neutrinos has been extensively discussed. An incomplete list is as follows: T. Endoh, S. Kaneko, S. K. Kang, T. Morozumi, and M. Tanimoto, Phys. Rev. Lett. **89**, 231601 (2002); M. Raidal and A. Strumia, Phys. Lett. B **553**, 72 (2003); G. C. Branco, R. G. Felipe, F. R. Joaquim, I. Masina, M. N. Rebelo, and C. A. Savoy, Phys. Rev. D **67**, 073025 (2003); V. Barger, D. A. Dicus, H. J. He, and T. j. Li, Phys. Lett. B **583**, 173 (2004); W. l. Guo and Z. z. Xing, Phys. Lett. B **583**, 163 (2004); R. G. Felipe, F. R. Joaquim, and B. M. Nobre, Phys. Rev. D **70**, 085009 (2004); A. Abada, S. Davidson, F. X. Josse-Michaux, M. Losada, and A. Riotto, J. Cosmol. Astropart. Phys. 04 (2006) 004; A. Abada, S. Davidson, A. Ibarra, F.-X. Josse-Michaux, M. Losada, and A. Riotto, J. High Energy Phys. 09 (2006) 010; S. Antusch, S. F. King, and A. Riotto, J. Cosmol. Astropart. Phys. 11 (2006) 011; W. l. Guo, Z. z. Xing, and S. Zhou, Int. J. Mod. Phys. E **E16**, 1 (2007); S. Antusch, P. Di Bari, D. A. Jones, and S. F. King, Phys. Rev. D **86**, 023516 (2012); J. Zhang and S. Zhou, J. High Energy Phys. 09 (2015) 065; F. Bjorkeroth, F. J. de Anda, I. de Medeiros Varzielas, and S. F. King, J. High Energy Phys. 10 (2015) 104; T. Kitabayashi and M. Yasue, Phys. Rev. D **94**, 075020 (2016); M. Fukugita, Y. Kaneta, Y. Shimizu, M. Tanimoto, and T. T. Yanagida, Phys. Lett. B **764**, 163 (2017);
[46] L. Covi, E. Roulet, and F. Vissani, Phys. Lett. B **384**, 169 (1996).

[47] W. Buchmuller, P. Di Bari, and M. Plumacher, Ann. Phys. (Amsterdam) **315**, 305 (2005).
[48] W. Buchmuller, R. D. Peccei, and T. Yanagida, Annu. Rev. Nucl. Part. Sci. **55**, 311 (2005).
[49] S. Davidson, E. Nardi, and Y. Nir, Phys. Rep. **466**, 105 (2008).
[50] A. Abada, S. Davidson, A. Ibarra, F.-X. Josse-Michaux, M. Losada, and A. Riotto, J. High Energy Phys. 09 (2006) 010.
[51] A. Abada, S. Davidson, F. X. Josse-Michaux, M. Losada, and A. Riotto, J. Cosmol. Astropart. Phys. 04 (2006) 004.
[52] S. Pascoli, S. T. Petcov, and A. Riotto, Nucl. Phys. **B774**, 1 (2007).
[53] E. Nardi, Y. Nir, E. Roulet, and J. Racker, J. High Energy Phys. 01 (2006) 164.
[54] G. F. Giudice, A. Notari, M. Raidal, A. Riotto, and A. Strumia, Nucl. Phys. **B685**, 89 (2004).
[55] P. Chen, G. J. Ding, F. Gonzalez-Canales, and J. W. F. Valle, Phys. Rev. D **94**, 033002 (2016).
[56] D. A. Sierra, M. Losada, and E. Nardi, Phys. Lett. B **659**, 328 (2008); D. A. Sierra, L. A. Munoz, and E. Nardi, Phys. Rev. D **80**, 016007 (2009); J. Phys. Conf. Ser. **171**, 012078 (2009); L. A. Munoz, Frascati Phys. Ser. **48**, 13 (2009).
[57] P. Chen, G. J. Ding, F. Gonzalez-Canales, and J. W. F. Valle, Phys. Lett. B **753**, 644 (2016).
[58] C. Patrignani *et al.* (Particle Data Group Collaboration), Chin. Phys. C **40**, 100001 (2016).
[59] P. A. R. Ade *et al.* (Planck Collaboration), Astron. Astrophys. **594**, A13 (2016); R. H. Cyburt, B. D. Fields, K. A. Olive, and T. H. Yeh, Rev. Mod. Phys. **88**, 015004 (2016).
[60] S. F. King, T. Neder, and A. J. Stuart, Phys. Lett. B **726**, 312 (2013).
[61] J. A. Escobar and C. Luhn, J. Math. Phys. (N.Y.) **50**, 013524 (2009).
[62] C. Y. Yao and G. J. Ding, Phys. Rev. D **92**, 096010 (2015).
[63] R. Acciarri *et al.* (DUNE Collaboration), arXiv:1601.05471; arXiv:1512.06148; arXiv:1601.02984; J. Strait *et al.* (DUNE Collaboration), arXiv:1601.05823.
[64] E. Kearns *et al.* (Hyper-Kamiokande Working Group Collaboration), arXiv:1309.0184; K. Abe *et al.* (Hyper-Kamiokande Working Group Collaboration), arXiv:1412.4673.
[65] K. Abe *et al.* (Hyper-Kamiokande Proto-Collaboration), arXiv:1611.06118.
[66] F. An *et al.* (JUNO Collaboration), J. Phys. G **43**, 030401 (2016).
[67] C. Jarlskog, Phys. Rev. Lett. **55**, 1039 (1985).